

ROLES OF BACTERIAL TOXIN RECEPTOR AND PIWI-  
INTERACTING RNA OF PACIFIC WHITE SHRIMP *Penaeus*  
*vannamei* IN RESPONSE TO *Vibrio parahaemolyticus*-  
CAUSING ACUTE HEPATOPANCREATIC NECROSIS  
DISEASE INFECTION



Miss Waruntorn Luangtrakul

จุฬาลงกรณ์มหาวิทยาลัย  
CHULALONGKORN UNIVERSITY

A Dissertation Submitted in Partial Fulfillment of the Requirements  
for the Degree of Doctor of Philosophy in Biochemistry and Molecular  
Biology

Department of Biochemistry  
FACULTY OF SCIENCE  
Chulalongkorn University  
Academic Year 2020

Copyright of Chulalongkorn University

บทบาทของตัวรับสัญญาณพิษจากแบคทีเรีย และ PIWI-interacting RNA และของกุ้ง  
ขาวแปซิฟิก *Penaeus vannamei* ในการตอบสนองต่อการติดเชื้อ *Vibrio*  
*parahaemolyticus* ก่อโรคตับและตับอ่อนวายเฉียบพลัน



วิทยานิพนธ์นี้เป็นส่วนหนึ่งของการศึกษาตามหลักสูตรปริญญาวิทยาศาสตรดุษฎีบัณฑิต  
สาขาวิชาชีวเคมีและชีววิทยาโมเลกุล ภาควิชาชีวเคมี  
คณะวิทยาศาสตร์ จุฬาลงกรณ์มหาวิทยาลัย  
ปีการศึกษา 2563  
ลิขสิทธิ์ของจุฬาลงกรณ์มหาวิทยาลัย

Thesis Title	ROLES OF BACTERIAL TOXIN RECEPTOR AND PIWI-INTERACTING RNA OF PACIFIC WHITE SHRIMP <i>Penaeus vannamei</i> IN RESPONSE TO <i>Vibrio parahaemolyticus</i> -CAUSING ACUTE HEPATOPANCREATIC NECROSIS DISEASE INFECTION
By	Miss Waruntorn Luangtrakul
Field of Study	Biochemistry and Molecular Biology
Thesis Advisor	Associate Professor KUNLAYA SOMBOONWIWAT, Ph.D.
Thesis Co Advisor	Professor Han-Ching Wang, Ph.D.

---

Accepted by the FACULTY OF SCIENCE, Chulalongkorn University in Partial Fulfillment of the Requirement for the Doctor of Philosophy

Dean of the FACULTY OF SCIENCE

( )

DISSERTATION COMMITTEE

..... Chairman  
 (Associate Professor TEERAPONG BUABOOCHA, Ph.D.)  
 Thesis Advisor  
 (Associate Professor KUNLAYA SOMBOONWIWAT, Ph.D.)  
 Thesis Co-Advisor  
 (Professor Han-Ching Wang, Ph.D.)  
 Examiner  
 (Associate Professor SUPAART SIRIKANTARAMAS, Ph.D.)  
 Examiner  
 (Assistant Professor Surasak Chunsriviro, Ph.D.)  
 External Examiner  
 (Associate Professor Chalernporn Ongvarrasopone, Ph.D.)

จุฬาลงกรณ์มหาวิทยาลัย  
 CHULALONGKORN UNIVERSITY

วรินทร์ เหลืองตระกุล : บทบาทของตัวรับสัญญาณพิษจากแบคทีเรีย และ PIWI-interacting RNA และของกุ้งขาวแปซิฟิก *Penaeus vannamei* ในการตอบสนองต่อการติดเชื้อ *Vibrio parahaemolyticus* ก่อโรคตับและตับอ่อนวายเฉียบพลัน. ( ROLES OF BACTERIAL TOXIN RECEPTOR AND PIWI-INTERACTING RNA OF PACIFIC WHITE SHRIMP *Penaeus vannamei* IN RESPONSE TO *Vibrio parahaemolyticus*-CAUSING ACUTE HEPATOPANCREATIC NECROSIS DISEASE INFECTION) อ.ที่ปรึกษาหลัก : รศ. ดร.กุลชา สมบูรณ์วิวัฒน์, อ.ที่ปรึกษาร่วม : ศ. ดร.ฮานซิง หวัง

การระบาดของโรคตับและตับอ่อนวายเฉียบพลันหรือโรคตายด่วนในกุ้ง เกิดจากแบคทีเรียก่อโรคชนิด *Vibrio parahaemolyticus* AHPND (VP<sub>AHPND</sub>) ส่งผลให้เกิดการสูญเสียผลผลิตกุ้งจำนวนมาก ในงานวิจัยนี้จึงสนใจศึกษาการตอบสนองและหน้าที่ของอิน/โปรตีนและอาร์เอ็นเอขนาดเล็กของระบบภูมิคุ้มกันต่อโรคตายด่วนโดยแบ่งเนื้อหาออกเป็น 2 ส่วน งานวิจัยส่วนแรกทำการค้นหาอินที่คาดว่าเป็นตัวรับสารพิษจาก VP<sub>AHPND</sub> จากข้อมูลทรานสคริปโตมของกุ้งขาวที่ติดเชื้อ VP<sub>AHPND</sub> และขึ้นต้นหน้าที่ในการรับสัญญาณสารพิษนั้น จากที่มีรายงานว่าอะมิโนเปปติเดสเอ็น (Aminopeptidase N; APN) เป็นตัวรับสัญญาณสำหรับสารพิษจาก *Bacillus thuringiensis* CryIA(c) ซึ่งเป็นโปรตีนที่มีโครงสร้างคล้ายกับสารพิษจาก VP<sub>AHPND</sub> (VP<sub>AHPND</sub> toxin) จึงไปค้นหาข้อมูลขึ้นดังกล่าวในฐานข้อมูลพิษ *LvAPN1* และ *LvAPN2* เมื่อศึกษาการแสดงออกของอินพบว่าอิน *LvAPN1* เท่านั้นที่มีการแสดงออกเพิ่มขึ้น ในกระเพาะ ตับและตับอ่อน และเซลล์เม็ดเลือดหลังจากติดเชื้อ VP<sub>AHPND</sub> และหลังจากได้รับ VP<sub>AHPND</sub> toxin จึงเลือกอิน *LvAPN1* มาศึกษาการแสดงออกของอินในกุ้งที่ได้รับ VP<sub>AHPND</sub> toxin พบว่ามีผลทำให้กุ้งมีอัตราการตายสะสม รอยโรคจากการติดเชื้อ และจำนวนแบคทีเรียในกระเพาะหลังจากติดเชื้อ VP<sub>AHPND</sub> ลดลง อีกทั้งเมื่อนำเซลล์เม็ดเลือดไปตรวจสอบสัณฐานวิทยาด้วย scanning electron microscope พบว่าเซลล์เม็ดเลือดไม่ถูกทำลายโดย VP<sub>AHPND</sub> toxin ดังที่พบในกุ้งกลุ่มควบคุมที่เซลล์เม็ดเลือดเกิดความเสียหายอย่างมาก และการศึกษาในระดับโปรตีนพบว่าโปรตีนรีคอมบิแนนท์ *LvAPN1* มีปฏิสัมพันธ์โดยตรงกับโปรตีนรีคอมบิแนนท์ PirA และ PirB ของ VP<sub>AHPND</sub> toxin จากผลการทดลองชี้ให้เห็นว่านอกจากกระเพาะและตับและตับอ่อนแล้ว เซลล์เม็ดเลือดยังเป็นเนื้อเยื่อเป้าหมายของ VP<sub>AHPND</sub> toxin เช่นกัน โดยมี *LvAPN1* เป็นตัวรับสัญญาณพิษจาก VP<sub>AHPND</sub> toxin งานวิจัยส่วนที่สองมีเป้าหมายเพื่อศึกษาการตอบสนองของอาร์เอ็นเอขนาดเล็กชนิด piRNA ต่อการติดเชื้อ VP<sub>AHPND</sub> โดยทำการค้นหา piRNA จากฐานข้อมูลอาร์เอ็นเอขนาดเล็กของกุ้งขาวโดยพบ piRNA ที่มีการแสดงออกตอบสนองต่อการติดเชื้อ VP<sub>AHPND</sub> คล้ายกับในสิ่งมีชีวิตอื่นจำนวน 150 ชนิด และนำไปวิเคราะห์อินเป้าหมายของ piRNA เหล่านี้ พบอินเป้าหมาย 53 อิน ที่มีหน้าที่เกี่ยวข้องกับการแสดงออกของอิน การสังเคราะห์โปรตีน และการสลายโปรตีน เมื่อนำมาวิเคราะห์หา piRNA ที่มีการแสดงออกเปลี่ยนแปลงที่เป็นผลมาจากการติดเชื้อ VP<sub>AHPND</sub> พบว่ามี piRNA 2 ชนิดที่มีการแสดงออกเพิ่มขึ้นและ piRNA อีก 4 ชนิดที่มีการแสดงออกลดลง เมื่อตรวจสอบการแสดงออกของ piRNA ข้างต้นเทียบกับของอินเป้าหมายพบว่ามี piRNA เพียง 2 ชนิด คือ piR-lva-29948104 และ piR-lva-26449194 ที่แสดงออกแบบมีความสัมพันธ์เชิงลบกับอินเป้าหมาย คือ E3 ubiquitin-protein ligase RNF26-like (RNF26) และ circadian locomoter output cycles protein kaput-like (Clock) จึงคาดว่า piRNA ทั้ง 2 ชนิดนี้มีบทบาทในการควบคุมการแสดงออกของอิน การสังเคราะห์โปรตีนและการสลายโปรตีนในกุ้งที่ติดเชื้อ VP<sub>AHPND</sub> จากงานวิจัยนี้ทำให้ต้องค้นคว้าความรู้ใหม่ที่เกี่ยวข้องการทำงานของโปรตีนตัวรับสัญญาณ *LvAPN1* ในการรับสัญญาณพิษ VP<sub>AHPND</sub> toxin และการแสดงออกของ piRNA ที่ตอบสนองต่อการติดเชื้อ VP<sub>AHPND</sub> ซึ่งองค์ความรู้เหล่านี้จะเป็นประโยชน์สำหรับการหาวิธีการในการแก้ไขปัญหาการติดเชื้อ VP<sub>AHPND</sub> ในอุตสาหกรรมเลี้ยงกุ้งได้

สาขาวิชา ชีวเคมีและชีววิทยาโมเลกุล  
ปีการศึกษา 2563

ลายมือชื่อนิสิต .....  
ลายมือชื่อ อ.ที่ปรึกษาหลัก .....  
ลายมือชื่อ อ.ที่ปรึกษาร่วม .....

# # 5872048123 : MAJOR BIOCHEMISTRY AND MOLECULAR BIOLOGY

KEYWORD: Aminopeptidase N, VPAHPND, *Vibrio parahaemolyticus*, VPAHPND toxin, Early mortality syndrome (EMS), Acute Hepatopancreatic Necrosis Disease (AHPND), Small RNA, piRNA, PIWI-interacting RNA, Pacific white shrimp, *Litopenaeus vannamei*

Waruntorn Luangtrakul : ROLES OF BACTERIAL TOXIN RECEPTOR AND PIWI-INTERACTING RNA OF PACIFIC WHITE SHRIMP *Penaeus vannamei* IN RESPONSE TO *Vibrio parahaemolyticus*-CAUSING ACUTE HEPATOPANCREATIC NECROSIS DISEASE INFECTION. Advisor: Assoc. Prof. KUNLAYA SOMBOONWIWAT, Ph.D. Co-advisor: Prof. Han-Ching Wang, Ph.D.

Acute hepatopancreatic necrosis disease (AHPND) or Early mortality syndrome (EMS) caused by virulent strains of *Vibrio parahaemolyticus* AHPND (VP<sub>AHPND</sub>) has been a leading cause of significant losses of shrimp production. In this study, we aim to explore the response and the role of immune-related gene/protein and small RNA in the VP<sub>AHPND</sub>-infected shrimp. This research was divided into 2 parts. In the first part, we identified candidate genes of VP<sub>AHPND</sub> toxin receptor and further confirmed its function as a VP<sub>AHPND</sub> toxin receptor. APN has been reported as a Cry toxin from *Bacillus thuringiensis*, whose structure is similar to VP<sub>AHPND</sub> toxin. Therefore, we identified aminopeptidase N (APN) from the transcriptomic data of VP<sub>AHPND</sub>-infected *Litopenaeus vannamei* hemocyte. According to *Lv*APN1 and *Lv*APN2 gene expression analysis, only *Lv*APN1 were highly upregulated in stomach, hepatopancreas and hemocyte after VP<sub>AHPND</sub> infection and VP<sub>AHPND</sub> toxin injection. Silencing of *Lv*APN1 gene reduced mortality, the clinical signs of AHPND in the hepatopancreas and the number of virulent VP<sub>AHPND</sub> bacteria in the stomach. In addition, observation of hemocyte morphology by scanning electron microscope showed that the *Lv*APN1 silencing prevented severe damage of hemocyte morphology causing by VP<sub>AHPND</sub> toxin like what clearly observed in the control group. At the protein level, r*Lv*APN1 directly bind to the recombinant protein of PirA and PirB toxins. Our results indicated that not only stomach and hepatopancreas, but also hemocytes are the target tissues of VP<sub>AHPND</sub> toxin and act as the VP<sub>AHPND</sub> toxin receptor. The second part aims to study on piRNAs that are expressed in response to VP<sub>AHPND</sub> infection. Firstly, we identified piRNAs from small RNA-Seq data of VP<sub>AHPND</sub>-infected *L. vannamei*. Totally 150 types of piRNA homologs were identified. Target gene identification of those piRNA identified 53 target genes involving in gene expression and protein synthesis/degradation. Six differentially expressed piRNAs (DEPs) were discovered. Two DEPs were upregulated whereas another 4 DEPs were downregulated after VP<sub>AHPND</sub> infection. Expression analysis of DEPs and the target genes showed that only 2 piRNAs such as piR-lva-29948104 and piR-lva-26449194 had the negative expression correlation with their mRNA targets which are E3 ubiquitin-protein ligase RNF26-like (RNF26) and circadian locomotor output cycles protein kaput-like (Clock), respectively. According to target gene's function, these 2 piRNAs might play the role in gene expression and protein synthesis/degradation processes in VP<sub>AHPND</sub>-infected shrimp. Collectively, our study provides the new insight into the role of VP<sub>AHPND</sub> toxin receptor, *Lv*APN1, and the expression of piRNA in response to VP<sub>AHPND</sub> infection. This knowledge will provide alternative strategies for fighting against VP<sub>AHPND</sub> infection in shrimp farming.

Field of Study:	Biochemistry and Molecular Biology	Student's Signature .....
Academic Year:	2020	Advisor's Signature .....
		Co-advisor's Signature .....

## ACKNOWLEDGEMENTS

On the completion of my thesis, I would like to express my deepest gratitude to my superlative supervisor, Assoc. Prof. Kunlaya Somboonwiwat, for her excellent guidance, supervision, encouragement, and supports throughout the study. The great suggestion and discussion with you have become essential keys for developing my research outcome. Especially, I have to thank you very much for your hard effort to teach, improve and inspire me into an efficient researcher.

To Prof. Han-Ching Wang (my co-supervisor), thank you for your warm welcome in National Cheng Kung University as well as your great supports and advice all the time while I was studying in Taiwan. Moreover, I did not only gain a lot of knowledge of science from you but I also got your worth experiences of science that you kindly shared with me. I also would like to thank TLAB members for all their support, suggestion, and discussion on my works in Taiwan.

I also thank Dr. Phattarunda Jaree and Dr. Pakpoom Boonchuen for their suggestion and help to keep me run the experiment smoothly. They always give a hand whenever needed. Thanks to the Marine Shrimp Broodstock Research Center II (MSBRC-2), Charoen Pokphand Foods PCL for providing *V. parahaemolyticus* AHPND strains.

All of my friends (TeamAy and Cems lab members) are greatly appreciated for their helpful suggestions and discussion. Additional great appreciation is extended to Assoc. Prof. Teerapong Buaboocha, Assoc. Prof. Dr. Supaart Sirikantaramas, Asst. Prof Dr. Surasak Chunsrivirod and Assoc. Prof. Dr. Chalernporn Ongvarrasopone for giving me your precious time on being my thesis's defense committee.

I wish to acknowledge the 100th Anniversary Chulalongkorn University Fund for Doctoral Scholarship, and the 90th Anniversary of Chulalongkorn University Fund for my student fellowship as well as the financial supports from the Overseas Research Experience Scholarship for Graduate

Students from the Graduate School, Chulalongkorn University. Financial support from Chulalongkorn University under the Ratchadaphisek Somphot Endowment (CU\_GR\_62\_79\_23\_30) and the Thailand Research Fund (International Research Network Scholar (No. IRN61W0001) are acknowledged. Additional support from the Ministry of Science and Technology, Taiwan (MOST-108-2314-B-006-096-MY3).

Finally, I would like to express my deepest gratitude to indispensable people including my parents and all family members for their guide, understanding, encouragement, endless love, care, and support throughout my lifetime.

Waruntorn Luangtrakul

## TABLE OF CONTENTS

	<b>Page</b>
.....	iii
ABSTRACT (THAI) .....	iii
.....	iv
ABSTRACT (ENGLISH).....	iv
ACKNOWLEDGEMENTS.....	v
TABLE OF CONTENTS.....	vi
LIST OF TABLES.....	ix
LIST OF FIGURES .....	x
CHAPTER I INTRODUCTION.....	1
1.1 Connection between two manuscripts .....	1
1.2 Introduction to the research problem and its significance .....	5
1.2.1 Shrimp aquaculture problem .....	5
1.2.2 VP <sub>AHPND</sub> and pathogenesis .....	5
1.2.3 Shrimp immunity.....	6
1.2.4 RNA interference-based shrimp immunity .....	8
1.2.5 Research significance.....	11
1.3 Objectives .....	11
1.4 Research scope.....	12
1.5 Beneficial outcome from research .....	13
CHAPTER II MANUSCRIPTS.....	13
2.1 Manuscript I.....	13
Cytotoxicity of <i>Vibrio parahaemolyticus</i> AHPND toxin on shrimp hemocytes, a newly identified target tissue, involves binding of toxin to aminopeptidase N1 receptor.....	13
2.1.2 Abstract .....	14
2.1.2 Introduction .....	15

2.1.3 Materials and Methods .....	19
2.1.4 Results .....	31
2.1.4.1 Characterization of the putative LvAPN protein.....	31
2.1.4.2 LvAPN1 is upregulated in response to AHPND .....	34
2.1.4.3 LvAPN1 as a putative VP <sub>AHPND</sub> toxin receptor .....	37
2.1.4.4 LvAPN1 knockdown reduced cell damage in toxin-challenged hemocytes .....	40
2.1.4.5 LvAPN1 plays crucial role in toxin translocation from cell membrane to cytoplasm of hemocytes .....	42
2.1.4.6 LvAPN1 gene silencing reduces the number of AHPND virulence plasmids in stomach.....	43
2.1.4.7 ELISA assay of protein-protein interactions between LvAPN1 and the PirA <sup>VP</sup> and PirB <sup>VP</sup> toxins.....	44
2.1.5 Discussion .....	46
2.2 Manuscript II .....	52
Identification of novel shrimp PIWI-interacting RNA (piRNA) involved in <i>Vibrio parahaemolyticus</i> AHPND infection .....	52
2.2.1 Abstract .....	53
2.2.2 Introduction .....	54
2.2.3 Materials and Methods .....	57
2.2.4 Results .....	63
2.2.4.1 Sequence analysis of shrimp piRNAs .....	63
2.2.4.2 Differentially expressed piRNAs (DEPs) in NHS-treated and NLHS-treated <i>L. vannamei</i> upon VP <sub>AHPND</sub> challenge.....	67
2.2.4.3 RT-qPCR validation of significant differentially expressed piRNAs (DEPs) .....	69
2.2.4.4 Target gene of upregulated- piRNA in response to VP <sub>AHPND</sub> infection .....	72
2.2.4.5 Validation of target gene expression .....	76
2.2.5 Discussion .....	78



CHAPTER III CONCLUSIONS .....	83
3.1 Conclusions.....	83
3.1.1 Cytotoxicity of <i>Vibrio parahaemolyticus</i> AHPND toxin on shrimp hemocytes, a newly identified target tissue, involves binding of toxin to aminopeptidase N1 receptor.....	83
3.1.2 Identification of novel shrimp PIWI-interacting RNA (piRNA) involved in <i>Vibrio parahaemolyticus</i> AHPND infection .....	84
3.2 Research limitations.....	84
3.3 Suggestions in research or perspective for further research .....	85
REFERENCES .....	87
VITA.....	95



## LIST OF TABLES

		<b>Page</b>
<b>Table 1</b>	Primers used for qRT-PCR, dsRNA synthesis and recombinant protein expression.....	21
<b>Table 2</b>	Primers used for the first-strand cDNA synthesis of piRNAs and qRT-PCR.....	62
<b>Table 3</b>	Primers used for top3 target genes of interesting piRNA in qRT-PCR.....	63
<b>Table 4</b>	Summary of sequences identified from small RNA libraries	67
<b>Table 5</b>	List of differentially expressed piRNAs.....	70
<b>Table 6</b>	List of six VP <sub>AHPND</sub> responsive DEPs and its top3 target genes	74

## LIST OF FIGURES

		<b>Page</b>
<b>Figure 1</b>	<i>Lv</i> APN1 characteristics analysis.....	32
<b>Figure 2</b>	Characterization of the putative <i>Lv</i> APN1 protein.....	33
<b>Figure 3</b>	Partially purification of VP <sub>AHPND</sub> toxin.....	35
<b>Figure 4</b>	Expression of the <i>Lv</i> APN1 gene upon VP <sub>AHPND</sub> and..... VP <sub>AHPND</sub> toxin challenges.....	36
<b>Figure 5</b>	The effect of <i>Lv</i> APN1 silencing in AHPND-causing..... bacteria pathogenesis.....	38
<b>Figure 6</b>	The mRNA expression levels of the <i>Lv</i> APN2 gene in..... hemocyte of <i>Lv</i> APN1 knockdown shrimp.....	39
<b>Figure 7</b>	The effect of <i>Lv</i> APN1 silencing on shrimp hemocyte..... homeostasis.....	41-42
<b>Figure 8</b>	Reducing of AHPND-causing bacteria plasmid in stomach... of <i>Lv</i> APN1 silenced shrimp.....	44
<b>Figure 9</b>	Recombinant protein purification analysis	46
<b>Figure 10</b>	Binding ability of rPirA <sup>VP</sup> and rPirB <sup>VP</sup> on immobilized..... recombinant truncated <i>Lv</i> APN1-His determined by ELISA...	47
<b>Figure 11</b>	Schematic representation of AHPND pathogenesis showing... the proposed role of <i>Lv</i> APN1 in hemocyte.....	52
<b>Figure 12</b>	Length distribution, abundance and composition of small RNA size of 24 to 31 nt from libraries of VP <sub>AHPND</sub> -infected..... NHS-treated and VP <sub>AHPND</sub> -infected NLHS-treated..... <i>L. vannamei</i> hemocytes.....	66
<b>Figure 13</b>	piRNA characteristics.....	67
<b>Figure 14</b>	Differential expression of piRNA.....	69
<b>Figure 15</b>	Relative expression analysis of piRNAs in response to.....	

	VP <sub>AHPND</sub> infection in <i>L. vannamei</i> hemocytes.....	72
<b>Figure 16</b>	Network analysis for piRNA/mRNA interaction.....	75
<b>Figure 17</b>	piRNA/mRNA interaction analysis	76-77
<b>Figure 18</b>	Relative expression analysis of target genes in the.....	
	VP <sub>AHPND</sub> infection.....	78



# CHAPTER I

## INTRODUCTION

### 1.1 Connection between two manuscripts

Shrimp innate immunity rapidly respond to invading microbes through intracellular signaling cascades which lead to the activation of cellular and humoral immune responses (Tassanakajon, Somboonwiwat, Supungul, & Tang, 2013). The humoral responses are mediated by macromolecules in hemolymph. The important humoral responses are the melanin synthesized through the prophenoloxidase (proPO) system, the blood clotting system and the generation of circulating antimicrobial peptides (AMPs). On the other hand, the cellular responses, particularly those in the circulating system are apoptosis, phagocytosis, nodule formation and encapsulation of the intruders (Flegel & Sritunyalucksana, 2011). Therefore, the majorities of the defense and homeostasis mechanisms are carried out in the hemolymph and the cells that are involved called “hemocytes” (Soderhall, Bangyeekhun, Mayo, & Soderhall, 2003). During the past few decades, shrimp production has declined due to the emergence of a bacterial disease called acute hepatopancreatic necrosis disease (AHPND) or Early mortality syndrome (EMS) causing by *Vibrio parahaemolyticus* ( $VP_{AHPND}$ ), which is a common halophilic gram-negative bacterium become a new virulent strain by acquiring the plasmid pVA1 producing PirAB<sup>VP</sup> binary toxin which is so called  $VP_{AHPND}$  toxin in this research (Han, Tang, Tran, & Lightner, 2015; Kondo et al., 2014).  $VP_{AHPND}$  infection causes high mortality in shrimp (70–100% in *Penaeus monodon* and *Litopenaeus vannamei*). PirAB<sup>VP</sup> proteins have been identified as the

virulence factor of AHPND (Lee et al., 2015; Tinwongger et al., 2016). The protein structure of PirAB<sup>VP</sup> toxin is very similar to that of Cry toxin, which are produced by *Bacillus thuringiensis* (Lee et al., 2015). The target tissue of AHPND is obviously the hepatopancreas, which displays hemolytic infiltration and cell sloughing post infection (Tran et al., 2013). In addition, PirAB<sup>VP</sup> were detected in the hepatopancreas, stomach and hemolymph of *L. vannamei* that had been infected with VP<sub>AHPND</sub> (Lai et al., 2015). Recently, there are several reports on shrimps exhibit an innate immune response against VP<sub>AHPND</sub> infections. Transcriptomics studies of VP<sub>AHPND</sub>-infected shrimp hemocytes and stomach have yielded a list of differentially expressed immune genes on various immune pathways, including penaeidins, crustins, serpins, lectins and antilipoplysaccharide factors (Maralit, Jaree, Boonchuen, Tassanakajon, & Somboonwiwat, 2018; Soonthornchai et al., 2016). The single-WAP domain-containing protein (SWD) is a type III crustin antimicrobial peptide that acts as a proteinase inhibitor for subtilisin in *L. vannamei* and also was upregulated in hemocytes of AHPND-infected shrimps (Visetnan, Supungul, Tassanakajon, Donpuksa, & Rimphanitchayakit, 2017). In addition, haemocyanin is a protein involved in the storage and transport of oxygen in shrimp haemolymph. However, a recent report suggests that it also shows an antibacterial immune response in *L. vannamei* specifically the agglutination of VP<sub>AHPND</sub> (Boonchuen, Jaree, Tassanakajon, & Somboonwiwat, 2018). Among the identified genes, the host receptor to VP<sub>AHPND</sub> toxin have not been identified.

The knowledge of VP<sub>AHPND</sub> infection mechanism and how the shrimp immune system response to VP<sub>AHPND</sub> infection is essential for the development of effective and efficient management strategies for the disease. Thus, in this study, we analyzed the

transcriptome data including RNA-Seq and small RNA-Seq data from hemocyte of *L. vannamei* challenged with VP<sub>AHPND</sub> reported previously by Boonchuen et al. (2020) to identify and characterize VP<sub>AHPND</sub> toxin receptor and VP<sub>AHPND</sub>- responsive PIWI-interacting RNA (piRNA), respectively (Boonchuen, Maralit, Jaree, Tassanakajon, & Somboonwiwat, 2020). In the first manuscript, we identified the candidate genes of VP<sub>AHPND</sub> toxin receptor from RNA-Seq, and its function has been elucidated. First, amino acid sequences of the candidate genes were analyzed for structural features such as transmembrane domain, the peptidase-M1 domain, Cry toxin binding region. Then, gene expression levels after VP<sub>AHPND</sub> infection and the partially purified VP<sub>AHPND</sub> toxin injection were validated in stomach, hepatopancreas and hemocytes by qRT-PCR. To study the function of the candidate VP<sub>AHPND</sub> toxin receptor in VP<sub>AHPND</sub>-infected shrimp, the candidate gene was silenced by RNA interference technique and observed shrimp mortality as well as clinical sign of AHPND in hepatopancreas after VP<sub>AHPND</sub> toxin challenge. Moreover, we detected the number of VP<sub>AHPND</sub> virulence plasmids in stomach to investigate the effect on bacterial colonization. It is well known that hemocyte is a major immune tissue producing various immune effectors to fight against infection. We would like to know whether shrimp hemocyte is another target tissue of VP<sub>AHPND</sub>. The hemocyte morphology of VP<sub>AHPND</sub> toxin-challenge shrimp after VP<sub>AHPND</sub> toxin receptor gene silencing was observed under scanning electron microscope. Also, the total hemocyte count as well as hemocyte cell viability were counted. To study the effect of VP<sub>AHPND</sub> toxin receptor gene silencing on VP<sub>AHPND</sub> toxin localization on hemocyte cell, we performed the immunofluorescence. Furthermore, ELISA assay was performed to confirm the interaction between rPirAB<sup>VP</sup> toxin and the candidate genes of VP<sub>AHPND</sub> toxin receptor. This finding provides the crucial information about how

VP<sub>AHPND</sub> toxin damage shrimp hemocyte which deepen our understanding in VP<sub>AHPND</sub> pathogenesis mediated by VP<sub>AHPND</sub> toxin/host cell interaction.

During VP<sub>AHPND</sub> infection, several shrimp immune pathways including RNA interference (RNAi) respond to VP<sub>AHPND</sub> infection. It is known that small RNA such as microRNA (miRNA) and PIWI-interacting RNA (piRNA) are key molecules of RNAi pathway that regulate gene expression in biological processes including immune pathway. Recently, Boonchuen et al. (2020) reported the functional roles of miRNAs in shrimp immunity involving in prophenoloxidase-activating system, hemocyte homeostasis, and antimicrobial peptide production, and these responses enhance VP<sub>AHPND</sub> resistance in *L. vannamei*. piRNA pathway is a conserved small RNA system that protects animal germ cell genomes from the harmful effects of transposon mobilization (Czech et al., 2018; Toth, Pezic, Stuwe, & Webster, 2016). Therefore, in the second manuscript we reanalyzed the small RNA-Seq data and identified piRNAs that are expressed in response to VP<sub>AHPND</sub> infection. Homologs of piRNA were identified according to size range from 24-31 nucleotides and piRNA characteristics which are 5' uridine at position 1 and adenine at position 10. The differentially expressed piRNA were identified and confirmed for their expression in the VP<sub>AHPND</sub>-infected shrimp. We explore their target genes to predict their function during VP<sub>AHPND</sub> infection to further elucidate the involvement of piRNA pathway in gene regulation during VP<sub>AHPND</sub> infection. These two manuscripts highlight the new finding of function of a protein act as VP<sub>AHPND</sub> toxin receptor and piRNAs as gene regulators in the hemocyte of VP<sub>AHPND</sub>-infected shrimp.



## 1.2 Introduction to the research problem and its significance

### 1.2.1 Shrimp aquaculture problem

Shrimp farming is an important aquaculture industry in many countries. Thailand has been the world's leading exporter of cultured shrimp since 1992 (Wyban, 2007). Unfortunately, the production of the black tiger shrimp *P. monodon* had rapidly been decreased because the outbreaks of bacterial and viral diseases (Mohan et al., 1998). Due to the serious problems of the black tiger shrimp production loss, Thailand had changed to culture the pacific white shrimp, *L. vannamei*. However, shrimp farming has been continuing affected by serious infectious disease outbreaks caused mainly by viruses and bacteria especially the white spot syndrome virus (WSSV) and *Vibrio* species. Shrimp production in Thailand has decreased rapidly near 50 percent in 2013 because of Acute hepatopancreatic necrosis disease (AHPND) or early mortality syndrome (EMS). Although, the early diagnosis and detection of AHPND makes better control and prevention of AHPND in shrimp farm, the effective treatment for AHPND is urgently required.

### 1.2.2 VP<sub>AHPND</sub> and pathogenesis

AHPND was caused only by strains of *V. parahaemolyticus* that possessed an extrachromosomal plasmid encoding the binary toxin PirA<sup>VP</sup> and PirB<sup>VP</sup>. This virulence plasmid is pVA1 with size of ~69 kbp. The pVA1 plasmid includes conjugative transfer and plasmid mobilization genes that make the plasmid self-transmissible (Tran et al., 2013). *V. parahaemolyticus* is initially colonizes only the shrimp stomach then the PirA<sup>VP</sup>/PirB<sup>VP</sup> binary toxin (PirAB<sup>VP</sup> toxin), which show structural similarities to the *Bacillus* Cry insecticidal proteins, are secreted into the extracellular environment

causing the hepatopancreas damage leading to shrimp death (Han et al., 2015; Lai et al., 2015; Lin et al., 2014). It has further been shown that the virulence of VP<sub>AHPND</sub> depends on the amount of PirAB<sup>VP</sup> toxin released and not on the gene copy number of the plasmid (Tinwongger et al., 2016). Histological examinations further showed that PirAB<sup>VP</sup> toxins caused shrimp HP cell death and led to the characteristic sloughing of the damaged epithelial cells into the HP Tubules (Lai et al., 2015). Recently, Kumar et al (2019) reported that PirAB<sup>VP</sup> toxins bind to the digestive tract of brine shrimp larvae and seem to be responsible for generating characteristic AHPND lesions and damaging enterocytes in the midgut and hindgut regions (Kumar et al., 2019). In addition, it was found that not only digestive tract was affected by PirB<sup>VP</sup>, but PirB<sup>VP</sup> interact with histones in shrimp hemocytes leading to cell apoptosis (Z. Zheng et al., 2021).

As stated before, the structure of PirAB<sup>VP</sup> toxin is similar to *Bacillus thuringiensis* Cry toxins, in which its interaction with aminopeptidase N (APN) receptor leading to cell damage. In case of the *B. thuringiensis* Cry toxin, the initial interaction is between domain III of Cry1A toxin and the GalNAc sugar on the APN receptor, and this facilitates further binding of domain II to another region of the same receptor (Lee et al., 2015; Xu, Wang, Yu, & Sun, 2014). This binding promotes the localization and accumulation of additional molecules of the activated toxins. The toxin oligomer then inserts into the membrane, leading to pore formation and cell lysis. (Xu et al., 2014).

### 1.2.3 Shrimp immunity

Major defense systems of shrimp are carried out in the hemolymph containing cells called hemocytes producing many immune effectors. Shrimp immunity is innate

immunity that can be divided into 2 groups of cellular and humoral immunities. The humoral responses of shrimp are the important part of shrimp immune defense system for they are a first line of defense against pathogens. To prevent the loss of hemolymph upon such injury and the invasion of infected microorganisms, the rapid blood coagulation system at the site of injury is a prominent immune mechanism (Yeh, Kao, Huang, & Tsai, 2006). The responses to microbial infections are rapid and very strong involving the secretion of immune proteins from the granular hemocytes into the circulating system and, then, the re-synthesis of said proteins in the immune cells. The humoral responses arise when the extracellular signal molecules from pathogens, such as the pathogen-associated molecular patterns (PAMPs) or the viral protein antigens, are detected by cell-surface receptors or pattern recognition proteins (PRPs) resulting in the activation of NF- $\kappa$ B signaling pathways (Janeway, 2013; F. Li & Xiang, 2013). Melanization by the activation of proPO system is the major innate immune responses in shrimp. Upon infection, pathogens are recognized by host PRRs and this leads to activation of serine proteinase cascade resulting in melanin formation around invading microorganisms (Amparyup, Promrungreang, Charoensapsri, Sutthangkul, & Tassanakajon, 2013). The JAK/STAT signaling pathway involve in antiviral immunity that mediate signal transduction response to control the WSSV immediate early gene (*ie1*) transcription (F. Liu, Li, Liu, & Li, 2017). The activation triggers the secretion of circulating antimicrobial peptides and other immune proteins to eradicate the infection.

The shrimp immune system exhibits an innate immune response against bacterial infection. Junprung et al. (2017) found that non-lethal heat shock induced the expression of heat shock proteins HSP70 and HSP90 in *L. vannamei*. These HSPs regulated the immune genes proPO and crustin and caused VP<sub>AHPND</sub> tolerance in

shrimps (Junprung, Supungul, & Tassanakajon, 2017). The penlectin5 protein was induced during VP<sub>AHPND</sub> infection (Angthong, Roytrakul, Jarayabhand, & Jiravanichpaisal, 2017). Also, haemocyanin which is a protein involved in the storage and transport of oxygen in shrimp haemolymph was reported as an antibacterial immune response specifically the agglutination of VP<sub>AHPND</sub> (Boonchuen et al., 2018).

#### 1.2.4 RNA interference-based shrimp immunity

Recently, the role of RNA interference (RNAi) pathway mediated by small non-coding RNAs in AHPND has been widely researched. In general, RNAi can be mediated by siRNA, miRNA or piRNA. For siRNA-mediated RNAi, the exogenous dsRNAs, repetitive sequences and transcripts that can form long hairpins, are processed by Dicer into siRNA duplex (Caplen & Mousset, 2003). Then, the siRNA duplex forms the precursor RNAi-induced silencing complex (pre-RISC) with Ago protein. The mature RISC eventually targets the complementary mRNAs, leading to translational repression (Caplen & Mousset, 2003). In *Marsupenaeus japonicus*, it is reported that Dicer2 and Ago2 proteins are required for the biogenesis and function of siRNA in *M. japonicus* shrimp. The knockdown of Dicer2 can promote virus infection in shrimp (T. Huang & Zhang, 2013).

In the miRNA-mediated RNAi pathway, miRNAs are derived from the endogenous noncoding RNA transcripts that fold into stem-loop structures. Firstly, primary miRNAs (pri-miRNAs) are transcribed from the genome and then trimmed by Drosha called pre-miRNA. Subsequently, the pre-miRNAs are transported into cytoplasm and processed into miRNA duplexes by Dicer. The miRNA duplex is

denatured leading to a mature RNA that subsequently bind to RISC complex containing Ago protein. The mature miRNA directs the complex to the target mRNA for post-transcriptional gene silencing (Carthew & Sontheimer, 2009). In *M. japonicus*, it has been reported that shrimp miRNAs can promote cellular phagocytosis and apoptosis via targeting specific genes, resulting in the suppression of virus infection. It is also found that shrimp miRNA can simultaneous activate multiple immune pathways to suppress virus infection (Shu & Zhang, 2017). Previously, next generation sequencing of WSSV-infected *Penaeus monodon* hemocyte revealed differentially expressed miRNA responding to WSSV infection. Their mRNA target is involved in several immune-related genes such as genes encoding antimicrobial peptides, signaling transduction proteins, oxidative stress proteins, proteinases or proteinase inhibitors, proteins in blood clotting system, apoptosis-related proteins and other immune molecules (Kaewkascholkul et al., 2016). In case of bacterial infection, miRNA expression studies in response to various bacterial infections have revealed common miRNAs as key players in the host innate immune response (Eulalio, Schulte, & Vogel, 2012). For example, miR-146 along with miR-155, were found to be coordinately unregulated in immune cells in response to various bacterial pathogens, including *Salmonella enteric* (Sharbati, Sharbati, Hoeke, Bohmer, & Einspanier, 2012) *Mycobacterium* species (Spinelli et al., 2013), and *Francisella tularensis* (Cremer et al., 2019). Recently, a comparative transcriptomic analysis of *L. vannamei* hemocyte infected with VP<sub>AHPND</sub> and non-VP<sub>AHPND</sub> was used to identify miRNA candidates that dysregulated during VP<sub>AHPND</sub> infection. These miRNAs were involved in the immune system, metabolism and apoptosis pathways (H. Zheng, Guo, Zheng, Cheng, & Huang, 2018). A VP<sub>AHPND</sub>-responsive miRNAs such as lva-miR-4850 has been characterized

recently as a suppressor of proPO2 (PO2) and proPO activating factor 2 (PPAF2) genes and down regulation of lva-miR-4850 in the VP<sub>AHPND</sub>-infected shrimp resulting in proPO activation. (Boonchuen, Jaree, Somboonviwat, & Somboonwiwat, 2021).

piRNA is the largest class of small non-coding RNAs (~24-31 nucleotides) that form RNA-protein complexes through interactions with PIWI proteins. These complexes repress transposons via transcriptional or posttranscriptional mechanisms and maintain germline genome integrity, particularly those in spermatogenesis. piRNA is a small single stranded RNA with a 5' end containing a monophosphate group and a strong uracil bias, and its 3' end 2-OH is methylated (Hirakata & Siomi, 2016). piRNA is mainly found in the intergenic region and has the characteristics of a clustering distribution, while it is relatively rarely found in the gene region (Iwasaki, Siomi, & Siomi, 2015). In *Drosophila*, the piRNA in germ cells was processed from lncRNA precursors with the participation of the Zucchini nuclease (H. Huang et al., 2014). After primary piRNA passes through the nuclear membrane to the cytoplasm, the Aub and AGO3 endonuclease Slicer activate the activity of the PIWI endonuclease (Wang et al., 2015). They then cleave the RNA to form secondary piRNA and amplify the piRNA in cells by a mechanism called the “Ping-Pong” cycle. So far, studies have highlighted the importance of the piRNA pathway as a germline-specific mechanism. However, recently the somatic function of the piRNA pathway has been verified in at least 12 insect species, as well as other arthropods (Lewis et al., 2018). Though the central and conserved function of the piRNA pathway seems to be TE repression. The role of piRNAs in regulating host gene expression is identified. Since the discovery of piRNA pathway, there have been reported host protein-coding genes regulating by *Drosophila*

piRNAs in development and stem cell (Rojas-Rios & Simonelig, 2018). In the present day, thousands of piRNAs have been identified in several organisms including invertebrates such as *Drosophila melanogaster* (Khurana et al., 2011), *Pinctada fucata* (S. Huang et al., 2019) and *Biomphalaria glabrata* (Queiroz et al., 2020) but not in shrimp through the application of high-throughput sequencing technologies.

### 1.2.5 Research significance

Study on shrimp innate immune response against VP<sub>AHPND</sub> infection in term of molecular interaction between host receptor and the bacterial virulent factor and the gene regulation by piRNA, will provide the crucial information for the development of methods to solve AHPND outbreak. Identification of VP<sub>AHPND</sub> toxin receptor expressed on the major immune cells like hemocyte and determination if hemocyte is also affected VP<sub>AHPND</sub> toxin could provide as a clue to prevent the damage effect of toxin by inhibiting by expression of VP<sub>AHPND</sub> toxin receptor. Moreover, piRNA and the target genes that plays role during VP<sub>AHPND</sub> infection identified for the first time in shrimp in the role of piRNAs in shrimp immune response against VP<sub>AHPND</sub> infection. This study might shed light on how VP<sub>AHPND</sub> toxin induces severe damage to the shrimp cell and the shrimp response to VP<sub>AHPND</sub> infection.

## 1.3 Objectives

1.3.1 To identify and characterize candidate VP<sub>AHPND</sub> toxin receptor from the VP<sub>AHPND</sub>- infected *L. vannamei* hemocyte transcriptome database

1.3.2 To identify piRNAs and target gene in shrimp immune response against *Vibrio parahaemolyticus* AHPND infection

## 1.4 Research scope

### 1.4.1 Cytotoxicity of *Vibrio parahaemolyticus* AHPND toxin on shrimp hemocytes, a newly identified target tissue, involves binding of toxin to aminopeptidase N1 receptor

This part aims to identify of the VP<sub>AHPND</sub> toxin receptor gene from the VP<sub>AHPND</sub>-infected *L. vannamei* transcriptome database by bioinformatic approaches. Also, the effect of VP<sub>AHPND</sub> toxin on *Lv*APN1-silenced shrimp was determined by observing shrimp mortality upon VP<sub>AHPND</sub> infection, hemocyte morphology on scanning electron microscope (SEM), total hemocyte counts (THC) and VP<sub>AHPND</sub> toxin localization on shrimp hemocyte. Furthermore, the number of binary Pir toxin producing plasmid in *Lv*APN1-silenced shrimp stomach during VP<sub>AHPND</sub> infection was measured to investigate the effect of *Lv*APN1 knockdown on bacterial colonization on stomach as well as the clinical sign of AHPND in hepatopancreas. Moreover, the interaction between *Lv*APN1 and PirAB<sup>VP</sup> toxin was confirmed by ELISA assay.

### 1.4.2 Identification of novel shrimp PIWI-interacting RNA (piRNA) involved in *Vibrio parahaemolyticus* AHPND infection

This project aims to gain more insight into the knowledge of small RNA function in shrimp immunity against VP<sub>AHPND</sub> infection. We identified piRNA from small RNA-Seq of VP<sub>AHPND</sub>-infected shrimp hemocyte and identified their protein-coding genes target from transcribed *L. vannamei* genome. In addition, expressed correlation of piRNA and their target in VP<sub>AHPND</sub>-infected shrimp hemocyte was determined to show the implication of piRNA in gene expression regulation during VP<sub>AHPND</sub> infection.



## 1.5 Beneficial outcome from research

Due to the decline of Thai shrimp production from the spread of AHPND, the effective strategies to cope with the disease is urgent needed. Our research provides the useful information on what the receptor of VP<sub>AHPND</sub> toxin is. In addition, the new target tissue of VP<sub>AHPND</sub> toxin was identified. Moreover, in terms of small RNA expression in response to VP<sub>AHPND</sub> infection, our research identified shrimp VP<sub>AHPND</sub>-responsive piRNAs and its target genes that might be the regulator for gene expression during VP<sub>AHPND</sub> infection. The knowledge obtained can be used to develop an effective control strategy to prevent VP<sub>AHPND</sub> infection in shrimp. This will be profit to shrimp aquaculture leads to sustainability of the industry.



**CHAPTER II**  
จุฬาลงกรณ์มหาวิทยาลัย  
**CHULALONGKORN UNIVERSITY**  
**MANUSCRIPTS**

### 2.1 Manuscript I

**Cytotoxicity of *Vibrio parahaemolyticus* AHPND toxin on shrimp hemocytes, a newly identified target tissue, involves binding of toxin to aminopeptidase N1 receptor**

**(Published on Journal of Plos Pathogens. 26 March, 2021. Volume 17. Page e1009463.)**

**[Impact factor: 6.218 (Teir1)]**

Waruntorn Luangtrakul<sup>1</sup>, Pakpoom Boonchuen<sup>1,2</sup>, Phattarunda Jaree<sup>3</sup>, Ramya Kumar<sup>4,5</sup>, Han-Ching Wang<sup>4,5\*</sup>, Kunlaya Somboonwiwat<sup>1\*</sup>

<sup>1</sup>Center of Excellence for Molecular Biology and Genomics of Shrimp, Department of Biochemistry, Faculty of Science, Chulalongkorn University, Bangkok, Thailand.

<sup>2</sup>School of Biotechnology, Institute of Agricultural Technology, Suranaree University of Technology, Mueang, Nakhon Ratchasima, Thailand

<sup>3</sup> Center of Applied Shrimp Research and Innovation, Institute of Molecular Biosciences, Mahidol University, Salaya, Nakhon Pathom, Thailand

<sup>4</sup>Department of Biotechnology and Bioindustry Sciences, College of Biosciences and Biotechnology, National Cheng Kung University, Tainan, Taiwan

<sup>5</sup>International Center for the Scientific Development of Shrimp Aquaculture, National Cheng Kung University, Tainan, Taiwan

**\*Corresponding author: Kunlaya Somboonwiwat**

## 2.1.2 Abstract

Acute hepatopancreatic necrosis disease (AHPND) caused by PirAB<sup>VP</sup>-producing strain of *Vibrio parahaemolyticus*, VP<sub>AHPND</sub>, has seriously impacted the shrimp production. Although the VP<sub>AHPND</sub> toxin is known as the VP<sub>AHPND</sub> virulence factor, a receptor that mediates its action has not been identified. An in-house transcriptome of *Litopenaeus vannamei* hemocytes allows us to identify two proteins from the aminopeptidase N family, LvAPN1 and LvAPN2, the proteins of which in insect are known to be receptors for Cry toxin. The membrane-bound APN, LvAPN1, was characterized to determine if it was a VP<sub>AHPND</sub> toxin receptor. The increased

expression of *Lv*APN1 was found in hemocytes, stomach, and hepatopancreas after the shrimp were challenged with either VP<sub>AHPND</sub> or the partially purified VP<sub>AHPND</sub> toxin. *Lv*APN1 knockdown reduced the mortality, histopathological signs of AHPND in the hepatopancreas, and the number of virulent VP<sub>AHPND</sub> bacteria in the stomach after VP<sub>AHPND</sub> toxin challenge. In addition, *Lv*APN1 silencing prevented the toxin from causing severe damage to the hemocytes and sustained both the total hemocyte count (THC) and the percentage of living hemocytes. We found that the r*Lv*APN1 directly bound to both rPirA<sup>VP</sup> and rPirB<sup>VP</sup> toxins, supporting the notion that silencing of *Lv*APN1 prevented the VP<sub>AHPND</sub> toxin from passing through the cell membrane of hemocytes. We concluded that the *Lv*APN1 was involved in AHPND pathogenesis and acted as a VP<sub>AHPND</sub> toxin receptor mediating the toxin penetration into hemocytes. Besides, this was the first report on the toxic effect of VP<sub>AHPND</sub> toxin on hemocytes other than the known target tissues, hepatopancreas and stomach.

**Keywords:** Aminopeptidase N1; *Litopenaeus vannamei*; Acute hepatopancreatic necrosis disease (AHPND); *Vibrio parahaemolyticus* causing AHPND (VP<sub>AHPND</sub>); VP<sub>AHPND</sub> toxin receptor

### 2.1.2 Introduction

Acute hepatopancreatic necrosis disease (AHPND), initially referred to as early mortality syndrome (EMS), has caused severe mortalities in farmed penaeid shrimp throughout Southeast Asia including China in 2009 before it spread to Vietnam in early 2011 and Thailand in late 2011 (Flegel, 2012; Lightner et al., 2012) AHPND can cause up to 100% mortality within 30 days after stocking, and has also resulted in production losses of more than US \$1 billion per year in the Asian shrimp farming industry (De

Schryver, Defoirdt, & Sorgeloos, 2014). The causative agent of AHPND was found to be a specific strain of the Gram-negative halophilic marine bacterium *Vibrio parahaemolyticus* (Tran et al., 2013). AHPND-causing bacteria initially colonize in the stomach of infected shrimp (Lai et al., 2015; Tran et al., 2013) to produce observable symptoms that include lethargy, an empty stomach and midgut, and pale to white atrophied hepatopancreas. Histological analysis of the hepatopancreas reveals sloughing of tubule epithelial cells in the early stage of AHPND and massive hemocytic infiltration in the late stage of infection (Nunan, Lightner, Pantoja, & Gomez-Jimenez, 2014; Soto-Rodriguez, Gomez-Gil, Lozano-Olvera, Betancourt-Lozano, & Morales-Covarrubias, 2015; Tran et al., 2013).

All AHPND-causing *V. parahaemolyticus* strains carry a virulent pVA1 plasmid (VP<sub>AHPND</sub>) which encodes the binary toxins PirA<sup>VP</sup> and PirB<sup>VP</sup>. These toxins are homologous to the *Photobacterium luminescens* insect-related (Pir) toxins (Lee et al., 2015), and they are secreted into the extracellular environment. Reverse gavage experiments have shown that the bacteria-free supernatant of the bacterial culture is sufficient to induce typical AHPND symptoms (Tran et al., 2013), and in fact that AHPND-like symptoms can be produced by the reverse gavage injection of purified recombinant PirB<sup>VP</sup> toxin alone (Lee et al., 2015).

An analysis of the binary toxins crystal structure found that *V. parahaemolyticus* PirA<sup>VP</sup> and PirB<sup>VP</sup> form a heterodimer and that the overall structural topology of the PirAB<sup>VP</sup> toxins is very similar to that of *Bacillus thuringiensis* crystal insecticidal (Cry) toxin (Lee et al., 2015). This similarity suggested that the putative PirAB<sup>VP</sup> heterodimer might have similar functional domains to the Cry protein, with the N-terminal domain of PirB<sup>VP</sup> corresponding to Cry domain I (pore-forming activity), the C-terminal domain

of PirB<sup>VP</sup> corresponding to Cry domain II (receptor binding), and PirA<sup>VP</sup> corresponds to Cry domain III, which is thought to be related to receptor recognition and membrane insertion (Soberon et al., 2010; Xu et al., 2014). In the case of the *B. thuringiensis* Cry toxin, cell death is induced by a series of processes which include receptor binding, oligomerization and pore forming (Xu et al., 2014). Briefly, the initial interaction is between domain III of Cry1A toxin and the GalNAc sugar on the aminopeptidase N (APN) receptor, and this facilitates further binding of domain II to another region of the same receptor (Lee et al., 2015; Soberon et al., 2010; Xu et al., 2014). This binding promotes the localization and accumulation of additional molecules of the activated toxins. This assemblage of toxins then binds to another receptor, cadherin, and this promotes the proteolytic cleavage of the toxin's N-terminal  $\alpha$ 1 helix. This cleavage in turn induces the formation of the pre-pore oligomer and increases the oligomer binding affinity to the glycosylphosphatidylinositol (GPI)-anchored APN and alkaline phosphatase (ALP) receptors. The oligomer then inserts into the membrane, leading to pore formation and cell lysis (Xu et al., 2014). The PirAB<sup>VP</sup> toxins are known to mainly target the shrimp hepatopancreas. Recently, it was found that, in the brine shrimp larvae, PirAB<sup>VP</sup> toxin challenge induced damage to the digestive tract upon binding to epithelial cells and produces characteristic symptoms of AHPND. The extensive necrosis and damages epithelial cells in the midgut and hindgut regions, resulting in pyknosis, cell vacuolisation, and mitochondrial and rough endoplasmic reticulum (RER) damage (Kumar et al., 2019). However, while the PirAB<sup>VP</sup> binary toxins is thought to use a mechanism that is similar to that of the Cry pore forming toxin, the details of this mechanism remain unclear. In the present study we therefore investigate

the role of APN, which is one of the receptors that are already known to be central to this process in insects.

The APN family is composed of a class of zinc metalloproteinases that preferentially cleave single neutral amino acids from the N-terminus of polypeptides (Pigott & Ellar, 2007). APNs are major proteins in the midgut of insect larvae, where they occur either as soluble enzymes or in association with the microvillar membrane (Terra et al., 1994). APNs are involved in several functions in a wide range of species. For example, APNs in the lepidopteran larval midgut play an important role in the digestion of dietary protein (Wang et al., 2015). The typical features present in classical lepidopteran APNs include a potential signal peptide at the N-terminus, a characteristic zinc-binding motif HEXXH(X)<sub>18</sub>E essential for their enzymatic activity, a highly conserved GAMEN motif forming part of the active site and a GPI anchor signal sequence at the C-terminal attaching them to the membrane (Hooper, 1994; Pigott & Ellar, 2007).

In the present study, we retrieved *Lv*APN1 and *Lv*APN2 sequences from our transcriptomic database of VP<sub>AHPND</sub>-challenged *Litopenaeus vannamei* hemocytes (Boonchuen et al., 2020). Gene expression of *Lv*APN1 was analyzed after challenge with AHPND-causing bacteria and partially purified VP<sub>AHPND</sub> toxins. Next, the role and importance of the *Lv*APN1 receptor were investigated by using a gene silencing technique. Lastly, we provide a preliminary schematic representation that shows how *Lv*APN1 in hemocytes might be involved in AHPND pathogenesis.

## 2.1.3 Materials and Methods

### 2.1.3.1 Ethics Statement

The experiments involving animals received ethical approval from Chulalongkorn University Animal Care and Use Committee (protocol review No. 1923019). The biosafety concerns of experiments performed was approved by the Institutional Biosafety Committee of Chulalongkorn University (SCCU-IBC-008/2019).

### 2.1.3.2 DNA sequence analysis

*L. vannamei* APN genes (*LvAPN1* and *LvAPN2*) were found in our transcriptomic database of VP<sub>AHPND</sub>-challenged *L. vannamei* hemocytes (Boonchuen et al., 2020). The full-length sequences of *LvAPN1* were retrieved from the in-house transcriptomic database and deposited into GenBank database (accession number MW259048) whereas that of *LvAPN2* was retrieved from GenBank database (accession number XP\_027218958). The amino acid sequence alignment was performed using the aminopeptidase N of various species from previous reports (Tamura, Stecher, Peterson, Filipski, & Kumar, 2013). The amino acid sequences of the two *LvAPN* proteins were analyzed for conserved motifs by SMART (<http://smart.embl-heidelberg.de>) scanning. Prediction of a signal peptide at the N-terminus of each protein was conducted with SignalP 4.1 (Petersen et al., 2011). A GPI anchor signal at the C-terminus was predicted using PredGPI, FragAnchor, and big-PI Predictor. *N*-glycosylation and *O*-glycosylation sites were predicted by the NetNglyc 1.0 Server (Blom, Sicheritz-Ponten, Gupta, Gammeltoft, & Brunak, 2004) and NetOglyc 4.0 Server (Julenius, Molgaard,

Gupta, & Brunak, 2005), respectively. Transmembrane helices of *Lv*APN amino acids were predicted by the TMHMM 2.0 Server (<http://www.cbs.dtu.dk/services/TMHMM/>).

### 2.1.3.3 Tissue distribution analysis

Tissue distribution for the *Lv*APN1 and *Lv*APN2 genes was analyzed in 7 tissues (gill, heart, hemocytes, lymphoid organ, hepatopancreas, intestine, stomach) from three individuals. Total RNA was isolated from these tissues using GENEzol reagent (Geneaid). RevertAid First Strand cDNA Synthesis Kit (Thermo Scientific) was used for reverse transcription. Gene expression analysis was done by semi-quantitative RT-PCR using specific primers for *Lv*APN1, *Lv*APN2 and EF-1 $\alpha$ . The sequences for all primer sets are listed in Table 1. Among three biological replicates, a representative result is shown.

**Table 1** Primer used for qRT-PCR, dsRNA synthesis and recombinant protein expression



Usage	Gene	Primer name	Primer sequence (5'-3')	
Real-time PCR/ PCR	<i>Lv</i> APN1	<i>Lv</i> APN1-F	GGGCAAGGAGGTCAAATGGA	
		<i>Lv</i> APN1-R	CAACGCCACTGTTGCATTGA	
	<i>Lv</i> APN2	<i>Lv</i> APN2-F	GACGTCACGACCTCGGCTG	
		<i>Lv</i> APN2-R	GCCAGGTACCTTGCTCTCCC	
	<i>Lv</i> EF-1 $\alpha$	EF-1 $\alpha$ -F	CGCAAGAGCGACAACATGA	
		EF-1 $\alpha$ -R	TGGCTTCAGGATACCAGTCT	
dsRNA synthesis	<i>Lv</i> APN1	dsAPN1_knd_F_XbaI	CATTCTAGAAGAGAAAAGGTATATCGCTACCACC	
		dsAPN1_knd_R_NcoI	CATCCATGGCTACAAGGTATGTGCTCATTTCAC	
		dsAPN1_knd_F_BamHI	CATGGATCCAGAGAAAAGGTATATCGCTACCACC	
		dsAPN1_knd_R_NdeI	TTCATATGCTACAAGGTATGTGCTCATTTCAC	
	EGFP	dsEGFP_knd_F_XbaI	CATTCTAGAATCATGGCCGACAAGCAGAA	
		dsEGFP_knd_R_NcoI	CATCCATGGAACCCAGCAGGACCATGTG	
		dsEGFP_knd_F_BamHI	CATGGATCCATCATGGCCGACAAGCAGAA	
		dsEGFP_knd_R_NdeI	TTCATATGAACTCCAGCAGGACCATGTG	
		<i>Lv</i> APN1	APN1_CBR_BamHI-F	CGTCAGGATCCGGATGAGATTTTACGTCGAGGAAG
			APN_CBR_SalI-R	AGACGTCGACGATTACTACTACTACTACTACCAC GAGTCCATCCTCCAAGC

APN, aminopeptidase N, EF, Elongation factor, knd, knockdown, EGFP, enhanced green fluorescent protein, CBR, Cry toxin binding region.

#### 2.1.3.4 Bacterial strains

For VP<sub>AHPND</sub> challenge by immersion, *V. parahaemolyticus* strains 5HP (AHPND-causing strain) and S02 (non-AHPND-causing strain) were used. In case of VP<sub>AHPND</sub> toxin challenge, the VP<sub>AHPND</sub> strain TM isolated from a shrimp culture farm in Thamai, Chanthaburi province, Thailand, was used for VP<sub>AHPND</sub> toxin purification. The non-AHPND causing strain, the non-VP<sub>AHPND</sub> strain MC isolated from a shrimp culture farm in Mahachai, Samut Sakhon province, Thailand, was used for non-VP<sub>AHPND</sub> toxin purification. All *V. parahaemolyticus* strains were cultured and maintained on thiosulfate citrate bile salts sucrose medium (TCBS) (BD Biosciences) (Lai et al., 2015; Nunan et al., 2014).

#### 2.1.3.5 Preparation of the partially purified VP<sub>AHPND</sub> toxin

To prepare the partially purified VP<sub>AHPND</sub> toxins and non-VP<sub>AHPND</sub> toxins, bacterial suspension of either the AHPND-causing (TM) or non-AHPND-causing strains (MC) of *V. parahaemolyticus*, was cultured in tryptic soy broth (TSB) supplemented with 1.5% NaCl incubated at 30 °C with shaking for 16 h. Subsequently, the bacterial culture was inoculated 1:100 in 400 ml TSB and cultivation continued with shaking for approximately 2-3 h until the OD<sub>600</sub> reached 2 (equivalent to 10<sup>8</sup> colony forming unit; CFU per ml). After centrifugation at 8,000 ×g for 15 min at 4 °C, the supernatant was collected and subjected to ammonium sulfate precipitation (AS) as described by Sirikharin et al. (2015) (Sirikharin et al., 2015). Total protein concentration of the partially purified VP<sub>AHPND</sub> toxins derived from TM strain and non-VP<sub>AHPND</sub> toxins derived from MC strain was determined using Bradford reagent (Bio-Rad) and stored at -80 °C. The protein quality was analyzed by SDS-PAGE and Western blot analysis using specific antibodies to PirA<sup>VP</sup> and PirB<sup>VP</sup> proteins.

#### **2.1.3.6 Challenge with VP<sub>AHPND</sub> bacteria and the partially purified VP<sub>AHPND</sub> toxins**

After acclimatization, shrimp were challenged with *V. parahaemolyticus* strain 5HP and S02 by immersion in tanks that were inoculated with a bacterial suspension as described by Boonchuen et al., (2018) (Boonchuen et al., 2018). The median lethal dose (LD<sub>50</sub>) of the 5HP bacterial inoculant at 24 h was determined in 10 shrimp, and this resulted in a final bacterial concentration of 2.5×10<sup>5</sup> CFU/ml in the immersion tanks. The LD<sub>50</sub> at 24 h for the partially purified VP<sub>AHPND</sub> toxins was similarly determined as 0.25 µg/g shrimp. The VP<sub>AHPND</sub> toxins were diluted in 1×PBS mixed with a red food-grade dye and intramuscular injected into shrimp. The red food-grade dye was used to make sure that VP<sub>AHPND</sub> toxins was properly entered into the shrimp muscle. The effect

of all the above challenges was also confirmed by observation of morphological changes in the hepatopancreas such as paling and atrophy as well as lethargy in shrimp.

#### **2.1.3.7 Quantitative real-time RT-PCR (qRT-PCR) analysis of *Lv*APN1 expression after challenge with AHPND-causing bacteria and the partially purified VP<sub>AHPND</sub> toxins**

Shrimp (n = 12 per group) were challenged with *V. parahaemolyticus* strain 5HP or VP<sub>AHPND</sub> toxins as described above, and the stomach, hepatopancreas and hemocytes were collected from three shrimp in each experimental group at either unchallenge, 12 or 24 h post challenge. Total RNA was isolated, and cDNA was synthesized using REzol C&T reagent (Protech Technology Enterprise Co., Ltd.) as per the manufacturer's protocol and a RevertAid First Strand cDNA Synthesis Kit (Thermo Scientific) was used to synthesize the cDNA. The cDNA samples were used as templates in the qRT-PCR reaction. The S02-infected and non-VP<sub>AHPND</sub> toxin-injected shrimp were used as controls.

To determine the expression level of *Lv*APN1 gene and EF-1 $\alpha$  internal control gene, the qRT-PCR analysis was performed using an appropriate amount of cDNA for each gene, specific oligonucleotide primers (Table 1) and qPCR Master Mix (KAPA Biosystem) in CFX96 Touch RealTime PCR System (Bio-Rad) under the following conditions: 95 °C for 3 min, 40 cycles at 95 °C for 30 s, 60 °C for 30 s, and 72 °C for 30 s. The experiments were done in three biological replicates. Relative expression level was calculated using the mathematical model of Pfaffl (2001) (Pfaffl, 2001). Data were analyzed using one-way ANOVA followed by Duncan's new multiple ranges test

and presented as means  $\pm$  standard deviations (SD). The level of statistical significance was set at  $P$ -value  $< 0.05$

#### **2.1.3.8 dsRNA silencing of *Lv*APN1 expression**

To investigate the functional importance of *Lv*APN1 as a putative VP<sub>AHPND</sub> toxin receptor, we used an RNA interference (RNAi) approach to silence the expression of *Lv*APN1 by the injection of double-stranded RNA (dsRNA). For dsRNA production using bacteria system, the recombinant plasmid pET-19b containing a 230 bp sense-antisense construct targeted to *Lv*APN1 mRNA was transformed into the ribonuclease III-deficient *Escherichia coli* strain HT115 (DE3) to produce dsRNA-*Lv*APN1 (dsAPN1) and the recombinant plasmid pET-19b containing a 400 bp sense-antisense construct targeted to EGFP mRNA was used to produce dsRNA-GFP (dsGFP), a dsRNA control. The dsRNAs were expressed and extracted as by described in Posiri et al. (2013) (Posiri, Ongvarrasopone, & Panyim, 2013). 20  $\mu$ g of dsAPN1, dsGFP or 0.85% NaCl were injected into each shrimp (~5 g body weight), and 24 h later, the shrimp were injected with 0.25  $\mu$ g/g shrimp of VP<sub>AHPND</sub> toxins or 1 $\times$ PBS pH 7.4 for the control. The stomach, hepatopancreas and hemocytes were collected at 24 h post VP<sub>AHPND</sub> toxin injection from three shrimp in each experimental group. Total RNA was isolated and cDNA was synthesized. Also, the gene expression level of *Lv*APN1 and EF-1 $\alpha$ , internal control gene, was analyzed by the qRT-PCR as described above to verify the efficiency of dsRNA silencing.

#### **2.1.3.9 Susceptibility of VP<sub>AHPND</sub> toxin-challenged *L. vannamei* after *Lv*APN1 silencing**

Shrimp (3 groups of 10 individuals) were injected intramuscularly with dsAPN1, dsGFP or 0.85% NaCl, respectively, in the lateral area of the fourth abdominal segment. Twenty-four h later, the treated shrimp were injected with 50  $\mu$ L of 0.25  $\mu$ g/g shrimp of VP<sub>AHPND</sub> toxins using a syringe with a 29-gauge needle. In the corresponding control groups (3 groups of 10 individuals), the shrimp were injected with 1 $\times$ PBS pH 7.4 instead of VP<sub>AHPND</sub> toxins. After the last injection, the shrimp mortality was monitored twice daily for 7 days. The experiments were done in three replicates.

#### **2.1.3.10 Effect of *Lv*APN1 silencing on the hepatopancreas damage caused by VP<sub>AHPND</sub> toxin**

Individual live shrimp samples (n=3) were also taken from each group dsAPN1-, dsGFP-, and NaCl-injected shrimp at 0, 3, 12, and 24 h post the partially purified VP<sub>AHPND</sub> toxin injection. Individual shrimp were fixed with Davison's fixative 48 h and subsequently stored in ethanol as described by Lightner (1996) (Lightner, 1996). The cephalothorax was then sectioned and stained with H&E stain following standard histological methods. Hepatopancreatic structures were examined using light microscopy, and necrosis of hepatopancreas tubules and hemocytic infiltration in the hepatopancreas were evaluated. Among 3 individuals examined, the representative result is shown.

#### **2.1.3.11 Total Hemocyte Count (THC)**

Prior to counting, the pooled samples of the hemolymph/anticoagulant mixture of each experimental knockdown group (NaCl, dsGFP and dsAPN1) after 24 h-

VP<sub>AHPND</sub> toxin challenge that were set aside from the immunofluorescence assay were kept on ice. To conduct the total hemocyte count, 4% (w/v) paraformaldehyde was added at the ratio 1:1 to immobilize the hemocytes, and the hemocytes were then counted using hemocytometer and a phase contrast microscope (Nikon, Japan). The observed number of hemocytes on the hemocytometer plate, the total hemocyte count in 1 mL hemolymph was then calculated. To determine the proportion of dead vs alive hemocytes, the cells were stained with 0.4% trypan blue prior to immobilization to distinguish between viable and non-viable cells. The experiments were done in three replicates.

#### **2.1.3.12 Effect of *Lv*APN1 silencing on the morphology of VP<sub>AHPND</sub> toxin-challenged shrimp hemocytes by SEM**

To investigate the direct effect of the partially purified VP<sub>AHPND</sub> toxins on hemocyte morphology in shrimp either with or without *Lv*APN1 silencing, 20 µg of dsAPN1, dsGFP, or NaCl were injected into each shrimp (~5 g body weight), and 24 h later, the shrimp were injected with 0.25 µg/g shrimp of VP<sub>AHPND</sub> toxins or 1×PBS, pH 7.4 for the control. At 24 h post challenge, shrimp hemolymph was collected using a sterile 1-ml syringe with anticoagulant. The hemocytes were collected, fixed in 2% glutaraldehyde and the hemocyte morphology was then observed under scanning electron microscope. The experiments were done in triplicate and the representative result is shown.

#### **2.1.3.13 Determination of partially purified VP<sub>AHPND</sub> toxins localization on shrimp hemocytes by immunofluorescence**

To investigate the localization of the VP<sub>AHPND</sub> toxins on hemocytes, three individual shrimp in each experimental knockdown group (NaCl, dsGFP, and dsAPN1) were challenged with VP<sub>AHPND</sub> toxins, and after 24 h, approximately 1.0 ml of *L. vannamei* hemolymph was collected from each shrimp under equal volume of an anticoagulant. After seeding aside some of the pooled hemolymph for the THC assay (see above), the hemocytes in these samples were isolated by centrifugation (800×g; 10 min; 4 °C), with the hemocyte pellet being immediately fixed in 4% (w/v) paraformaldehyde in 1×PBS pH 7.4 at ratio of 1:1 and kept at 4°C until use. Cells (5×10<sup>5</sup> cells/ml) were fixed onto the poly-L-lysine (Sigma) coated-coverslips in a 24-well plate and washed three times with 0.02% Triton X-100 in 1×PBS pH 7.4 followed by cell membrane staining with Cell Brite cytoplasmic membrane dye (Biotium) at the ratio of 1:200 in blocking solution (0.02% Triton X-100, 10% FBS and 1% BSA in 1×PBS pH 7.4) for 10 min. Cells were washed three times and permeabilized with 1×PBS pH 7.4 containing 0.2% gelatin, 1% BSA and 0.02% Triton X-100 for 30 min. Cells were then washed three times and blocked with 1×PBS pH 7.4 containing 10% FBS and 0.02% Triton X-100 for 2 h. Cells were washed again and probed with the rabbit anti-PirB<sup>vp</sup> primary antibody at ratio of 1:5 000 in 1×PBS pH 7.4 containing 10% FBS and 0.02% Triton X-100 at 4 °C overnight, followed by washing and incubation with anti-rabbit secondary antibody conjugated with Alexa Fluor 488 (ratio 1:5 000) at room temperature for 2 h. The nuclei were stained with Hoechst 33342 (Thermo Scientific). The coverslips were mounted with EverBrite Mounting Medium (Biotium) and sealed on glass slides. Fluorescence images were detected with an LSM 800 laser scanning confocal microscope (Carl Zeiss). The experiments were done in triplicate and the representative result is shown.

#### **2.1.3.14 Effect of *Lv*APN1 silencing on stomach colonization by AHPND-causing bacteria**

At 24 h after *Lv*APN1 knockdown, shrimp stomach was collected before (unchallenge) and after challenge with the 5HP (AHPND-causing) or S02 (non-AHPND causing) strains of *V. parahaemolyticus*, stomach samples were collected for DNA extraction using a DTAB/CTAB DNA extraction kit (GeneReach Biotechnology Corp.). The DNA isolated from shrimp stomach was screened for the presence of both the Toxin 1 sequence (which includes parts of both PirA<sup>VP</sup> and PirB<sup>VP</sup> genes) and the part of pVA1 sequence (which lies elsewhere on the pVA1 AHPND plasmid) using an IQ REAL AHPND/EMS Quantitative System on a CFX96 real-time machine (Bio-Rad) according to the supplier's instructions. The IQ REAL system included artificial DNA that contained partial sequences of the PirAB<sup>VP</sup> gene (Toxin 1) and the part of pVA1 region, which were used as standards to obtain standard curves. Copy numbers of the binary Pir toxin sequence and the pVA1 sequence were normalized against the number of host genome copies as measured by an IQ REAL WSSV Quantitative System (Gene Reach Biotechnology Corp). The data are represented as the mean±SD of triplicate tests.

#### **2.1.3.15 ELISA assay of interaction between recombinant truncated r*Lv*APN1 protein and the recombinant PirA<sup>VP</sup> and PirB<sup>VP</sup> toxins**



To investigate the direct binding affinity between the PirA<sup>VP</sup> and PirB<sup>VP</sup> toxins subunits and *Lv*APN1, the recombinant protein of PirA<sup>VP</sup>-His, PirB<sup>VP</sup>-GST, GST, and truncated *Lv*APN1-His (r*Lv*APN1) was prepared. The recombinant PirA<sup>VP</sup>-His and PirB<sup>VP</sup>-GST proteins were produced from *E. coli* BL-21 CodonPlus (DE3) clones harbouring plasmids to express the tagged PirA<sup>VP</sup> or PirB<sup>VP</sup> proteins; these were kindly provided by Dr. Kallaya Dangtip, Center of Excellence for Shrimp Molecular Biology and Biotechnology (CENTEX SHRIMP, Mahidol University, Thailand). The recombinant His tagged rPirA<sup>VP</sup> and the GST-tagged rPirB<sup>VP</sup> were overproduced and then purified using Ni-NTA and Glutathione-beads, respectively (Sirikharin et al., 2015). The recombinant truncated *Lv*APN1-His is N-terminal region of *Lv*APN1 composing of CBR and the active site of peptidase-M1 domain fused with 6×-His tag. The *E. coli* BL-21 (DE3) clone harbouring pET-28b-His-truncated *Lv*APN1 was constructed by cloning the *Lv*APN1 fragment encoding for 388 amino acids truncated *Lv*APN1 containing a CBR (<sup>205</sup>Aspartic acid to <sup>591</sup>Valine) to pET-28b-His vector. It was further expressed in LB broth at 37 °C and induced with 1 mM IPTG at 30 °C for 3 h. The crude r*Lv*APN1 was then purified by Ni-NTA. The purified truncated r*Lv*APN1-His, rPirA<sup>VP</sup>-His, rPirB<sup>VP</sup>-GST and rGST were then dialyzed against 1×PBS, pH 7.4. Western blots using anti-His (Biomax Scientific) and anti-GST (Cell Signaling Technology) antibodies were used to confirm the expression of the respective proteins.

The interaction of toxin proteins (rPirA<sup>VP</sup> and rPirB<sup>VP</sup>) and purified truncated r*Lv*APN1 was determined by ELISA technique as described by Boonchuen et al. (2018) (Boonchuen et al., 2018) with modifications. Briefly, 20 µg of the purified truncated r*Lv*APN1 was coated overnight with 0.1 M carbonate/bicarbonate buffer pH 9.6 in 96-well microtiter plate at 4 °C. The wells were washed 3 times with TBS (20 mM Tris-

HCl, 150 mM NaCl; pH 8.0) containing 0.1% (v/v) Tween 20 (TBST) for 15 min at room temperature. After that, the coated truncated *Lv*APN1 was blocked with TBS, pH 8.0 containing 0.5% (w/v) BSA (Sigma Aldrich) for 3 h. After washing 3 times with TBST, 100  $\mu$ l of either rPirA<sup>VP</sup>, rPirB<sup>VP</sup> or rGST at various concentration (0-10  $\mu$ M in TBS) were incubated with the truncated r*Lv*APN1-coated 96-well plate and incubated at 4 °C overnight. The wells were then washed with TBST. The bound proteins (rPirA<sup>VP</sup> and rPirB<sup>VP</sup>) were detected using 1: 5 000 specific primary antibodies; (rabbit anti-PirA<sup>VP</sup> polyclonal antibody and rabbit anti-PirB<sup>VP</sup> polyclonal antibody, respectively) and a secondary antibody, HRP-conjugated goat anti-rabbit antibody, diluted 1:5 000 fold. The HRP substrate was added and A<sub>450</sub> was measured by spectrophotometry. The specific antibodies for PirA<sup>VP</sup> and PirB<sup>VP</sup> were gifts from Professor Dr. Chu Fang Lo, Department of Biotechnology and Bioindustry Sciences, National Cheng Kung University, Tainan, Taiwan. All assays were performed in triplicate. rGST was used instead of rPirA<sup>VP</sup> and rPirB<sup>VP</sup> for the negative control, which was detected by anti-GST antibody. GraphPad Prism 6 software (Graph-Pad Software, Inc.), was used to analyzed and graphically present the data. The data were fitted to a one-site binding-specific binding model and the K<sub>d</sub> value was determined from the nonlinear curve fitting as  $A = A_{\max} [L]/(K_d + [L])$ , where A is the absorbance, which is proportional to the bound concentration, A<sub>max</sub> is the maximum binding, and [L] is the concentration of the recombinant proteins. The data are represented as the mean $\pm$ SD of triplicate tests.

## 2.1.4 Results

### 2.1.4.1 Characterization of the putative *Lv*APN protein

A comparison of the *Lv*APN1 and *Lv*APN2 deduced amino acid sequences showed that the encoded proteins both have high similarity to other aminopeptidases. While both *Lv*APNs have a Cry toxin binding region (CBR), the N-terminus of *Lv*APN1 but not *Lv*APN2 contains a transmembrane domain (Fig 1A). Considering the peptidase-M1 domain, both proteins have the HEXXH(X)<sub>18</sub>E domain which is characteristic of the zinc-dependent metalloprotease gluzincins, as well as the GAMEN domain which is normally found in other APNs (Fig 1A). Also present is an ERAP1 domain, which plays a central role in N-terminal peptide trimming. The putative *N*-glycosylation sites and *O*-glycosylation sites were also identified (Fig 2). No glycosylphosphatidylinositol (GPI) anchor sites were found in the C-terminal region, and no signal peptide was predicted.

Sequence alignment of the CBRs from *Lv*APNs and other APNs is shown in Fig 1B. The CBR located in the N-terminal region of the *Lv*APNs conformed to the specific CBR motif TxFxxTxARxAFPCxDEP that is found in the Cry-binding APNs of toxin-susceptible insects. We also found that both *Lv*APN1 and *Lv*APN2 were constitutively expressed in all tested immune-related tissue samples from healthy shrimp including stomach, hepatopancreas and hemocytes (Fig 1C).

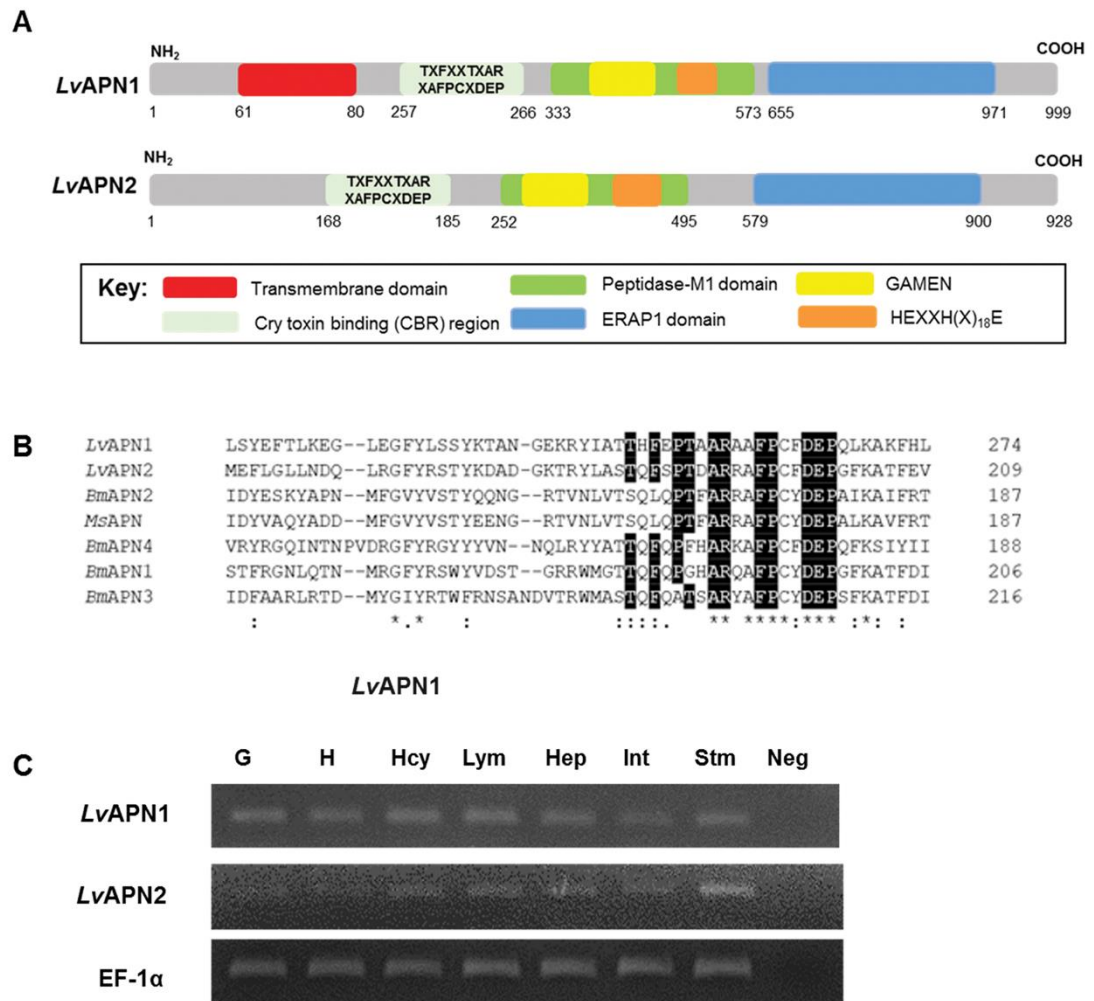


**Fig 1. *LvAPN1* characteristics analysis.** (A) Schematic presentation of specific motifs and other components in the *LvAPN* sequence. Predicted positions of the putative N-terminal transmembrane domain, Cry-binding region (CBR), peptidase-M1 domain, and the GAMEN and HEXXH(X)<sub>18</sub>E zinc-binding site motifs are shown in red, grey, green, yellow, blue and orange, respectively. (B) Alignment of the Cry1Aa toxin-binding region (CBR) of *Litopenaeus vancouverensis*, *Bombyx mori* and *Manduca sexta* APNs. The sequences of *LvAPN1* (XP\_027215499.1); *LvAPN2* (XP\_027218958.1); *BmAPN1* (AFK85020); *BmAPN2* (AB011497); *BmAPN3* (AF352574); *BmAPN4* (AB013400) and *MsAPN* (CAA66466) were compared. Perfectly conserved amino acid residues have black backgrounds. (C) Aminopeptidase N transcript expression

analysis in various *L. vannamei* tissues by RT-PCR. The tissues examined were gill (G), heart (H), hemocyte (Hcy), lymphoid (Lym), hepatopancreas (Hep), intestine (Int) and stomach (Stm). EF1- $\alpha$  was used as the internal reference and PCR control. Neg is a negative control. A representative data of 3 biological replicates is shown.

```

MEGPMRMSDVLNSQPHNNYNTLNNEE[SSGSPNESGFMVNKRAMYEPGAVMVC[SO]KRACCVVTLG
FVAIIAVALIVAFTKPG[CPEA]TYT[GEPLPGOSIRP]TSSPPT[PPTATNGELFPWTSVRLPTHVRPLHYDLSL
HP[LT]SRYVKGELTIKLTAEETQQIVIHGHDLN[VT]SYKLNKYEKPIGISKFLEYPAHQQYLKLEILRRG
S[NY]TLRLSYEFTLKEGLEGFYSSYKTANGEKRYIAT[TH]FEPTAARA[AFFCFDEP]QLKAKFHLSIYREPHQ
FTLFNMPLQTSVKAEDSDLILDQFQESVEMSTYLVAFFVVCDDYDHTV[NT]KTSN[NS]VSVSVYAPPMMISQASY
ALR[MA]TQILD[FE]SFFGVPYPLPKODLIAIPDFGAGAMENWGLITYRETALMFD[PT]HTSSRAOQRVT[VI]
AHELAHQWFGN[LV]TMAWWSDLWLNEGFASFMENLGTGVAEPGWAMQEQFIVEKMQPALSLDALLAS
HPIS[IP]VDDPAQIESIFDTISYKKGASII[GM]LESFIGQDMLKAGLRLLYLEAHRYGNAATDDLWEALTRILKK
SGHNLDIK[GIM]DTWTLOAGFPLISVGLLEDGLVTASQARFLVCEE[VT]DPNEPL[ST]LGYKWHVPLTYVTS
ANPK[ET]MHWM[LT]DVEFEV[GE]VKWIKFNVGQ[RG]FYRVTYDEGGWDALIHVLQTEPHTLSPADRASL
LDDAFTLVKAGT[NAT]VALN[SL]YKRESLYIPWHTALNHLFSWVQLLFN[YS]AHTLMLEYIHTLILPHYERV
GWMDTGTHIERLLRSEILMAAVECGNIAIEEAQKRFAAWRNK[ES]IPPNLRSVYKTVRYGTEEDWR
HCWQVY[NT]SSIPSEKSLMLKAMAQTRDPWLMQQYLEYTLDGSKIRPQDVMIVLSEVSNP[GG]RLSAWR
MVRQHW[QT]ISQLFGHGSFTIGAIKAV[IS]PFTSAFDLGEVESFFSNVDVGPGERALAAQALETIRLHIQWHE
HNLDDVTQWLHQQLSQPEGRDE

```

**Fig 2 Characterization of the putative *Lv*APN1 protein.** The putative N-terminal transmembrane domain is boxed. The GAMEN and HEXXH(X)<sub>18</sub>E zinc-binding site motifs are shown in bold with a grey background. The predicted Cry toxin binding region is highlight in yellow. Two conserved domains, the peptidase M1 domain and ERAP1-like C-terminal domain, are underlined and dash-underlined, respectively. Putative *N*-glycosylated asparagine residues predicted by the NetNGlyc 1.0 server, and putative *O*-glycosylated threonines and serine residues predicted by the NetOGlyc 3.1 server are shown in black.

#### 2.1.4.2 *Lv*APN1 is upregulated in response to AHPND

As shown in Fig 1A, *Lv*APN2 has no transmembrane domain, and since it would therefore presumably be expressed only in soluble form rather than as a membrane-bound protein receptor, our subsequent experiments focused only on *Lv*APN1.

First, we used Western blot to confirm that both PirA<sup>VP</sup> and PirB<sup>VP</sup> toxins were present in the purified proteins extracted from Thamai strain (TM) and absent from the proteins extracted from Mahachai strain (MC) (Fig 3). Next, in order to analyze the expression of *Lv*APN1 that was identified from the transcriptomic data, we challenged adult *L. vannamei* with either the non-AHPND causing *Vibrio parahaemolyticus* strain S02 or the virulent AHPND-causing strain 5HP as shown in panel (i), or else with the partially purified toxins or non-toxins extracted from TM strain and MC strain as shown in panel (ii), respectively. Using qRT-PCR to analyze the expression patterns of *Lv*APN1 in the stomach (Fig 4A), hepatopancreas (Fig 4B) and hemocytes (Fig 4C), we found that at 12 and 24 hpi, the expression profiles of *Lv*APN1 in the hepatopancreas were significantly upregulated after challenge with either 5HP or the partially purified VP<sub>AHPND</sub> toxins. Similarly, in the stomach, *Lv*APN1 expression was upregulated at 12 hpi by the partially purified VP<sub>AHPND</sub> toxins and at 24 hpi by 5HP. Meanwhile, in hemocytes, although *Lv*APN1 was significantly upregulated at 12 hpi after 5HP challenge and at 24 hpi after challenge with the partially purified VP<sub>AHPND</sub> toxins, we also observed some unexpected downregulation of *Lv*APN1 at 12 hpi (Fig 4).

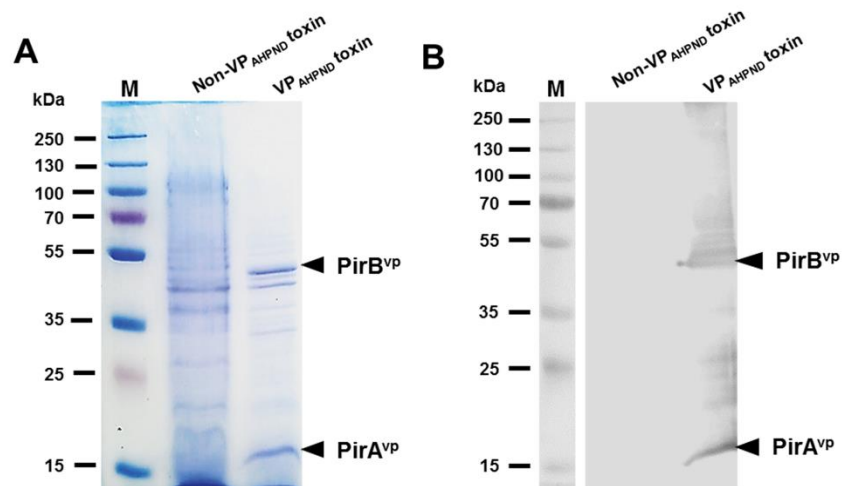


**Fig 3 Partially purification of VP<sub>AHPND</sub> toxin.** (A) SDS-PAGE analysis and (B) Western blot analysis with PirAB<sup>VP</sup> polyclonal antibodies of the partially purified ammonium sulfate fractions from the culture medium of the non-AHPND isolate S02 and the VP<sub>AHPND</sub> isolate 5HP. The 2 major toxin bands (PirA<sup>VP</sup> at ~16 kDa and PirB<sup>VP</sup> at ~50 kDa) in lanes for partially purified 5HP proteins are absent from the proteins derived from S02.

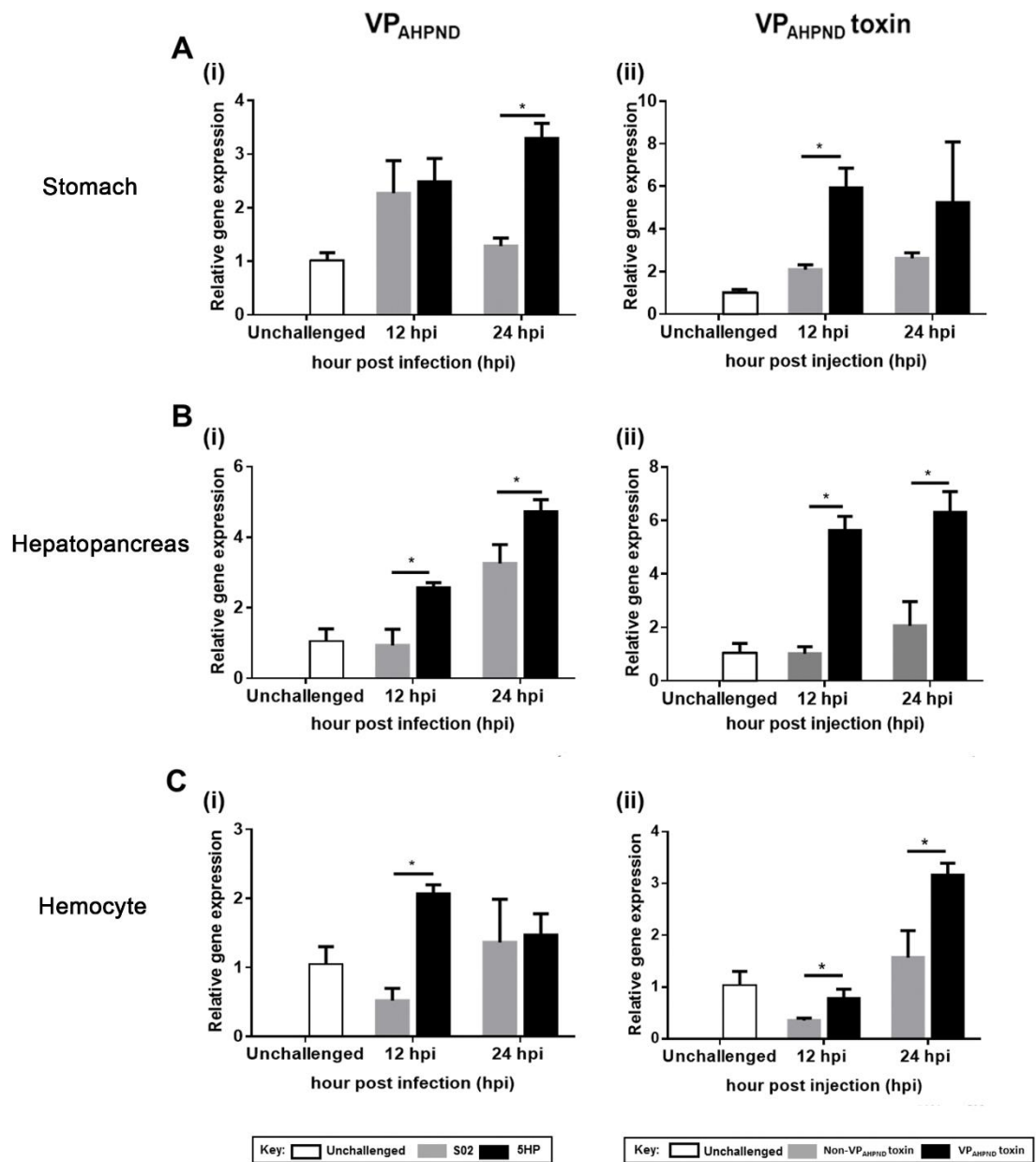


**Fig 4. Expression of the *LvAPN1* gene upon VP<sub>AHPND</sub> and VP<sub>AHPND</sub> toxin challenges.** (A) Stomach, (B) hepatopancreas, and (C) hemocyte of *L. vannamei* were collected before infection (unchallenged) and after challenge with 5HP (i) or the partially purified VP<sub>AHPND</sub> toxins (ii) at 12 and 24 h. *LvAPN1* expression was analyzed by qRT-PCR using EF-1 $\alpha$  as the internal control gene. The data represent fold change of *LvAPN1* expression in the 5HP or VP<sub>AHPND</sub> producing strain challenged group



compared to the S02 or non-VP<sub>AHPND</sub> toxin producing strain-challenge control. The experiments were done in triplicate. Each bar represents the mean  $\pm$  standard deviation (SD). Asterisks indicate significant difference ( $P < 0.05$ ).

#### 2.1.4.3 *Lv*APN1 as a putative VP<sub>AHPND</sub> toxin receptor

Next, to investigate the functional importance of *Lv*APN1 as a putative VP<sub>AHPND</sub> toxin receptor, we used an RNA interference (RNAi) approach to silence the expression of *Lv*APN1 by the injection of double-stranded RNA (dsRNA). At 24 h after injection of purified *Lv*APN1-specific dsRNA, *Lv*APN1 transcription levels were significantly reduced in stomach, hepatopancreas and hemocytes, relative to the dsGFP-injected and NaCl-injected controls (Fig 5A). The *Lv*APN1 specific dsRNA was also shown to have no effect on the expression of *Lv*APN2 (Fig 6). Furthermore, Fig 5B further shows that silencing of *Lv*APN1 significantly increased the survival of adult *L. vannamei* that were challenged with the partially purified VP<sub>AHPND</sub> toxins; although none of the shrimp in the NaCl-treated and dsGFP-treated groups survived beyond 5 days, 77% of the *Lv*APN1 silenced shrimp survived the same challenge through to the end of the experiment at 7 days.

PirAB<sup>VP</sup> toxins released from VP<sub>AHPND</sub> is the major cause of AHPND symptom of hepatopancreas necrosis. So, the effect of *Lv*APN1 knockdown on the hepatopancreas morphology of shrimp challenged with the partially purified VP<sub>AHPND</sub> toxin was observed (Fig 5C). As expected, histological examination showed that *Lv*APN1 silencing largely prevented the characteristic AHPND clinical signs of sloughed epithelial cells and cellular disruption, whereas in the NaCl-treated and

dsGFP-treated control shrimp, both sloughing of the tubule cells and hemocyte infiltration were observed. This result suggested the putative role of *Lv*APN1 as a  $VP_{AHPND}$  toxin receptor.

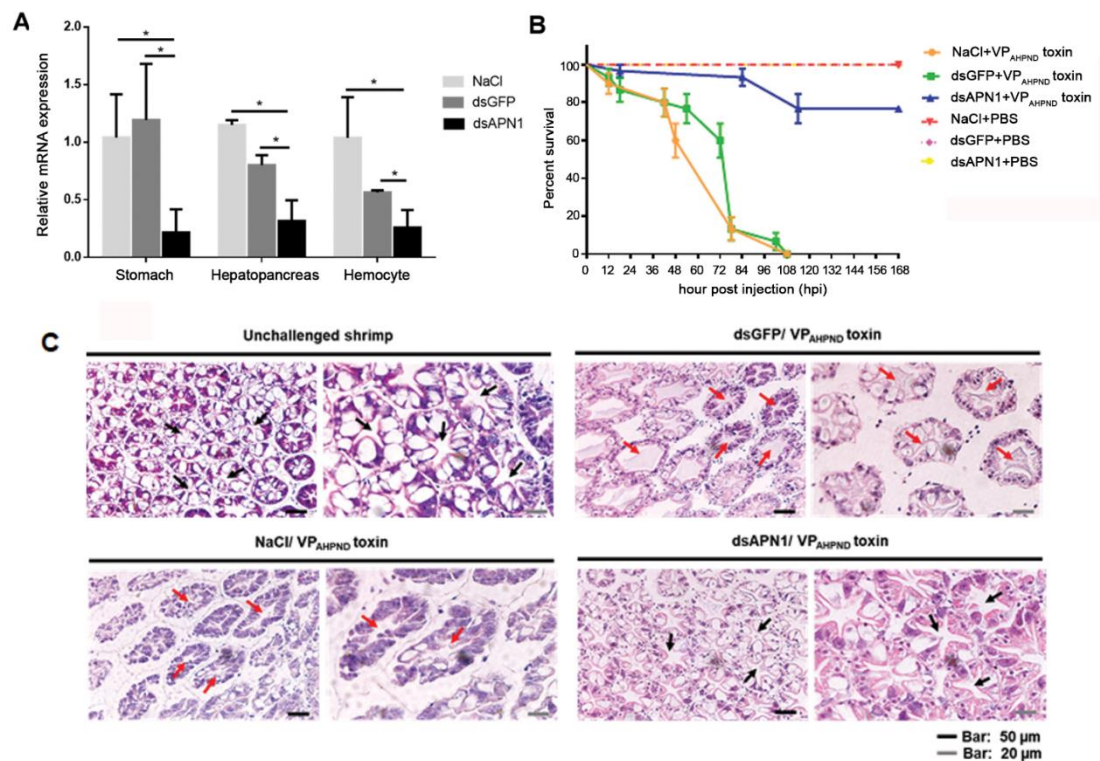


**Fig 5. The effect of *Lv*APN1 silencing in AHPND-causing bacteria pathogenesis.**

(A) Confirmation of *Lv*APN1 gene knockdown in *L. vannamei*. The mRNA expression levels of the *Lv*APN1 gene in the stomach, hepatopancreas and hemocyte of shrimp injected with 0.85% NaCl, 20  $\mu$ g/g shrimp of dsGFP, or 20  $\mu$ g/g shrimp of dsAPN1 were determined by qRT-PCR and expressed in relative to EF-1 $\alpha$ . Each bar represents the mean  $\pm$  SD, derived from triplicate experiments. Asterisks indicate significant difference ( $P < 0.05$ ). (B) *Lv*APN1 silencing reduced mortality in shrimp challenged with partially purified  $VP_{AHPND}$  toxins. Cumulative mortality was monitored in 3 groups of 10 shrimp for each of the individual experimental conditions. NaCl-injected

shrimp were challenged with partially purified VP<sub>AHPND</sub> toxin (●), dsGFP-injected shrimp were challenged with partially purified VP<sub>AHPND</sub> toxin (■), dsAPN1-injected shrimp were challenged with partially purified VP<sub>AHPND</sub> toxin (▲), NaCl-injected shrimp were challenged with PBS (▼), dsGFP-injected shrimp were challenged with PBS (◆), dsAPN1-injected shrimp were challenged with PBS (●). Shrimp survival was observed every 12 h post treatment for 7 days. All experiments were performed in triplicate and the survival percentage calculated as mean ± 1 standard error (SE) at each time point as shown. (C) A representative data of haematoxylin and eosin-stained hepatopancreas collected from shrimp at 24 h after challenge with VP<sub>AHPND</sub> toxin. Normal hepatopancreatic tubules (black arrow) are observed in the unchallenged group and dsAPN1-injected group, whereas typical AHPND lesions with necrotic, sloughed epithelial cells (red arrow) were found in both the dsGFP- and NaCl-injected groups.

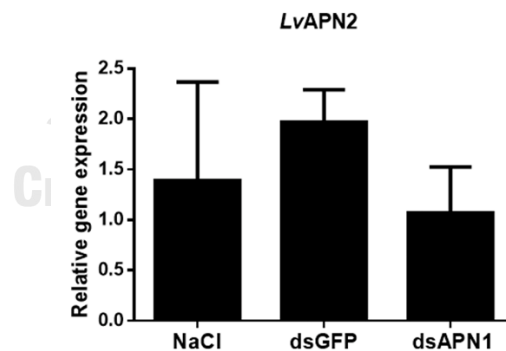


**Fig 6** The mRNA expression levels of the *LvAPN2* gene in hemocyte of *LvAPN1* knockdown shrimp. Shrimp were injected with 0.85% NaCl, 20 µg/g shrimp of dsGFP, or 20 µg/g shrimp of dsAPN1 were determined by qRT-PCR. Relative expression of *LvAPN2* gene is shown here in relative to that of EF-1α.

#### 2.1.4.4 *LvAPN1* knockdown reduced cell damage in toxin-challenged hemocytes

As observed earlier that *LvAPNs* were constitutively expressed in all tested immune-related tissues especially hepatopancreas and stomach that are destroyed upon  $VP_{AHPND}$  infection. However, there is no evidence of damages on other tissues reported so far. It is well known that hemocyte is a major immune tissue producing various immune effectors to fight against infection. Here, we showed that the  $VP_{AHPND}$  toxins significantly decreased the total hemocyte count (THC) in the NaCl-treated and dsGFP-treated shrimp at 24h (Fig 7A). By contrast, the silencing of *LvAPN1* results in a THC that is similar to that of the unchallenged PBS-treated group. In addition, we also found that 83% of the hemocytes in the *LvAPN1* knockdown group were alive, compared to 63% and 58% in the NaCl and dsGFP control groups, respectively (Fig 7B).

To further determine if hemocytes are one of  $VP_{AHPND}$  toxin target tissue, the morphology of the  $VP_{AHPND}$ -challenged shrimp hemocytes was observed (Fig 7C). Scanning electron microscopy (SEM) showed a clear morphological change in the hemocyte cell surface after  $VP_{AHPND}$  toxin challenge in the NaCl- and dsGFP-treated shrimp. These changes included cell disruption, pore formation on the cell surface and bursting. Meanwhile, in the *LvAPN1* knockdown shrimp, there was no observable morphological damage to the hemocytes after  $VP_{AHPND}$  toxin challenge. These results infer that hemocytes are a  $VP_{AHPND}$  toxin target tissue where *LvAPN1* is involved in penetration of toxins into cell.

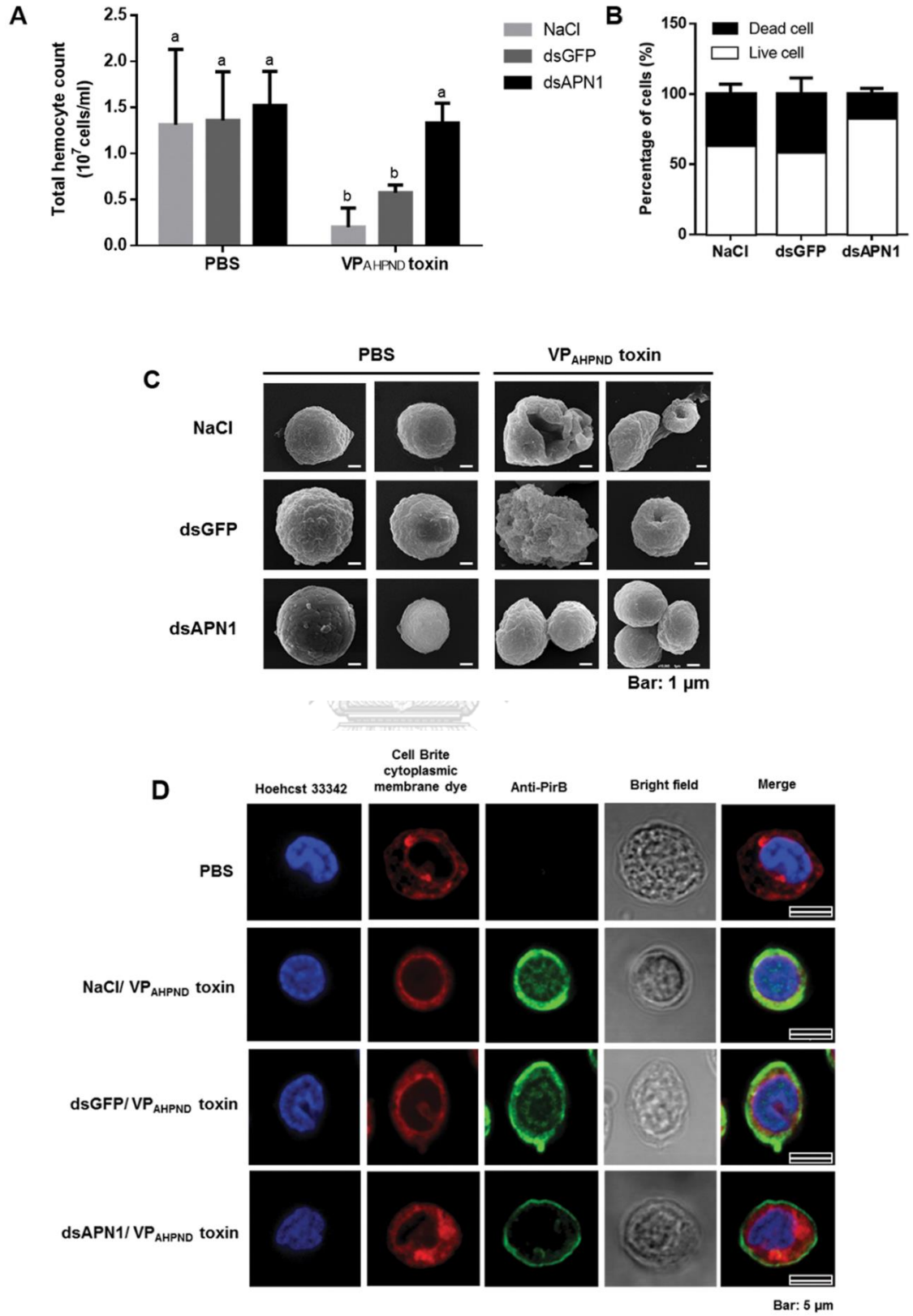


**Fig 7. The effect of *Lv*APN1 silencing on shrimp hemocyte homeostasis** (A) Effect of *Lv*APN1 silencing on the total hemocyte count after challenge with the partially purified VP<sub>AHPND</sub> toxins. Experimental groups were the same as those used in Fig 3B. PBS was used as a control. THC values for each treatment condition were derived from at least three shrimp. (B) Percentage of dead and viable hemocytes in the *Lv*APN1 knockdown shrimp after partially purified VP<sub>AHPND</sub> toxins challenge was determined by trypan blue staining and observation under light microscopy. Asterisks indicate significant difference ( $P < 0.05$ ). (C) The representative SEM micrograph showing morphology of *Lv*APN1 knockdown shrimp hemocytes after partially purified VP<sub>AHPND</sub> toxin challenge. Experimental groups were the same as those used in Fig 3B. PBS was used as a control. (D) Localization of the VP<sub>AHPND</sub> toxin on shrimp hemocyte by immunofluorescence. The VP<sub>AHPND</sub> hemocytic nuclei, cytoplasmic membrane and PirB<sup>VP</sup> toxin are visualized in blue (Hoechst 33342), red (CellBrite cytoplasmic membrane) and green (Alexa Fluor 488) colors, respectively. PBS-injected shrimp was used as a control. The scale bar corresponds to 5  $\mu$ m. All experiments were done in triplicate.

#### **2.1.4.5 *Lv*APN1 plays crucial role in toxin translocation from cell membrane to cytoplasm of hemocytes**

To observe the effect of *Lv*APN1 silencing on the localization of VP<sub>AHPND</sub> toxins on shrimp hemocytes, we used immunofluorescence and confocal microscopy in conjunction with anti-PirB<sup>VP</sup> antibodies specific to PirB<sup>VP</sup>. Twenty-four h after challenge with the partially purified VP<sub>AHPND</sub> toxins, *Lv*APN1 knockdown shrimp hemocytes were collected, fixed and processed for the detection of PirB<sup>VP</sup> proteins.

Nuclei were stained with Hoechst 33342 (blue) and cell membranes were stained with CellBrite cytoplasmic membrane dye (red), while the VP<sub>AHPND</sub> toxin was visualized with Alexa Fluor 488 conjugated anti-PirB<sup>VP</sup> antibody (green). The fluorescent microscopic images revealed that while VP<sub>AHPND</sub> toxin was localized on both the hemocyte cell surface and the cytoplasm of the NaCl-treated and dsGFP-treated hemocytes, the VP<sub>AHPND</sub> toxin was only localized on the cell membrane not inside the cell of dsAPN1-treated shrimp (Fig 7D). These results suggest that in hemocytes, *Lv*APN1 is acting as a target receptor molecule of VP<sub>AHPND</sub> toxins and that it is a critical part of the mechanism that allows the toxins to pass through the cell membrane.

#### **2.1.4.6 *Lv*APN1 gene silencing reduces the number of AHPND virulence plasmids in stomach**

To investigate the effect of *Lv*APN1 silencing in the stomach of *L. vannamei*, we performed an immersion challenge using two strains of *V. parahaemolyticus*, S02 and 5HP. At 24 h after infection, a PCR-based AHPND detection kit was used to test stomach samples for the presence of two sequences in the pVA1 plasmid, one that overlaps both of the Pir toxin genes, and another more stable sequence known as AP2 (Kumar et al., 2020). As shown in both panels of Fig 8 after 5HP infection, the dsAPN1-injected group showed significantly lower counts for the pVA1 plasmids than the NaCl-treated and dsGFP-treated controls. All of the above results provide further evidence of *Lv*APN1 involvement in AHPND pathogenesis.

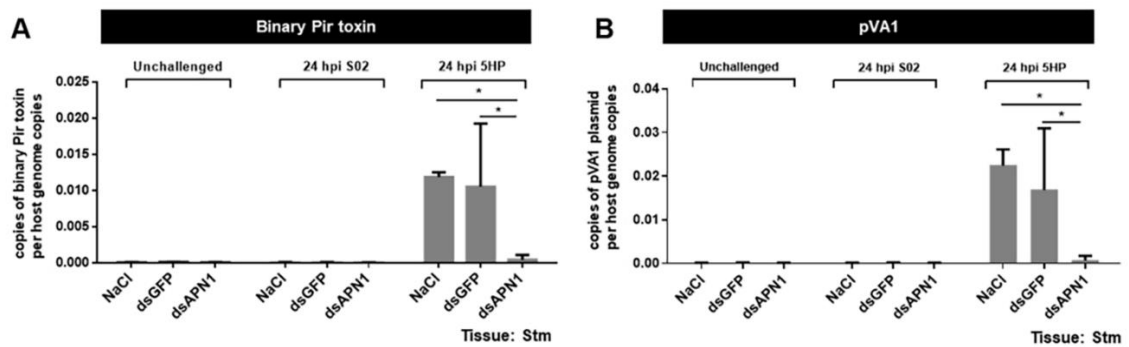


**Fig 8. Reducing of AHPND-causing bacteria plasmid in stomach of *LvAPN1* silenced shrimp.** PCR amplification of two different sequences in the genome of the pVA1 plasmid, (A) Binary Pir toxin sequence and (B) pVA1 sequence from the stomach of shrimp injected with 0.85% NaCl, 20  $\mu\text{g/g}$  shrimp of dsGFP, or 20  $\mu\text{g/g}$  shrimp of dsAPN1. Shrimp stomach were collected after dsRNA injection (unchallenged) and after infection with the AHPND-causing *V. parahaemolyticus* 5HP strain and non-AHPND causing *V. parahaemolyticus* S02 at 24 h. The data represent copies of pVA1 plasmid per host genome copies. Each bar represents the mean  $\pm$  standard deviation (SD) of triplicate experiments. Asterisks indicate significant difference ( $P < 0.05$ ).

#### 2.1.4.7 ELISA assay of protein-protein interactions between *LvAPN1* and the PirA<sup>VP</sup> and PirB<sup>VP</sup> toxins

After confirming the successful expression of the recombinant proteins truncated *LvAPN1*, PirA<sup>VP</sup>-His, PirB<sup>VP</sup>-GST and GST in a bacterial expression system (Fig 9), the purified truncated r*LvAPN1* was found to bind directly to rPirA<sup>VP</sup> and rPirB<sup>VP</sup> in a concentration-dependent manner (Fig 10). Assuming a one-site binding



model, the apparent dissociation constants ( $K_d$ ) of truncated *rLvAPN1* to *rPirA<sup>VP</sup>* and *rPirB<sup>VP</sup>*, as calculated from the saturation curves, were 3.2  $\mu$ M and 0.5  $\mu$ M, respectively. These results suggest that both  $VP_{AHPND}$  binary toxin subunits can bind directly to *LvAPN1* receptor.

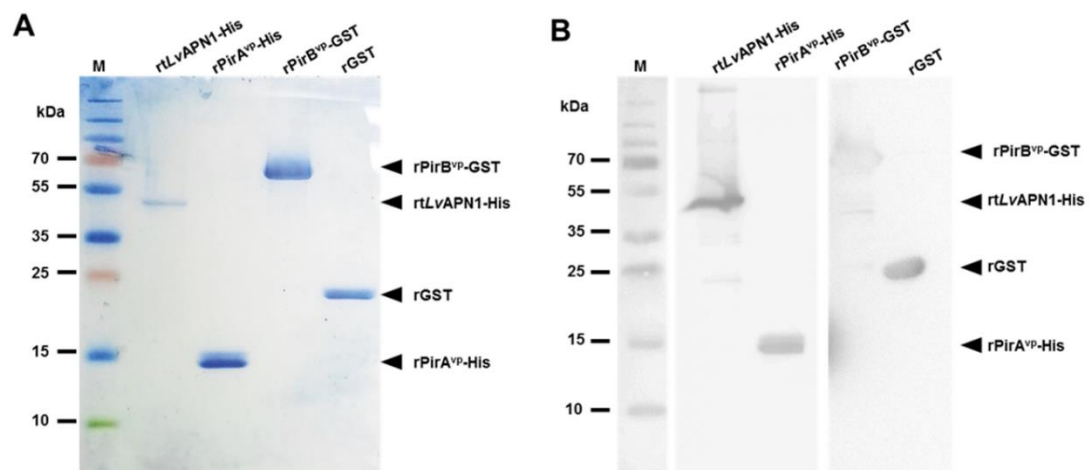


**Fig 9 Recombinant protein purification analysis.** (A) SDS-PAGE analysis and (B) Western blot analysis with anti-His and anti-GST antibodies of recombinant truncated *LvAPN1-His*, *rPirA<sup>VP</sup>-His*, *rPirB<sup>VP</sup>-GST* and *rGST* protein overexpressed in *E. coli*. The His-tagged *rLvAPN1* and *rPirA<sup>VP</sup>* were purified by Ni-NTA affinity chromatography. The deduced molecular weight for recombinant truncated *LvAPN1-His* and *PirA<sup>VP</sup>-His* were 53 and 16 kDa, respectively. The *rPirB<sup>VP</sup>-GST* fusion protein and *rGST* were purified by Sepharose 4B Glutathione beads. The estimated molecular weights for *rPirB<sup>VP</sup>-GST* and *rGST* were approximately 70 and 23 kDa, respectively.

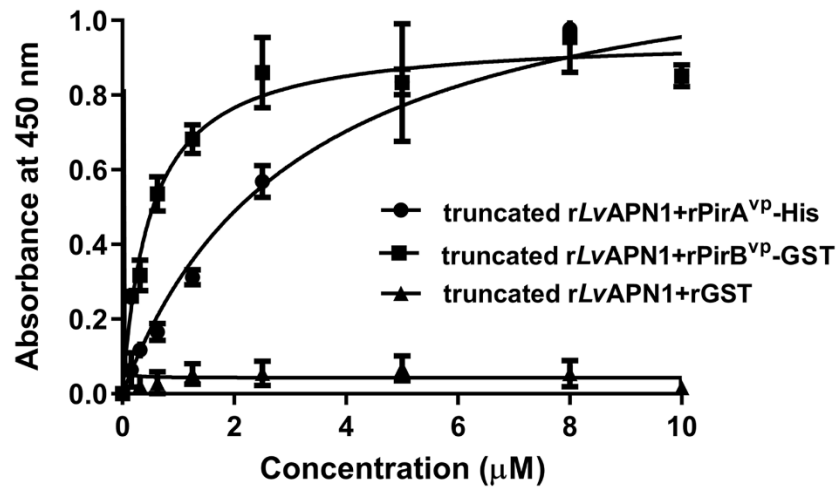


**Fig 10. Binding ability of rPirA<sup>VP</sup> and rPirB<sup>VP</sup> on immobilized recombinant truncated LvAPN1-His determined by ELISA.** The purified rPirA<sup>VP</sup>-His, rPirB<sup>VP</sup>-GST or rGST (0-10 μM) was added to a purified recombinant truncated LvAPN1-coated plate, followed by probing with the anti-PirB<sup>VP</sup> specific primary antibody and goat anti-rabbit-conjugated HRP secondary antibody. Finally, after addition of the tetramethylbenzidine (TMB) substrate, the absorbance at 450 nm ( $A_{450}$ ) was measured. Solid lines illustrate the fitted curves. The data are shown as the mean  $\pm$  1 standard error of mean (SEM), derived from triplicate experiments.

### 2.1.5 Discussion

APNs in insects have been extensively investigated for their interactions with *Bacillus thuringiensis* Cry toxins (Bravo, Gill, & Soberon, 2007). In the present study, we first identified aminopeptidase N 1 and 2 (LvAPN1 and LvAPN2) from the transcriptome of VP<sub>AHPND</sub>-challenged *L. vanna* hemocytes. LvAPN1 and LvAPN2, which were expressed in all immune-related and AHPND-affected tissues including

stomach, hepatopancreas and hemocytes (Fig 1C), possess the hallmark characteristics of lepidopteran APNs, so they appear to belong to the APN family (Fig 1A). There are at least four classes of APN in the insect midgut, where they occur either as soluble enzymes or in association with the microvillar membrane (Terra and Ferreira. 2014). While these four APNs are thought to differ in their amino acid specificity, they all function to cleave amino acids from peptides, a step which is necessary for amino acid co-transport into epithelial cells (Adang et al., 2014). Prediction of a transmembrane helix showed that *LvAPN1* is potentially a membrane-bound protein (Figs 1A and 2) while *LvAPN2* is not. The results of sequence alignment indicated that *LvAPN1* CBR shared moderate to high protein identity with the CBRs of other APN homologs, while the protein sequences beyond this consensus domain diverged considerably from those of the APNs found in Cry-susceptible insects (Fig 1B) (Shao et al., 2018). Nevertheless, based on the similarity of its domain structure, it seems likely that *LvAPN1* would have a similar function to the APN receptors in insects.

Specific binding of the Cry toxins to receptors on the epithelial cells of the midgut and hindgut is critical for their toxic effect on susceptible insects (Hofmann et al., 1988; Van Rie, Jansens, Hofte, Degheele, & Van Mellaert, 1990; S. Zhang et al., 2009), and previous study has shown that the *BmAPNs* were specifically or highly expressed in the midgut of *B. mori* after *B. bombysepticus* and *B. thuringensis* infection (Lin et al., 2014). Here, we found that the expression levels of the *LvAPN1* gene were increased after challenge with either the AHPND-causing bacteria or the VP<sub>AHPND</sub> toxin not only in stomach and hepatopancreas, but also in hemocytes (Fig 4). Interestingly, there are other reports in arthropods that their hemocytes are targeted by Cry toxins. For example, Cerstiaens et al., (2001) demonstrated the toxicity of Cry

toxins to the hemocoel in *Lymantria dispar* (Lepidoptera) and *Neobellieria bullata* (Diptera) (Cerstiaens et al., 2001). In addition, the *AjAPN1* protein of non-gut hemocoelic tissues was implicated as a Cry1Aa toxin receptor in these tissues in *Achaea Janata* (Ningshen, Aparoy, Ventaku, & Dutta-Gupta, 2013). All of these findings suggest that VP<sub>AHPND</sub> toxins targeting stomach, hepatopancreas, and hemocytes mediated by *LvAPN1* is required for AHPND pathogenesis in shrimp.

Silencing of *HaAPN1* in *Helicoverpa armigera* was found to decrease the susceptibility of larvae to Cry1Ac toxins (Sivakumar et al., 2007), while silencing of *HcAPN3* was also associated with reduced susceptibility of *Hyphantria cunea* to Cry1Ab (Y. Zhang et al., 2017). In the present study we likewise investigated the function of *LvAPN1* by dsRNA-mediated silencing. Our results show that *LvAPN1* dsRNA significantly silenced *LvAPN1* in the stomach, hepatopancreas and hemocytes (Fig 5A) and knockdown of *LvAPN1* reduced the mortality of VP<sub>AHPND</sub> toxins-challenged shrimp (Fig 5B). Recent research demonstrated that in the germ-free brine shrimp PirAB<sup>VP</sup> toxins bind to epithelial cell of the digestive tract and damage enterocytes in the midgut and hindgut regions (Kumar et al., 2019). In the Penaeid shrimp, it is known that VP<sub>AHPND</sub> toxins cause the damage on stomach and hepatopancreas tissues whereas no evidence is available for hemocytes. In this study we would like to prove that not only stomach and hepatopancreas but also hemocytes are target tissue of VP<sub>AHPND</sub> toxins. We investigated the effect of *LvAPN1* silencing on availability and morphology of hemocyte in VP<sub>AHPND</sub> toxin-challenged shrimp. We found that VP<sub>AHPND</sub> toxins cause severe damage of hemocyte leading to lowering total hemocyte number and cell death while silencing of *LvAPN1* prevented these effects (Figs 7A, 7B) emphasizing the participation of *LvAPN1* in VP<sub>AHPND</sub> toxin susceptibility

of hemocyte. Immunofluorescence assay further revealed that the VP<sub>AHPND</sub> toxins passed through the cell membrane and localized inside the cell, but when *LvAPN1* was silenced, the VP<sub>AHPND</sub> toxin was unable to gain entry and remained localized on the cell membrane (Fig 7D). Although these effects were observed in circulating hemocytes, the VP<sub>AHPND</sub> toxins presumably damages the hemocytes in the hepatopancreas in the same way. If so, then the hemocyte infiltration that occurs in the late stage of infection would include hemocytes that have already been damaged by the VP<sub>AHPND</sub> toxins (Kumar et al., 2020).

In insects, binding of the Cry toxins to receptors leads to membrane insertion into the host cell (Ningshen et al., 2013; Pacheco, Gomez, Gill, Bravo, & Soberon, 2009; Pigott & Ellar, 2007). Thus, for example Cry toxins form pores in the apical membrane of larvae midgut cells, destroying the cells and killing the larvae (Soberon et al., 2010). Our results showed that while challenge with the partially purified VP<sub>AHPND</sub> toxins led to cell death and pore formation in hemocytes in unsilenced shrimp, knockdown of *LvAPN1* not only inhibited pore formation by the VP<sub>AHPND</sub> toxins (Fig 7C), it also reduced both shrimp mortality (Fig 5B), and led to a reduction in the number of AHPND-causing bacteria in the stomach (Fig 8). The reason for reduction is still unclear, but one possibility is that the lack of *LvAPN1* receptors might somehow reduce susceptibility of hemocyte, stomach, and hepatopancreas cells to VP<sub>AHPND</sub> toxins.

Binding specificity between the receptor and the toxin is also critically important for Cry toxicity. In a previous report, ligand blotting showed that in *B. mori* and *H. cunea*, the APN receptors specifically bind to Cry1Aa toxins (Jenkins et al., 2001). Similarly, here we used ELISA to determine the binding of VP<sub>AHPND</sub> toxins and *LvAPN1* receptor. We found that the recombinant His-tagged N-terminal of *LvAPN1*

was able to directly bind to both the rPirA<sup>VP</sup> and rPirB<sup>VP</sup> toxins, and that it showed a slightly higher binding affinity to PirB<sup>VP</sup> than to PirA<sup>VP</sup> (Fig 10), suggesting that PirA<sup>VP</sup> subunit might first recognize and bind to LvAPN1 receptor, this binding possibly facilitate PirB<sup>VP</sup> subunit binding to the receptor with higher stability on hemocytes. The role of PirB<sup>VP</sup> as a ligand for cell surface receptor of shrimp target cells has been recently suggested as well. Victorio-De Los Santos et al (2020) suggested that PirB<sup>VP</sup> is a lectin that can bind to amino sugar ligand and exhibits the hemagglutinating activity as the PirAB<sup>VP</sup> complex (Victorio-De Los Santos et al., 2020). Taken together, our data suggests that LvAPN1 is likely to facilitate AHPND pathogenesis by functioning as a receptor for VP<sub>AHPND</sub> toxins, and that it is therefore likely to be involved in pore-formation and membrane insertion.

Lastly, we note that the ability of the VP<sub>AHPND</sub> toxins to enter and damage hemocytes (Fig 7) suggests that the pathological effects of AHPND are not limited to the stomach and hepatopancreas, but also extend to the hemocytes. Taking all of the results presented here we propose a model for the role of LvAPN1 in shrimp hemocytes (Fig 11). According to this model, the AHPND-causing *V. parahaemolyticus* enter into the shrimp. At the same time, the AHPND-causing *V. parahaemolyticus* release of PirAB<sup>VP</sup> toxins. Next, the PirAB<sup>VP</sup> toxins bind to LvAPN1 receptor located on cell membrane of shrimp hemocytes and then might induce PirAB<sup>VP</sup> toxin oligomerization. Noted that, PirB<sup>VP</sup> has higher affinity to LvAPN1 receptor than PirA<sup>VP</sup>. This interaction enhanced pore formation and membrane insertion which led to the hemocyte morphology changes and hemocyte lysis.

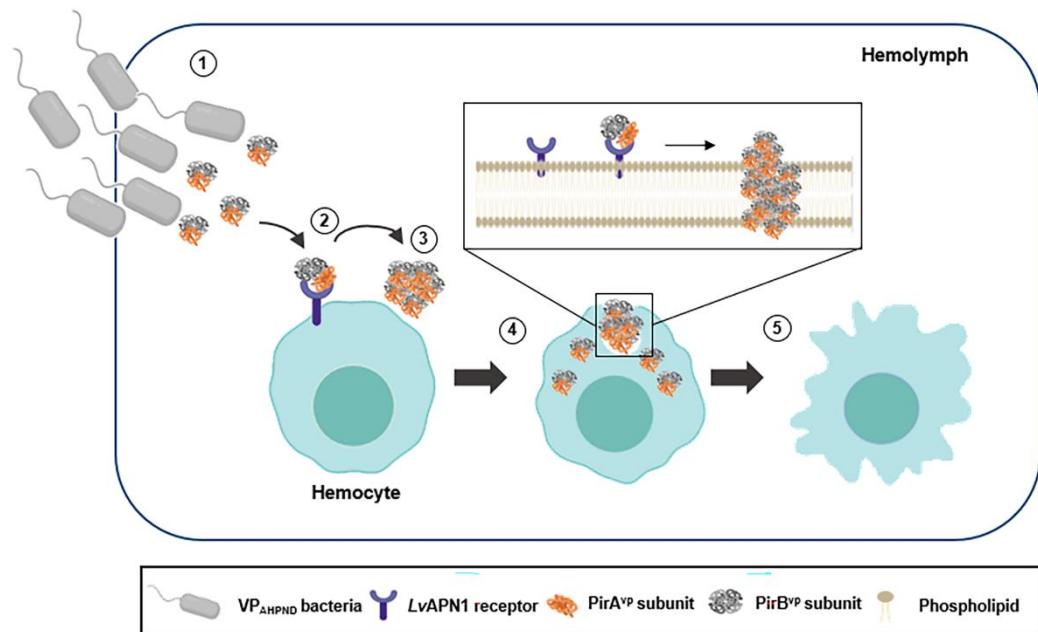


**Fig 11. Schematic representation of AHPND pathogenesis showing the proposed role of *LvAPN1* in hemocyte.** (1)  $VP_{AHPND}$  bacteria enter the shrimp and release PirAB<sup>VP</sup> toxin. (2) The PirB<sup>VP</sup> (with higher affinity) and PirA<sup>VP</sup> subunits recognize and bind to *LvAPN1* receptor which is embedded in cell membrane of shrimp hemocyte. (3) This interaction might induce  $VP_{AHPND}$  toxins oligomerization. (4)  $VP_{AHPND}$  toxins induce pore formation and insert into membrane. (5) Hemocyte is lysed and damaged causing by pore formation and membrane insertion.

## 2.2 Manuscript II

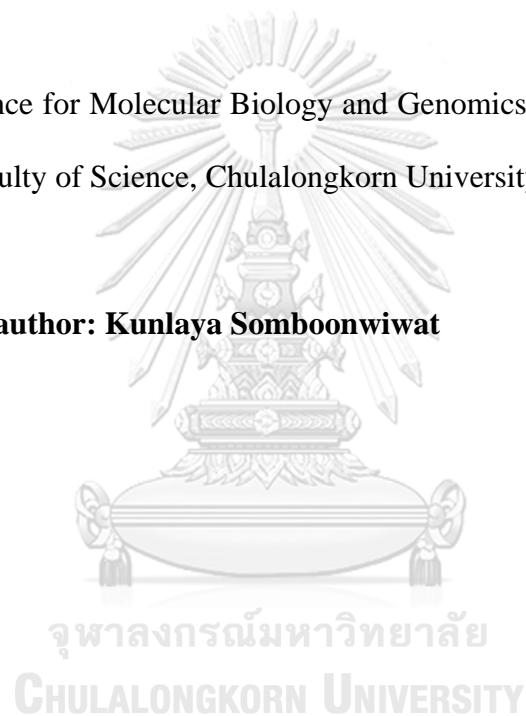
**Identification of novel shrimp PIWI-interacting RNA (piRNA) involved in *Vibrio parahaemolyticus* AHPND infection**

**(Preparing to publish on Journal of Fish & Shellfish immunology (Tier1))**

Waruntorn Luangtrakul, Kunlaya Somboonwiwat\*

Center of Excellence for Molecular Biology and Genomics of Shrimp, Department of Biochemistry, Faculty of Science, Chulalongkorn University, Bangkok, Thailand.

**\*Corresponding author: Kunlaya Somboonwiwat**





### 2.2.1 Abstract

Piwi-interacting RNA (piRNA) is the largest class of small non-coding molecules with 24-31 nts in length. It forms RNA-protein complexes through interactions with PIWI proteins. These piRNA/PIWI complexes suppress expression of transposons and protein-coding genes via transcriptional or posttranscriptional mechanisms. piRNAs have been identified in many living organisms but not in shrimp. Therefore, the aim of this study is to identify piRNAs from hemocyte of *Litopenaeus vannamei* infected with *V. parahaemolyticus* AHPND (VP<sub>AHPND</sub>). Our previous next generation sequencing data of small RNAs libraries derived from hemocyte of nonlethal heat shock-treated VP<sub>AHPND</sub>-infected shrimp hemocyte, were re-analyzed to identify VP<sub>AHPND</sub>-responsive piRNAs. A total of 150 piRNA homologs were found across all libraries. Only 6 piRNAs were differentially dysregulated during VP<sub>AHPND</sub> infection. Based on the seed sequence complementary criteria, the target gene of piRNA was bioinformatically identified from our in-house *L. vannamei* transcriptome database. The target gene of piR-lva-29948104 and piR-lva-26449194 were E3 ubiquitin-protein ligase RNF26-like (RNF26) and circadian locomotor output cycles protein kaput-like (Clock), respectively. The expression profile of each piRNA and the corresponding targets showed the negative correlation indicating that the piRNAs might regulate those transcripts. Taken together, for the first time in shrimp this work identified piRNA and their possible role in regulating gene expression during VP<sub>AHPND</sub> infection.

**Keywords:** PIWI-interacting RNA (piRNA); *V. parahaemolyticus* AHPND (VP<sub>AHPND</sub>); small non-coding RNA

### 2.2.2 Introduction

Shrimp farming is an economically important industry, but has been affected by serious infectious disease outbreaks caused by viruses and bacteria such as white spot syndrome virus (WSSV) and pathogenic *Vibrio* species, respectively. In 2013, Thai shrimp production has declined nearly 50 percent because of “early mortality syndrome” (EMS) or “acute hepatopancreatic necrosis disease” (AHPND). Due to the adverse effect of this disease, it is necessary to understand the underlying molecular mechanisms of the shrimp immune response against *V. parahaemolyticus* AHPND (VP<sub>AHPND</sub>) infection in order to find the effective ways for the disease control.

In eukaryotes ranging from yeasts to humans, RNAi is an evolutionarily conserved mechanism that regulates gene expression and protects against transposons, viruses and bacteria. Three classes of small RNAs (sRNAs) are involved in RNAi: microRNAs (miRNAs) with a length of 18–24 nt, small interfering RNAs (siRNAs) of 21–23 nt, and PIWI-interacting RNAs (piRNAs) of 24–31 nt. The RNA interference (RNAi) pathway degrades mRNAs or inhibits their translation via gene silencing mechanism. For siRNA and miRNA, silencing occurs through RNA-induced silencing complexes (RISCs) consisting of an Argonaute protein (AGO) and a guiding small RNA (sRNA) that is antisense to the mRNA target and eventually lead to the degradation or translational inhibition of the target genes (He, Zhao, Li, & Guo, 2015). Unlike siRNAs and miRNAs, the piRNAs are unique in terms of their biogenesis process and also in the cellular processes they are involved. Particularly, piRNAs form a separate category of small RNAs being characterized by their ability to associate and interact with PIWI proteins (Iwasaki et al., 2015).

piRNA function mainly repress TEs in animal germlines via transcriptional or posttranscriptional mechanisms and maintain germline genome integrity. Production of piRNAs is dicer-independent and relies on the activity of Piwi proteins, a subclass of the AGO family (Wang et al., 2015). In *Drosophila*, biogenesis of piRNA involves two steps: primary biogenesis and the ping-pong cycle. In the primary biogenesis pathway, the piRNA precursors are transcribed from genomic clusters-loci harboring transposon fragments. Noted that, these genomic clusters provide a genetic memory of past transposition invasion. The initiation of the biogenesis process RNA polymerase II produces long precursor piRNA transcripts that may originate from diverse sources, such as piRNA clusters, individual transposon insertions or 3' UTRs of particular protein-coding genes (X. Huang, Fejes Toth, & Aravin, 2017). The primary piRNAs (pri-piRNA) are then form complex with PIWI/Aubergine (AUB) protein called the piRNA-induced silencing complex (piRISC). PIWI-piRISCs are then imported into the nucleus to transcriptionally regulate transposons. In the ping-pong cycle, the piRISC guide AUB proteins to sense strand of transposon or mRNA target in cytoplasm, upon seed sequence complementary binding. AUB proteins use their slicer activity to cleave the target sequence to generate a sense piRNA called secondary piRNA. The secondary piRNA is incorporated into AGO3 protein and binds to new complementary antisense RNA. These processes can repress transposons and increases the abundance of piRNAs capable of targeting active transposons (Hutvagner & Simard, 2008).

As stated above that the main function of piRNA is suppression of transposon activity in the germline, there have been reported that pachytene piRNAs target lncRNAs, as well as protein-coding mRNAs, and induce their repression through the slicer activity of Miwi (Watanabe, Cheng, Zhong, & Lin, 2015). In *Culex pipiens*

*pallens*, piRNA-3878 modulated pyrethroids resistance by targeting P450 (CpCYP307B1) which might be involved in ecdysone biosynthesis may be related with cuticular resistance to insecticide in *Cx. pipiens pallens* (Ye et al., 2017). A recent study has shown that host protein-coding genes are regulated by *Drosophila* piRNAs in development and stem cell (Rojas-Rios & Simonelig, 2018). In the silkworm, a Feminizer-derived piRNA targets the CDS of the *Masculinizer* mRNA and determines the sex of the silkworm (Kiuchi et al., 2014). Interestingly, piRNA became connecting with antiviral immunity in insects. Mosquito piRNAs harbouring ping-pong production-specific characteristics have also been found to be expressed in somatic tissues. The viral-specific piRNAs (vpiRNAs) are essential for mosquito survival and viral tolerance. Inhibition of vpiRNAs formation leads to extreme susceptibility to viral infections, reduction of viral small RNAs due to an impaired immune response, and loss of viral tolerance (Goic et al., 2016). The function of piRNA in antibacterial infection still has not been clearly stated. Some studies reporting many dysregulated piRNAs were found and expressed in peripheral blood, which may be associated with the pathogenesis of pulmonary tuberculosis caused by *Mycobacterium tuberculosis* (X. Zhang et al., 2019).

It has been speculated in the previous study that no shrimp piRNAs were found in virus-derived small RNAs from the penaeid shrimp *Fenneropenaeus chinensis* during acute infection of the DNA virus WSSV (C. Liu et al., 2016), perhaps due to the lack of available shrimp genome data. In the present day, thousands of piRNAs have been identified in several organisms including invertebrates such as *Drosophila melanogaster* (Khurana et al., 2011), *Pinctada fucata* (S. Huang et al., 2019) and *Biomphalaria glabrata* (Queiroz et al., 2020), but not in shrimp through the application

of high-throughput sequencing technologies. Currently, PIWI protein has been identified and characterized in *P. monodon* testis and ovary, indicating its potential role in germ cell development (Sukthaworn, Panyim, & Udomkit, 2019). This is an evidence pointing out that the PIWI-piRNA pathway might exist in shrimp.

In this study, we identified piRNA that plays important role in VP<sub>AHPND</sub> response from small RNA data of the non-lethal heat stress-treated (NLHS-VP) and VP<sub>AHPND</sub>-infected *L. vannamei* hemocytes (NLHS-VP) reported by (Boonchuen et al., 2020).

## **2.2.3 Materials and Methods**

### **2.2.3.1 Ethics Statement**

The experiments involving animals received ethical approval from Chulalongkorn University Animal Care and Use Committee (protocol review No. 1923019). The biosafety concerns of experiments performed was approved by the Institutional Biosafety Committee of Chulalongkorn University (SCCU-IBC-008/2019).

### **2.2.3.2 Shrimp rearing**

Healthy shrimps, weighing 2–4 g, were obtained from a Charoen Pokphand Foods PCL farm at Petchaburi province (Thailand) and acclimatized in rearing tanks at ambient temperature ( $30\pm 2$  °C), water salinity of 20 parts per thousand, and constant aeration before use in the experiments.

### **2.2.3.3 Bacterial challenge experiments**

The VP<sub>AHPND</sub> inoculum was prepared by culturing the bacteria overnight in 3 mL of tryptic soy broth (TSB) containing 1.5% (w/v) NaCl at 30 °C with shaking at 250 rpm. The starter culture was then transferred to 200 mL TSB with 1.5% (w/v) NaCl and further incubated at 30 °C and 250 rpm until the optical density at 600 nm (OD<sub>600</sub>) reached 2.0 (approximately 10<sup>8</sup> colony forming units [CFU]/mL). Each shrimp was then challenged with VP<sub>AHPND</sub> by immersion in the bacterial inoculum at a final concentration of 1.5×10<sup>6</sup> CFU/mL (LD<sub>50</sub>=24 h).

#### **2.2.3.4 Small RNA-Seq and data analysis**

The raw reads of our small RNA sequencing database of VP<sub>AHPND</sub>-infected non-lethal heat stress (NLHS)-treated shrimp hemocytes at 0, 6, and 24 hpi and non-heat stress (NHS)-treated shrimp hemocytes at 0 and 6 hpi reported by Boonchuen et al., 2020 were used for the analysis. Five cDNA libraries of three biological replicates included 0 NLHS-VP, 6 NLHS-VP, 24 NLHS-VP, 0 NH-VP and 6 NH-VP. The high-quality sequences that passed initial quality filters (QC=30) with lengths shorter than 24 nucleotides, and longer than 31 nucleotides, were removed. Homology search for contaminating RNA, such as mRNA, rRNA, and tRNA was conducted using BLASTn against the NCBI nucleotide and Rfam database. After discarding the contaminating RNA, the remaining sequences were searched against piRBase (<http://www.pirbase.org/>) in order to identify known piRNA homologs, non-piRNA homologs were excluded.

To characterize the nucleotide composition of piRNA homologs, we generated motif logos for the first 20 nucleotides of piRNAs using WebLogo web server version 2.8.2 (<http://weblogo.berkeley.edu/logo.cgi>). We searched the ±3 bp flanking regions

at the 5' end of the piRNA homologs to determine the position of the nucleotide with the 5' uracil. If no uracil was present, we used the first nucleotide as the start position. We then searched the adenine at the 10<sup>th</sup> position downstream from the 5' end (Perera et al., 2019). Based on the number of reads cut off >5, the piRNA homologs were further analyzed to identify the differentially expressed piRNA (DEPs) which has the specific procedures were as follows: (1) treatment and control groups were normalized to the same orders of magnitude. Formula: Normalized piRNA = piRNA reads/total reads of the sample; (2) Normalized results were used to calculate the fold change. Formula: Heat response = Normalized piRNA of 0 NLHS-VP/ Normalized piRNA of 0 NHS-VP; VP response = Normalized piRNA of 6 NHS-VP/ Normalized piRNA of 0 NHS-VP; VP/Heat response = Normalized piRNA of 6 NLHS-VP/ Normalized piRNA of 0 NLHS-VP, Normalized piRNA of 24 NLHS-VP/ Normalized piRNA of 0 NLHS-VP. DEPs were with Log2 fold change  $\geq 1$  or  $\leq -1$ . Then, Log2 fold change of DEPs were contributed by Heatmapper software (<http://www.heatmapper.ca/expression/>) (Sash et al., 2016).

#### 2.2.3.5 Quantitative real-time PCR analysis

Shrimp were challenged with VP<sub>AHPND</sub> by immersion that were inoculated with a final bacterial concentration of  $2.5 \times 10^5$  CFU/ml ( $LD_{50} = 24$  h) in the tanks as described by (Boonchuen et al., 2018). The DEPs of interest consisting of piR-lva-29948104, piR-lva-26449194, piR-lva-51554355, piR-lva-16411750, piR-lva-50211863, and piR-lva-711939 were selected for expression analysis using stem-loop RT-qPCR. The pooled total small RNA samples from 3 shrimp individuals of VP<sub>AHPND</sub>-infected shrimp hemocyte at 0, 6, and 24 hpi were prepared using the miRNA Isolation

kit (Favogen). The extracted total small RNA was then used as a template for the first strand stem-loop cDNA synthesis using the stem-loop primers (Table 2) by RevertAid First Strand cDNA Synthesis Kit (ThermoFisher Scientific). The U6 gene expression was used as an internal control. Stem-loop RT-qPCR was performed using the RT-qPCR reactions comprised of 5-fold diluted cDNA templates for each piRNA specific oligonucleotide primers (Table 2), and Lunar Universal qPCR Master Mix (New England Biolabs inc.) in the CFX96 Touch™ Real-Time PCR Detection System (Bio-Rad) under the following conditions: 95 °C for 3 min, 40 cycles of 95 °C for 30 s, 60 °C for 30 s, and 72 °C for 30 s. Relative expression was calculated by the mathematical model of Pfaffl (2001). and data were analyzed using paired-sample t-tests and are presented as means±standard deviations. The fold change of the expression level at each time point was calculated by comparing to the piRNA expression level at 0 hpi. The up- or down- regulated piRNAs upon VP<sub>AHPND</sub> infection were those that have fold changes higher or lower than 1.5. The statistical significance was determined if *P*-values were < 0.05. Experiment was performed in triplicates.

**Table 2** Primers used for the first-strand cDNA synthesis of piRNAs and qRT-PCR

Gene	Primer name	Sequence (5'-3')
piR-lva-29948104	piR-104-F	ATCAAGGCCGAGAAGCTGATGACGAGC
	piR-104-RT	GTTGGCTCTGGTGCAGGGTCCGAGGTATTTCGACC AGAGCCAAC GCTCGT
piR-lva-26449194	piR-194-F	GAAGTGGCACGGACCAGGGGAATCCGACT



	piR-194-RT	GTTGGCTCTGGTGCAGGGTCCGAGGTATTTCGCACC AGAGCCAAC AGTCGG
piR-lva-51554355	piR-355-F	CATTTAAAGTGGTACGCGAGCTGG
	piR-355-RT	GTTGGCTCTGGTGCAGGGTCCGAGGTATTTCGCACC AGAGCCAAC CCAGCT
piR-lva-16411750	piR-750-F	CCGUAAUUGCAGUACCUCCGGAUUG
	piR-750-RT	GTTGGCTCTGGTGCAGGGTCCGAGGTATTTCGCACC AGAGCCAAC CAATCC
piR-lva-50211863	piR-863-F	ACTGGCACGGACCAGGGGAATCCGACT
	piR-863-RT	GTTGGCTCTGGTGCAGGGTCCGAGGTATTTCGCACC AGAGCCAAC AGTCGG
piR-lva-711939	piR-939-F	TGAAAGACATGGGTAGTGAGATGT
	piR-939-RT	GTTGGCTCTGGTGCAGGGTCCGAGGTATTTCGCACC AGAGCCAACACATCT
	Universal primer	GTGCAGGGTCCGAGGT
U6	U6-qRTF	GTA CTTGCTTCGGCAGTACATATAC
	U6-qRTR	TGGAACGCTTCACGATTTTGC

The expression of target genes was confirmed by qRT-PCR. The pooled total RNA from VP<sub>AHPND</sub>-infected shrimp hemocyte at 0, 6 and 24 hpi is extracted using miRNA Isolation kit (Favogen). The oligo(dT) primer will be used for cDNA synthesis. The *elongation factor 1-alpha* gene (*EF1-α*) will be used as an internal control. The target genes primers were used for qRT-PCR as shown in Table 3 and the qRT-PCR condition was used as described above. Relative expression level was calculated using the mathematical model of Pfaffl (2001). Relative expression was calculated and data were analyzed using paired-sample t-tests and are presented as means±standard deviations. The fold change of the expression level at each time point was calculated by comparing to the target gene expression level at 0 hpi. The up- or down- regulated target genes upon VP<sub>AHPND</sub> infection were those that have fold changes higher or lower than 1.5, respectively. The statistical significance was determined if *P*-values were < 0.05. Experiment was performed in triplicates.

**Table 3 Primers used for top3 target genes of interesting piRNA in qRT-PCR**

Gene	Primer name	Sequence (5'-3')
Cell wall protein IFF6	CWP_qPCR_F	CTCAACTAGCAACGCAAACG
	CWP_qPCR_R	TTATTCGAGGCTCCACTTGC
Probable dual specificity protein kinase madd-3	Kimadd3_qPCR_F	GATAAGGCGCTGCTTTTGAC
	Kimadd3_qPCR_R	AACAGCGGTTTAGGATGTCTG
E3 ubiquitin-protein ligase RNF26-like	E3ubiquitin_qPCR_F	AGGCAACGATTCTCAGATG
	E3ubiquitin_qPCR_R	TGATCCACCTGCTCTGTTTG
Attractin	Attractin_qPCR_F	TGAAGATTGTCCGGGTTAGG
	Attractin_qPCR_R	TGAAGGCAAGGTTGATAGG
Circadian locomoter output cycles protein kaput	Clock_qPCR_F	AACAGCAGCAACAGCAACAG
	Clock_qPCR_R	CCATCATCTGCATGAACTGG
Insulin-like growth factor-binding protein complex	IGFALS_qPCR_F	TCATGAAACTGCACGGACTC
	IGFALS_qPCR_R	TGTCGTTGTCTCGCAAGTTC
Epidermal growth factor receptor	EGFR_qPCR_F	ACAATGCTGAAGGTGGAAGC
	EGFR_qPCR_R	TCAGGGGAACATTCTCGAAC
Cholinesterase 1	ACHE_qPCR_F	ACAACCGTGTGACATCATC
	ACHE_qPCR_R	TCACCAATGAGCTTGACCAG
Bile salt-activated lipase	BSDL_qPCR_F	CGATTTGCAGTACCTGTTCG
	BSDL_qPCR_R	TGAAAACGCTCTGGGTACAG
<i>LvEF1-<math>\alpha</math></i>	EF1- $\alpha$ -F	CGCAAGAGCGCAACTATGA
	EF1- $\alpha$ -R	TGGCTTCAGGATACCAGTCT

### 2.2.3.6 piRNA target prediction

The piRNA targets were identified by comparing the piRNA sequences with transcribed database from *L. vannamei* genome (<http://www.shrimpbaseset.net/vannamei.html>) using CU-Mir software developed by our research group (<https://cumir.shrimp-genomes.org/>). The criteria used for the analysis was 1) the primary seed sequences (position 2-10 nt from 5' end) of piRNA can bind perfectly complementary and 2) at any different region on an open reading frame (ORF), 3'-untranslated region (UTR) and 5'-UTR. 3) The percent total length complementary cutoff was set at 65%. RNAhybrid software (<http://bibiserv.techfak.uni-bielefeld.de/rnahybrid/>) was also used to computationally predict piRNA/target

gene interaction by using a free energy of  $< -20.0$  kcal/mol (Kaewkascholkul et al., 2016).

### **2.2.3.7 piRNA/mRNA interaction network analysis.**

In order to define all possible DEPs-mRNA interactions involved in immune-related genes. mRNA targets were searched to identify their gene functions and classified as “Defense & Homeostasis”, “Energy & Metabolism”, “Cell cycle & DNA Synthesis/repair”, “Gene expression, regulation & protein synthesis, degradation”, “Receptor”, “Signaling & communication”, “Transport”, “Adhesive protein”, “Structural & cytoskeleton related proteins”, and “Unknown”. Subsequently, the DEPs/mRNA network were built using Cytoscape v3.8.2 software. The number of interactions between DEPs and their target gene functions were analyzed using Degree sorted layout tool. The size of node vary according to the number of interaction identified. Based on percent complementary, top 3 of target gene based on percent complementary of each interesting DEPs were selected and further validated the expression level by qRT-PCR as described above.

## **2.2.4 Results**

### **2.2.4.1 Sequence analysis of shrimp piRNAs**

The small RNA libraries of VP<sub>AHPND</sub>-infected NLHS-treated shrimp hemocyte at 0, 6, and 24 hpi was constructed by Boonchuen et al., 2020 (Boonchuen et al., 2020). To identify shrimp piRNAs, the raw reads were reanalyzed. After 5'-, 3'-adapter trimming and quality control filtering. The 1,086,629 total raw reads in the 0 NHS-VP,

879,272 in the 6 NHS-VP, 1,114,328 in the 0 NLHS-VP, 931,638 in 6 NLHS-VP and 1,252,728 in the 24 NLHS-VP were obtained. The 24-31 nt long sequence were selected and the size distribution were shown in Fig. 12A. Searching the NCBI nucleotide database revealed that, on average, 25% of the sequences were most likely contaminating RNAs (Fig. 12B). After removal of contaminating mRNA, rRNA, and tRNA homologs, the final counts of total sequences were 161,305; 31,806 in the 0 NHS-VP, 52,321 in the 6 NHS-VP, 42,585 in the 0 NLHS-VP, 31,300 in the 6 NLHS-VP and 3,293 in the 24 NLHS-VP. The small RNAs were mapped to piRBase identifying 150 piRNA homologs. The 338 total read counts of matched mature piRNA sequences were 82, 67, 91, 91 and 7, respectively, for the 0 NHS-VP, 6 NHS-VP, 0 NLHS-VP, 6 NLHS-VP, 24 NLHS-VP libraries (Table 4). Furthermore, in VP<sub>AHPND</sub>-infected shrimp hemocyte, 220 reads of piRNA-like transcript contain uridine signature at position 1 of the 5' end while 128 reads contain an adenosine signature at the 10<sup>th</sup> position downstream of the 5' end (Fig. 13).

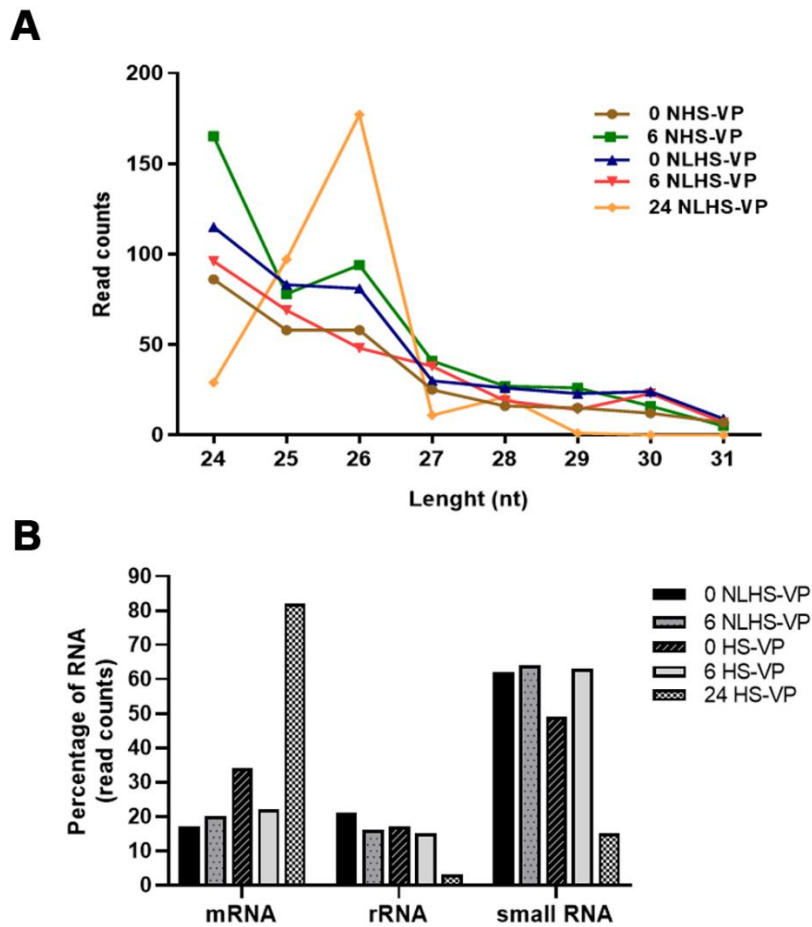


**Fig 12. Length distribution, abundance and compositions of small RNA size of 24 to 31 nt from libraries of VP<sub>AHPND</sub>-infected NHS-treated and VP<sub>AHPND</sub>-infected NLHS-treated *L. vannamei* hemocytes. (A) Length distribution and abundance of small RNAs from hemocytes of NHS-treated *L. vannamei* infected with VP<sub>AHPND</sub> at 0 (0 NHS-VP) and 6 (6 NHS-VP) hpi and NLHS-treated *L. vannamei* infected with VP<sub>AHPND</sub> at 0 (0 NLHS-VP), 6 (6 NLHS-VP) and 24 (24 NLHS-VP) hpi. (B) Composition of RNAs in each small RNA-Seq library.**

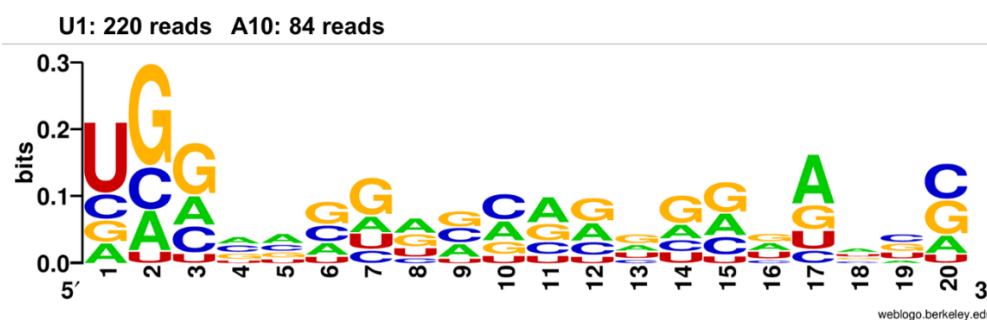


**Fig 13. piRNA characteristics.** Sequence logos of piRNA homologs. The sequence motifs were generated using the first 20 bp from the 5' end of piRNA homologs, allowing for  $\pm 3$  bp flanking region to determine the strand direction. The number of reads indicate a uridine signature at the 5' end (U1) and an adenine at the 10th position (A10).

**Table 4** Summary of sequences identified from small RNA libraries of heat and non-lethal heat- and non-heat stress treated *L. vannamei* after challenged with AHPND at 0, 6 and 24 hpi.

Type	Total Reads				
	0 NHS-VP	6 NHS-VP	0 NLHS-VP	6 NLHS-VP	24 NLHS-VP
Raw Reads	1086629	879272	1114328	931638	1252728
Passed-filter reads	948089	771799	956249	817019	1104193
Trimmed 3' and 5' adapter	42585	31300	40470	31,806	52321
Clean Reads	31806	52321	42585	31300	3293
Contaminating RNA	116	161	198	116	284
Unknown small RNA	193	282	193	198	52
piRNA Homolog	82	67	91	91	7
Non-piRNA homolog	88	115	102	108	45

NHS, non-heat stress; NLHS, non-lethal heat stress; VP, *Vibrio parahaemolyticus*

#### **2.2.4.2 Differentially expressed piRNAs (DEPs) in NHS-treated and NLHS-treated *L. vannamei* upon VP<sub>AHPND</sub> challenge.**

A piRNA was considered differentially expressed when the absolute value of log<sub>2</sub> fold change ratio of piRNA in the control (0 hpi) and experimental (6 hpi and 24 hpi) libraries is greater than 1 or lower than -1 ( $\geq 1$  or  $\leq -1$ ). Totally, 14 piRNAs were found to be differential expression upon heat and VP<sub>AHPND</sub> infection. Expression of 8 piRNAs were altered (4 up-regulated and 4 down-regulated piRNAs) in response to heat only (0 NHS-VP vs 0 NLHS-VP). All the DEPs were also clustered in a hierarchical heatmap where expression values are reported as Log<sub>2</sub> fold change values. As a result of VP<sub>AHPND</sub> infection both in non-heated and heated condition (0 NHS-VP vs 6 NHS-VP and 0 NLHS-VP vs 6, 24 NLHS-VP), only 6 piRNAs were found to be differentially expressed. In this study, we focused on VP<sub>AHPND</sub>-responsive piRNA; therefore, only 6 DEPs of VP response and VP/heat response groups were further analyzed and are listed in Table 5. As shown in the heatmap (Fig. 14) VP- and VP/heat-responsive piRNAs, included 2 up-regulated and 4 down-regulated piRNAs.

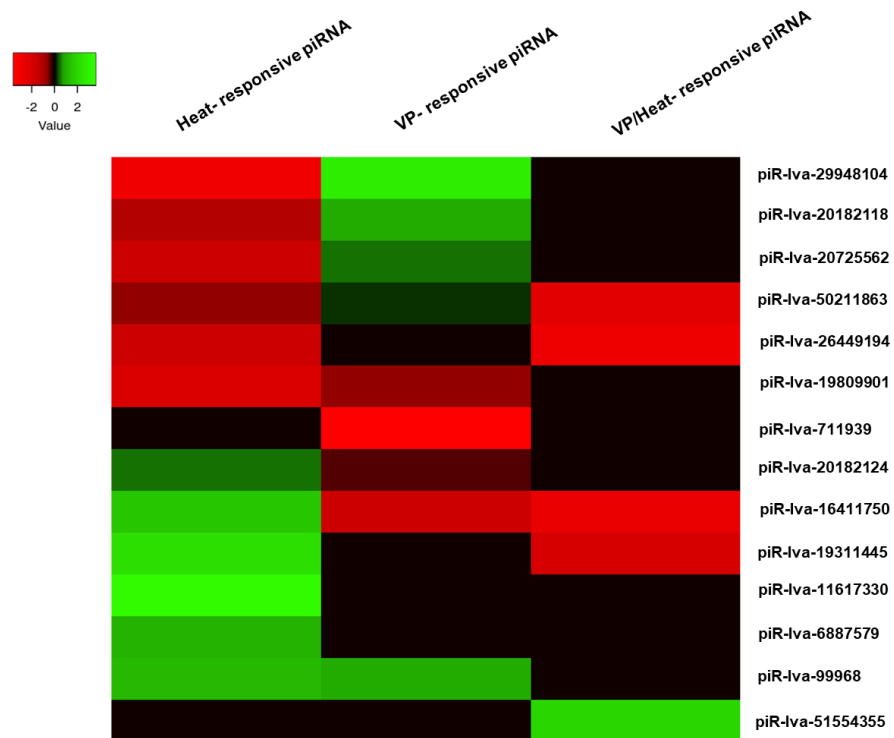


**Fig 14. Differential expression of piRNAs.** Heatmaps representing differentially expressed piRNAs that are considered as Heat-, VP-, and VP/Heat- responsive piRNAs with the fold change  $\geq 2$  or  $\leq -2$  and  $P$ -value  $< 0.05$ .



**Table 5** List of differentially expressed piRNAs

Response to	piRNA name	piRNA homolog	Sequence (5'-3')
Heat stress	piR-lva-20182118	piR-dme-20182118	TGGACGGAGAACTGATAAGGGCAT
	piR-lva-20182124	piR-dme-20182124	TGGACGGAGAACTGATAAGG
	piR-lva-11617330	piR-dme-11617330	AGGCACTGGAGGACCGAACCCACGTCT
	piR-lva-19311445	piR-mmu-19311445	TGCCCGATCGTCTAATGGCAGGACCGCT
	piR-lva-20725562	piR-dme-20725562	ATTGTACTIONCATCAGGTGCTCGGT
	piR-lva-6887579	piR-dme-6887579	TGAGATCATTGTGAAAGCTG
	piR-lva-19809901	piR-dme-19809901	TATCACAGCCAGCTTTGATGAGCG
	piR-lva-99968	piR-gga-99968	AGCTTGGACTATAGGATGGCTTGAG
VP	piR-lva-29948104	piR-mmu-29948104	ATCAAGGCCGAGAACTGATGACGAGC
	piR-lva-711939	piR-bmo-711939	TGAAAGACATGGGTAGTGAGATGT
VP/Heat stress	piR-lva-26449194	piR-mmu-26449194	ACTGGCACGGACCAGGGGAATCCGACT
	piR-lva-51554355	piR-mmu-51554355	CATTAAAGTGGTACGCGAGCTGG
	piR-lva-16411750	piR-dme-16411750	CCGGTATTGCAGTACCTCCGGGATTG
	piR-lva-50211863	piR-mmu-50211863	ACTGGCACGGACCAGGGGAATCCGACT

piRNA homologs is identified from piRBase and the best hits were selected based on % identity ( $\geq 90\%$ ).

#### 2.2.4.3 RT-qPCR validation of significant differentially expressed piRNAs (DEPs)

In order to confirm the expression of interesting DEPs that are expressed in response to VP<sub>AHPND</sub> infection, the expression profiles of 6 DEPs (piR-lva-29948104, piR-lva-26449194, piR-lva-51554355, piR-lva-16411750, piR-lva-50211863, and piR-lva-711939) were analyzed using stem loop RT-qPCR. The expression levels of 3 piRNAs (piR-lva-29948104, piR-lva-26449194 and piR-lva-51554355) were significantly upregulated after VP<sub>AHPND</sub> infection by about 1.5- to 600-fold in accordance with the small RNA-Seq data (Fig. 15). The piR-lva-29948104 expression was significantly up-regulated after VP<sub>AHPND</sub> infection at 6 and 24 hpi about 4- fold.

The piR-lva-26449194 expression were significantly up-regulated after VP<sub>AHPND</sub> infection at 6 and 24 hpi about 2.5- and 1.5- fold. The piR-lva-51554355 expression was significantly up-regulated after VP<sub>AHPND</sub> infection at 6 and 24 hpi about 600- and 300- fold. In contrast, another 3 piRNAs were not significantly changed after VP<sub>AHPND</sub> infection (piR-lva-16411750, piR-lva-50211863, and piR-lva-711939) and not correlated with the small RNA-Seq data. The piR-lva-16411750 expression was not significantly changed after VP<sub>AHPND</sub> infection while the small RNA-Seq data showed it was down-regulated after VP<sub>AHPND</sub> infection at 6 hpi about 0.25- fold. The piR-lva-50211863 expression was not significantly changed after VP<sub>AHPND</sub> infection whereas the small RNA-Seq data showed it was up-regulated after VP<sub>AHPND</sub> infection at 6 hpi about 1.2- fold. The piR-lva-711939 was not significantly changed after VP<sub>AHPND</sub> infection, but the small RNA-Seq data showed it was down-regulated after VP<sub>AHPND</sub> infection at 6 hpi about 0.1- fold.

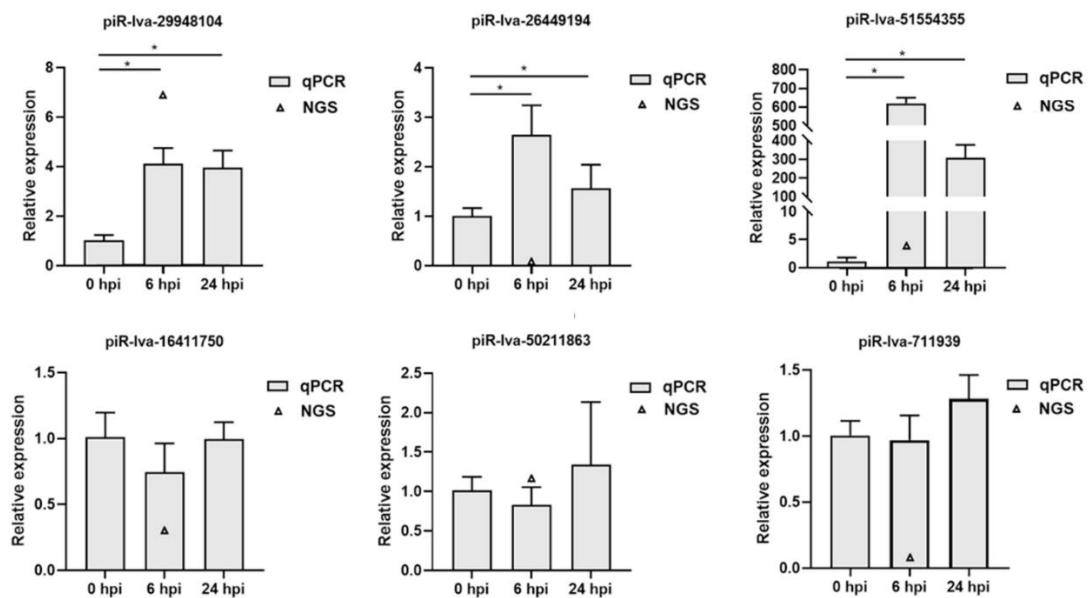


**Fig15. Relative expression analysis of piRNAs in response to VP<sub>AHPND</sub> infection in *L. vannamei* hemocytes.** Total small RNAs from hemocytes of VP<sub>AHPND</sub>-infected *L. vannamei* at 0, 6, and 24 hpi were used as templates for specific stem-loop first strand cDNA synthesis. Relative expression levels of 6 DEPs were determined by qRT-PCR and normalized against expression level of U6, the internal reference. The bar graphs represent means±standard deviations and triangles (▲) are data from the small RNA-Seq. The results were derived from triplicate experiments. Asterisks indicate significant differences ( $P < 0.05$ ) from the respective VP<sub>AHPND</sub>-infected shrimp at 0 hpi.

#### 2.2.4.4 Target gene of upregulated- piRNA in response to VP<sub>AHPND</sub> infection

Target mRNAs from the transcriptome of shrimp genome were analyzed using CU-mir software. This analysis facilitated the identification of specific piRNA-mRNA interactions, which then served as a clue to the general regulatory mechanisms underlying the immune response of shrimp under the VP<sub>AHPND</sub> infection. Table 6 shows the list of DEP target genes. The piRNA/target mRNA interaction network was then analyzed by Cytoscape v3.8.2 program. Among target genes identified, the biological functions of the target genes can be identified into “Defense & Homeostasis”, “Energy & Metabolism”, “Cell cycle & DNA Synthesis/ repair”, “Gene expression & Protein synthesis/degradation”, “Receptor”, “Signaling & Communication”, “Transporter”, and “Unknown”. Several piRNAs such as piR-lva-99968, piR-lva-20182118, piR-lva-11617330, piR-lva-51554355, piR-lva-29948104, piR-lva-26449194, and piR-lva-711939 had high degrees of connectivity and might play crucial roles in the shrimp immune regulatory network during VP<sub>AHPND</sub> infection. Meanwhile, genes involved in “Gene expression & Protein synthesis/degradation”, “Energy & Metabolism”, and “Defense & Homeostasis” were the most common piRNA targets (Fig. 16A). The top three target genes of each significantly expressed piRNAs were selected based on percent complementary to validate target gene expression levels (Fig. 16B). To further confirm prediction results, the spontaneous occurrence of the piRNA/target mRNA interaction was determined by RNAhybrid software. The results showed that piRNAs and the top3 target genes interaction have low mfe (approximately < -20 kcal/mol) (Fig. 17).

**Table 6** List of six VP<sub>AHPND</sub> responsive DEPs and its top3 target genes

piRNA name	Top3 target genes	Binding region
piR-lva-29948104	Cell wall protein IFF6	ORF
	Probable dual specificity protein kinase madd-3	ORF
	E3 ubiquitin-protein ligase RNF26-like	3' UTR
	Attractin	ORF
piR-lva-26449194	Circadian locomoter output cycles protein kaput	ORF
	Insulin-like growth factor-binding protein complex	5' UTR
piR-lva-51554355	Epidermal growth factor receptor	ORF
	Cholinesterase 1	ORF
	Bile salt-activated lipase	ORF
piR-lva-16411750	Triosephosphate isomerase A-like	ORF
	Triosephosphate isomerase B-like	ORF
	Vang-like protein 2	ORF
piR-lva-50211863	Armadillo segment polarity protein-like	ORF
	COP1-interactive protein 1-like	ORF
	Protein singed wings 2-like	ORF
piR-lva-711939	Transcription factor SOX-4-like	3' UTR
	MFS-type transporter SLC18B1-like	3' UTR
	Caspase-1-like	3' UTR

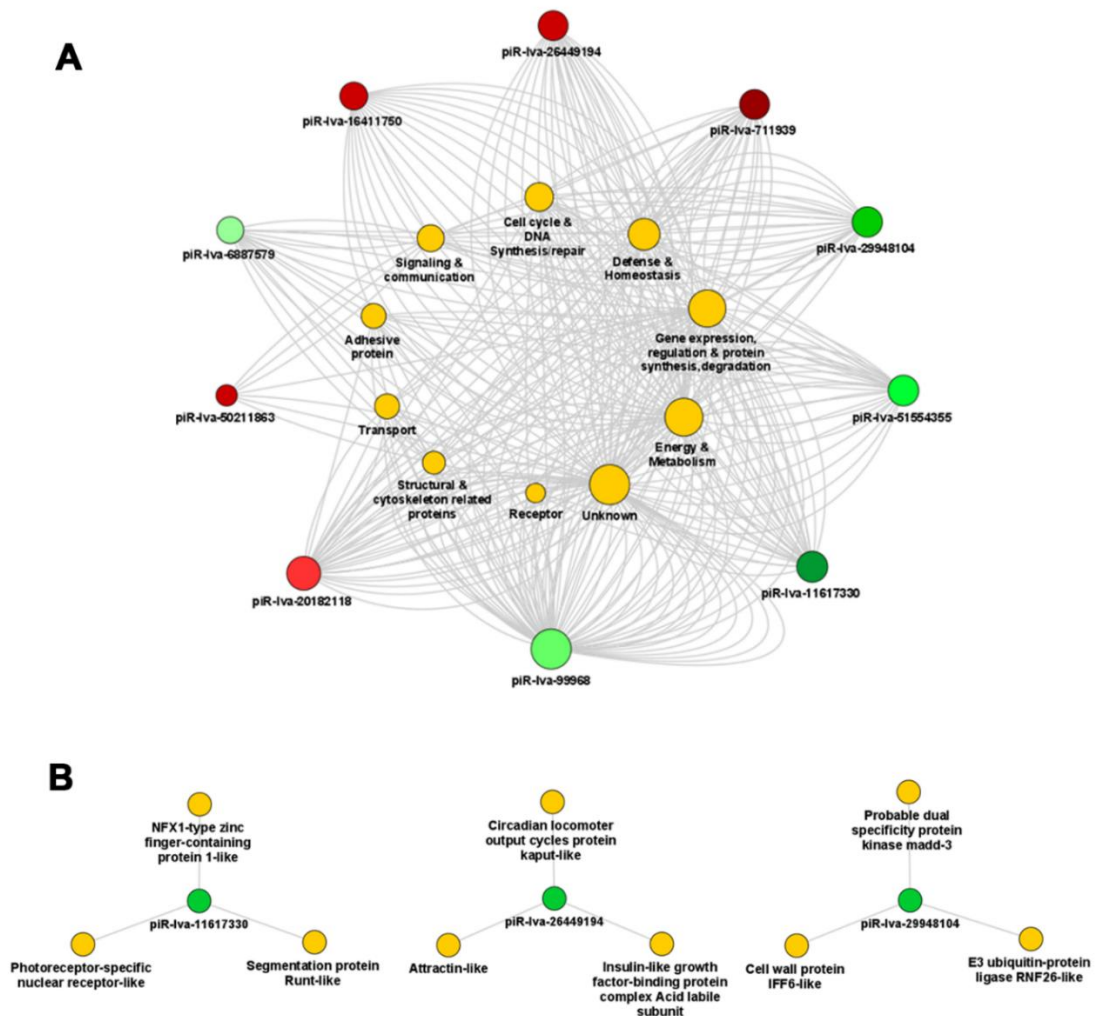


**Fig 16. Network analysis for piRNA/mRNA interaction.** (A) The piRNA/mRNA network based on the predicted DEP target function. The up-regulated piRNAs are green circle and down-regulated genes are red circle, whereas yellow circles are target functions. The darker color represents a higher differential expression while the lighter color represents a lower differential expression. The degree of connectivity, which represents the number of genes regulated by a given piRNA, is indicated by the size of the node. (B) The network of each significantly expressed piRNA and their top3 target genes based on percent complementary. The green and yellow circular nodes represent the up-regulated piRNA and their target genes, respectively.

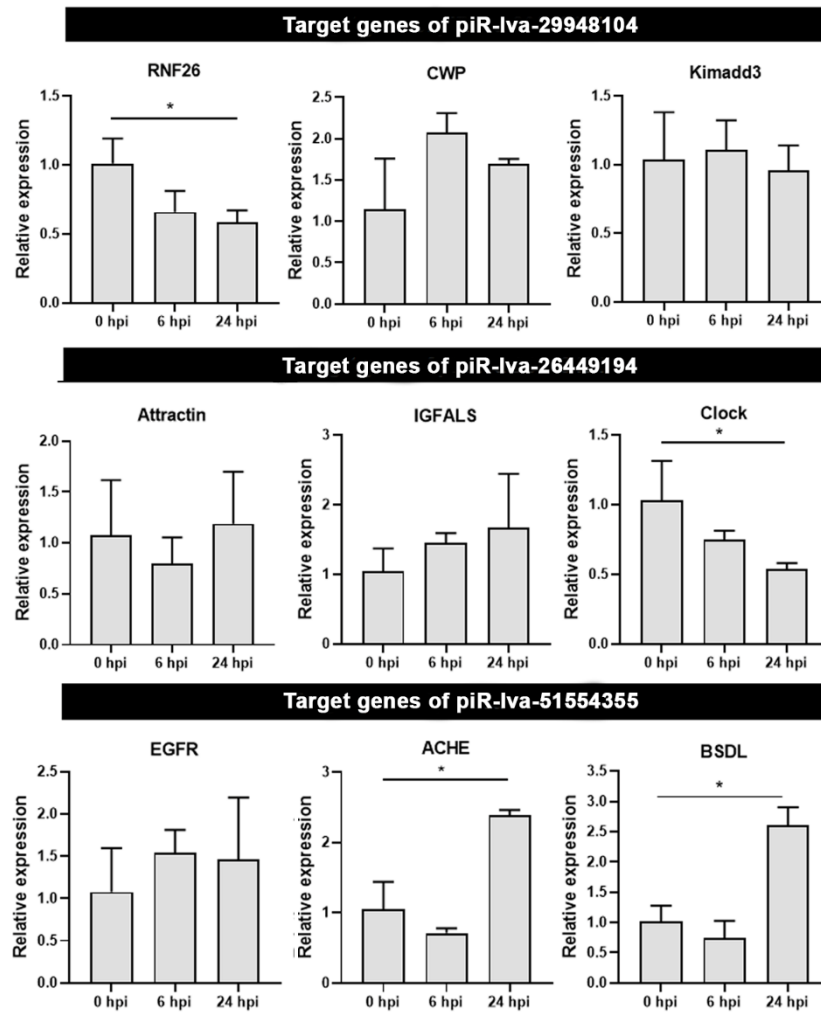


**Fig 17. piRNA/mRNA interaction analysis.** The top3 mRNA target of (A) piR-lva-29948104, (B) piR-lva-26449194 and (C) piR-lva-51554355 were predicted using RNAhybrid software.

#### 2.2.4.5 Validation of target gene expression

To validate the expression level of target genes with the predicted negative correlation with the piRNA expression level due to target gene expression regulated by piRNA, the top three target genes of each upregulated piRNA were selected and confirmed their expression level using specific primers as shown in Table 2. Fig. 18 shows the expression profile of target genes in VP<sub>AHPND</sub>-infected shrimp hemocyte at 0, 6, 24 hpi. The expression profile of RNF26, which is piR-lva-29948104 target gene, was down-regulated at 24 hpi during VP<sub>AHPND</sub> infection whereas other target genes were not significantly changed upon VP<sub>AHPND</sub> infection. RNF26 involved in gene expression & protein synthesis/degradation. Looking at the piR-lva-26449194 targets, Attractin and IGFALS, which are involved in defense & homeostasis and energy & metabolism, respectively, were not changed in expression upon VP<sub>AHPND</sub> infection. Meanwhile, Clock which is involved in gene expression & protein synthesis/degradation was down-regulated at 24 hpi. For piR-lva-51554355 targets, EGFR, ACHE and BSDL were significantly up-regulated in expression upon VP<sub>AHPND</sub> infection.





จุฬาลงกรณ์มหาวิทยาลัย

**Fig 18. Relative expression analysis of target genes in the VP<sub>AHPND</sub> infection.**

Expression level of E3 ubiquitin-protein ligase RNF26-like (RNF26), Cell wall protein IFF6 (CWP), Probable dual specificity protein kinase madd-3 (Kimadd3), Attractin-like (Attractin), Insulin-like growth factor-binding protein complex acid labile subunit (IGFALS), Circadian locomotor output cycles protein kaput (Clock), Epidermal growth factor receptor-like (EGFR), Cholinesterase 1 (ACHE) and Bile salt-activated lipase (BSDL) was determined by RT-qPCR in the hemocytes of VP<sub>AHPND</sub>-challenged *L. vannamei* at 0 hpi, 6 hpi and 24 hpi. Relative expression ratios are calculated using *Ef1-α* as the internal control. Relative expression level of each gene in hemocytes of

*L. vannamei* challenged with VP<sub>AHPND</sub> at each time point after infection was normalized to that of 0 hpi to determine the effect of VP<sub>AHPND</sub> challenge. The results were derived from triplicate experiments. Asterisks indicate significant differences at  $P < 0.05$  from the 0 hpi.

### 2.2.5 Discussion

The AHPND is known to be caused by VP<sub>AHPND</sub>, which accumulates in the stomach of shrimp and secretes PirAB<sup>VP</sup> toxins into circulation. PirAB<sup>VP</sup> toxins dose affect not only the digestive tracts of shrimp (i.e., stomach, hepatopancreas, etc.) (Kumar et al., 2019; Lai et al., 2015) but also hemocyte through binding of *Lv*APN1 receptor (Luangtrakul et al., 2021). There are several mechanisms involved in defense against VP<sub>AHPND</sub> infection such as activation of Toll and IMD pathways to produce antimicrobial peptides (AMPs) (Yeh et al., 2016), dysregulation of apoptosis-related genes in hemocyte (Z. Zheng et al., 2021) and non-coding small RNA that regulate gene expression (Boonchuen et al., 2020; Velazquez-Lizarraga et al., 2019; H. Zheng et al., 2018). The miRNA and mRNA interactions contribute to the modulation of NLHS-induced immune responses enhancing VP<sub>AHPND</sub> resistance in *L. vannamei* (Boonchuen et al., 2020). Although, it has been reported that no piRNA expression during acute infection of the DNA virus WSSV in *Fenneropenaeus chinensis* (C. Liu et al., 2016), the PIWI-interacting proteins that is participate in piRNA biogenesis and reproductive regulation, *PmPiwiI*, was found in gametogenesis *P. monodon* (Sukthaworn et al., 2019). Therefore, it is believed that piRNAs exist and play crucial role in gene regulation like what have been reported in other organisms (Lim, Anand,

Nishimiya-Fujisawa, Kobayashi, & Kai, 2014; Mohn, Handler, & Brennecke, 2015). In this study, we identified 150 piRNA homologs of 338 reads of hits and 458 reads of non-piRNA homologs from small RNA libraries of the NLHS-treated and VP<sub>AHPND</sub>-infected *L. vannamei* hemocytes (NHS-VP) (Table 3). piRNA characteristics were detected from those piRNA homologs identified in VP<sub>AHPND</sub>-infected *L. vannamei* hemocytes (Fig. 13). This is supported by several reports indicating that somatic piRNAs serve as primary piRNAs and prefer a uridine at position 1 of the 5' end. Some piRNAs contain an adenine at the 10<sup>th</sup> position (Ortoger et al., 2014; Perera et al., 2019). Although, the main function of piRNA is the silencing of transposable elements (TE) in the germline of animals, but it also silences mRNAs of mosquito protein-coding genes or non-retroviral endogenous virus elements, as well as viral replication intermediates produced during infection (Miesen, Joosten, & van Rij, 2016).

Previous study, Zhang et al. (2019) found piRNA responded to pulmonary tuberculosis causing by *Mycobacterium tuberculosis*. The piRNA mainly involved in transcription and protein binding in human peripheral blood (X. Zhang et al., 2019). In *C. elegans*, bacterial infection suppresses the downregulation of piRNAs by temperature stress (Belicard, Jareosettasin, & Sarkies, 2018). Among 150 piRNA homologs, 2 DEPs were upregulated and 4 DEPs were downregulated in response to VP<sub>AHPND</sub> infection (Fig. 14). These six highly conserved piRNA homolog sequences have already been described in *Mus musculus* (De Fazio et al., 2011), *Drosophila melanogaster* (fruit fly) (Olovnikov et al., 2013) and *Bombyx mori* (silkworm) (Xiol & Pillai, 2012). Noted that, in the current study, only piRNA homologs were reported. The remaining unknown sequences will be further analyzed against *L. vannamei*

genome to determine whether they are novel host piRNAs by computational prediction techniques.

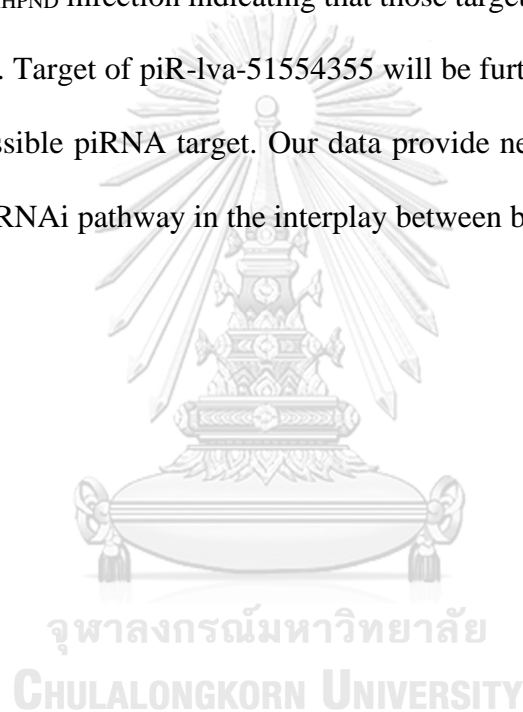
The piRNA expression level in hemocyte of VP<sub>AHPND</sub>-challenged *L. vannamei* were determined by stem-loop real-time qRT-PCR. Three out of 6 selected piRNAs from *L. vannamei* hemocyte were differentially expressed upon VP<sub>AHPND</sub> infection (Fig. 15). According to our report, the expression of piR-lva-29948104, piR-lva-26449194 and piR-lva-51554355 were increased after challenge with the AHPND-causing bacteria, but there are no reports their expression in other organisms. This result indicated that piRNAs might be involved in VP<sub>AHPND</sub> infection. In order to characterize piRNA function in shrimp bacterial response against VP<sub>AHPND</sub> infection, the target mRNAs of each piRNA were predicted. Since *L. vannamei* genome sequence is available, transcribed database was used in this analysis, the following criteria were taken into consideration: the perfect complementary match of piRNA seed sequence to target gene and the thermal stability of piRNA/mRNA duplex. Here our interactome showed that the predicted targets of VP<sub>AHPND</sub>-responsive piRNAs are protein-coding genes involving in several biological processes (Fig. 16A) such as gene expression & protein synthesis/degradation, energy & metabolism, and defense & homeostasis. In pulmonary tuberculosis patient, target genes of piRNAs were mainly involved in transcription and protein binding, which were enriched in many pathways related with immunity (Song et al., 2019). Most piRNAs target to 3' UTR of mRNA (Gainetdinov, Colpan, Arif, Cecchini, & Zamore, 2018; X. Z. Li, Roy, Moore, & Zamore, 2013). However, 3' UTR is not the only binding region for piRNAs, there is also sites located in 5'UTR or even within coding DNA sequence of mRNAs (Sarkar, Maji, Saha, & Ghosh, 2014). From our piRNA target prediction, the analyzed piRNAs were found to

target at all three regions of the mRNA including 3' UTR, ORF and 5' UTR (Table 6). To analyze the putative target mRNA for the differential expressed piRNAs, the expression level of top3 target genes of selected piRNAs were validated. Negative correlations were identified in the piRNA-mRNA pairs, which can be considered as evidence of piRNA targeting (X. Z. Li et al., 2013).

As previously report, ubiquitination plays a crucial role in regulating vital processes such as the cell cycle, cell signaling, and cell survival/death (Guo & Tadi, 2021). Ubiquitination is a major pathway in the elimination of accumulated toxic proteins and targeting of damaged proteins for degradation (Huang et al., 2010). RING finger proteins or RNF are often involved in the ubiquitin-mediated protein degradation pathway. RNF166 has been reported as a crucial role in RNA virus-induced innate immune responses and antibacterial autophagy. (Heath et al., 2016). In mammalian, RNF26 temporally regulates virus-triggered induction of type I IFNs. Knockdown of RNF26 promoted degradation of MITA (also known as STING) that acts as a scaffold protein to facilitate the phosphorylation of interferon regulatory factor 3 (IRF3) and STAT6. This suppression inhibited viral infection (Qin et al., 2014). However, no studies have elucidated the role of RNF26 in responding to bacterial infection. For our prediction, down-regulation of RNF26 targeted by piR-lva-29948104 might be involved in bacterial infection.

For Clock, the circadian clock regulates many aspects of immunity in plants and animals. Bacterial infections are affected by time of day, but the mechanisms involved remain undefined. Previously, *Drosophila* mutants lacking the circadian regulatory proteins Timeless and Period are sensitive to infection by *S. Pneumoniae* (Stone et al.,

2012). Recently, Kitchen et al., 2020 revealed that core clock protein BMAL1 regulates RhoA-dependent macrophage motility and bacterial engulfment, and loss of BMAL1 enhances antibacterial immunity (Kitchen et al., 2020). Taken together, it is interesting to further characterize the function of Clock, targeted by piR-lva-26449194, that probably enhance or inhibit antibacterial mechanism somehow. For target genes of piR-lva-51554355, the expression level of top3 target genes have not been changed in responding to VP<sub>AHPND</sub> infection indicating that those target genes are not regulated by piR-lva-51554355. Target of piR-lva-51554355 will be further selected to increase the opportunity of possible piRNA target. Our data provide new insights into the role of the piRNA-based RNAi pathway in the interplay between bacteria and shrimp.



## CHAPTER III

### CONCLUSIONS

#### 3.1 Conclusions

##### **3.1.1 Cytotoxicity of *Vibrio parahaemolyticus* AHPND toxin on shrimp hemocytes, a newly identified target tissue, involves binding of toxin to aminopeptidase N1 receptor**

This research identified VP<sub>AHPND</sub> toxin receptor namely “LvAPN1” from VP<sub>AHPND</sub>-infected *L. vannamei* hemocyte transcriptome. Suppression of LvAPN1 reduced the number of AHPND virulence plasmids in stomach and occurrence of AHPND clinical sign, sustained the number of total hemocyte count, and elevated the number of viable hemocyte. We demonstrated that VP<sub>AHPND</sub> toxin challenge induces hemocyte cell damage and it interacts with LvAPN1 *in vitro*. Collectively, our finding suggested that not only stomach and hepatopancreas but also hemocyte are the VP<sub>AHPND</sub> target tissues where LvAPN1 serves as a VP<sub>AHPND</sub> toxin receptor. This study provides novel insight into the contributions of LvAPN1 receptor towards the AHPND pathogenesis in shrimp and may extend to the development of AHPND preventive measure in shrimp.

### 3.1.2 Identification of novel shrimp PIWI-interacting RNA (piRNA) involved in *Vibrio parahaemolyticus* AHPND infection

This research predicts novel small RNA-based shrimp immunity called piRNA from VP<sub>AHPND</sub>-infected *L. vannamei* hemocyte small RNA sequencing. Six differentially expressed piRNAs were dysregulated in responding to VP<sub>AHPND</sub> infection. In addition, three out of 6 differentially expressed piRNAs were significantly upregulated during VP<sub>AHPND</sub> infection. Interestingly, piR-lva-26449194 and piR-lva-51554355 target protein-coding gene (RNF26 and Clock) in negative correlation, which involved in gene expression and protein synthesis/degradation during VP<sub>AHPND</sub> infection suggesting that these piRNA might regulate gene expression in shrimp immunity.

## 3.2 Research limitations

### 3.2.1 Cytotoxicity of *Vibrio parahaemolyticus* AHPND toxin on shrimp hemocytes, a newly identified target tissue, involves binding of toxin to aminopeptidase N1 receptor

In this study, we discovered *Lv*APN1 act as the VP<sub>AHPND</sub> toxin receptor in hemocyte. The present of *Lv*APN1 caused the severe damage of hemocyte, reduction of shrimp mortality and clinical sign of AHPND. The result from ELISA assay showed that rPirA<sup>VP</sup> and rPirB<sup>VP</sup> directly bind to truncated-r*Lv*APN1. However, the interaction between truncated-*Lv*APN1 and heterodimer of rPirA/B<sup>VP</sup> was not performed due to PirA/B<sup>VP</sup> complex is unstable and has a low binding affinity *in vitro*. The *Lv*APN1-PirA/B<sup>VP</sup> toxin interaction would be more clearly understand if we can confirm their interaction.



### **3.2.2 Identification of novel shrimp PIWI-interacting RNA (piRNAs) involved in *Vibrio parahaemolyticus* AHPND infection**

We found 150 piRNA homologs out of about 5 million sequences from 5 libraries of NLHS-VP shrimp and NHS-VP shrimp. Only 6 piRNAs were dysregulated in responding to VP<sub>AHPND</sub> infection. According to the low amounts VP<sub>AHPND</sub>-responsive piRNA, this is the limitation to obtain the interesting piRNA involving in shrimp immunity or VP<sub>AHPND</sub> infection. The first reason is that several novel piRNAs have not been annotated in piRNA database yet resulting in the piRNA homologs were less identified. Another reason is that most common piRNAs are well known to regulate and suppress TE, but it has a few studies of protein-coding gene targeting identification when compare to other small RNA like miRNA, which are well study in protein-coding gene regulation.

### **3.3 Suggestions in research or perspective for further research**

#### **3.3.1 Cytotoxicity of *Vibrio parahaemolyticus* AHPND toxin on shrimp hemocytes, a newly identified target tissue, involves binding of toxin to aminopeptidase N1 receptor**

3.3.1.1 According to Cry toxin mode of actions, there are other receptors involving in pore formation besides APN. Thus, we would like to identify VP<sub>AHPND</sub> toxin candidate receptors such as Cadherin and further determine VP<sub>AHPND</sub> toxin oligomerization.

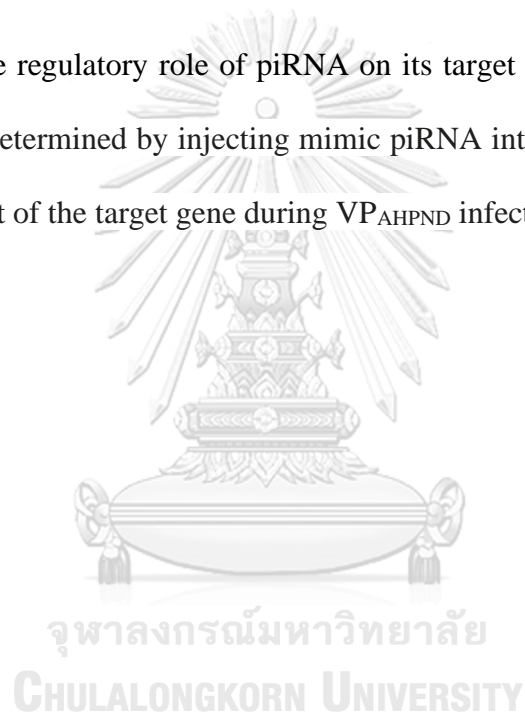
3.3.1.2 Our hypothesis of VP<sub>AHPND</sub> toxin pathogenesis is that once VP<sub>AHPND</sub> infects the shrimp, toxin might cause systematic damage in all shrimp tissue because LvAPN1 is expressed in all immune-related tissues. Therefore, this hypothesis needs to

be proved by *in situ* hybridization via tracking VP<sub>AHPND</sub> toxin localization in *Lv*APN1-silenced shrimp cephalothorax.

### **3.3.2 Identification of novel shrimp PIWI-interacting RNA (piRNA) involved in *Vibrio parahaemolyticus* AHPND infection**

3.3.2.1 Interaction of piRNA on its target will be validation by Luciferase reporter system

3.3.2.2 The regulatory role of piRNA on its target in shrimp during VP<sub>AHPND</sub> infection will be determined by injecting mimic piRNA into shrimp and investigating the silencing effect of the target gene during VP<sub>AHPND</sub> infection.



## REFERENCES

- Amparyup, P., Promrungreang, K., Charoensapsri, W., Sutthangkul, J., & Tassanakajon, A. (2013). A serine proteinase PmClipSP2 contributes to prophenoloxidase system and plays a protective role in shrimp defense by scavenging lipopolysaccharide. *Dev Comp Immunol*, *41*(4), 597-607. doi:10.1016/j.dci.2013.06.013
- Anghong, P., Roytrakul, S., Jarayabhand, P., & Jiravanichpaisal, P. (2017). Involvement of a tachylectin-like gene and its protein in pathogenesis of acute hepatopancreatic necrosis disease (AHPND) in the shrimp, *Penaeus monodon*. *Dev Comp Immunol*, *76*, 229-237. doi:10.1016/j.dci.2017.06.011
- Belicard, T., Jareosettasin, P., & Sarkies, P. (2018). The piRNA pathway responds to environmental signals to establish intergenerational adaptation to stress. *BMC Biol*, *16*(1), 103. doi:10.1186/s12915-018-0571-y
- Blom, N., Sicheritz-Ponten, T., Gupta, R., Gammeltoft, S., & Brunak, S. (2004). Prediction of post-translational glycosylation and phosphorylation of proteins from the amino acid sequence. *Proteomics*, *4*(6), 1633-1649. doi:10.1002/pmic.200300771
- Boonchuen, P., Jaree, P., Somboonwiwat, K., & Somboonwiwat, K. (2021). Regulation of shrimp prophenoloxidase activating system by lva-miR-4850 during bacterial infection. *Sci Rep*, *11*(1), 3821. doi:10.1038/s41598-021-82881-2
- Boonchuen, P., Jaree, P., Tassanakajon, A., & Somboonwiwat, K. (2018). Hemocyanin of *Litopenaeus vannamei* agglutinates *Vibrio parahaemolyticus* AHPND (VPAHPND) and neutralizes its toxin. *Dev Comp Immunol*, *84*, 371-381. doi:10.1016/j.dci.2018.03.010
- Boonchuen, P., Maralit, B. A., Jaree, P., Tassanakajon, A., & Somboonwiwat, K. (2020). MicroRNA and mRNA interactions coordinate the immune response in non-lethal heat stressed *Litopenaeus vannamei* against AHPND-causing *Vibrio parahaemolyticus*. *Sci Rep*, *10*(1), 787. doi:10.1038/s41598-019-57409-4
- Bravo, A., Gill, S. S., & Soberon, M. (2007). Mode of action of *Bacillus thuringiensis* Cry and Cyt toxins and their potential for insect control. *Toxicon*, *49*(4), 423-435. doi:10.1016/j.toxicon.2006.11.022
- Caplen, N. J., & Mousses, S. (2003). Short interfering RNA (siRNA)-mediated RNA interference (RNAi) in human cells. *Ann N Y Acad Sci*, *1002*, 56-62. doi:10.1196/annals.1281.007
- Carthew, R. W., & Sontheimer, E. J. (2009). Origins and Mechanisms of miRNAs and siRNAs. *Cell*, *136*(4), 642-655. doi:10.1016/j.cell.2009.01.035
- Cremer, S., Michalik, K. M., Fischer, A., Pfisterer, L., Jae, N., Winter, C., . . . Dimmeler, S. (2019). Hematopoietic Deficiency of the Long Noncoding RNA MALAT1 Promotes Atherosclerosis and Plaque Inflammation. *Circulation*, *139*(10), 1320-1334. doi:10.1161/CIRCULATIONAHA.117.029015
- Czech, B., Munafo, M., Ciabrelli, F., Eastwood, E. L., Fabry, M. H., Kneuss, E., & Hannon, G. J. (2018). piRNA-Guided Genome Defense: From Biogenesis to Silencing. *Annu Rev Genet*, *52*, 131-157. doi:10.1146/annurev-genet-120417-031441
- De Fazio, S., Bartonicek, N., Di Giacomo, M., Abreu-Goodger, C., Sankar, A., Funaya, C., . . . O'Carroll, D. (2011). The endonuclease activity of Mili fuels piRNA

- amplification that silences LINE1 elements. *Nature*, 480(7376), 259-263. doi:10.1038/nature10547
- De Schryver, P., Defoirdt, T., & Sorgeloos, P. (2014). Early mortality syndrome outbreaks: a microbial management issue in shrimp farming? *PLoS Pathog*, 10(4), e1003919. doi:10.1371/journal.ppat.1003919
- Eulalio, A., Schulte, L., & Vogel, J. (2012). The mammalian microRNA response to bacterial infections. *RNA Biol*, 9(6), 742-750. doi:10.4161/rna.20018
- Flegel, T. W. (2012). Historic emergence, impact and current status of shrimp pathogens in Asia. *J Invertebr Pathol*, 110(2), 166-173. doi:10.1016/j.jip.2012.03.004
- Flegel, T. W., & Sritunyalucksana, K. (2011). Shrimp molecular responses to viral pathogens. *Mar Biotechnol (NY)*, 13(4), 587-607. doi:10.1007/s10126-010-9287-x
- Gainetdinov, I., Colpan, C., Arif, A., Cecchini, K., & Zamore, P. D. (2018). A Single Mechanism of Biogenesis, Initiated and Directed by PIWI Proteins, Explains piRNA Production in Most Animals. *Mol Cell*, 71(5), 775-790 e775. doi:10.1016/j.molcel.2018.08.007
- Goic, B., Stapleford, K. A., Frangeul, L., Doucet, A. J., Gausson, V., Blanc, H., . . . Saleh, M. C. (2016). Virus-derived DNA drives mosquito vector tolerance to arboviral infection. *Nat Commun*, 7, 12410. doi:10.1038/ncomms12410
- Guo, H. J., & Tadi, P. (2021). Biochemistry, Ubiquitination. In *StatPearls*. Treasure Island (FL).
- Han, J. E., Tang, K. F., Tran, L. H., & Lightner, D. V. (2015). Photorhabdus insect-related (Pir) toxin-like genes in a plasmid of *Vibrio parahaemolyticus*, the causative agent of acute hepatopancreatic necrosis disease (AHPND) of shrimp. *Dis Aquat Organ*, 113(1), 33-40. doi:10.3354/dao02830
- He, F., Zhao, J., Li, L., & Guo, R. (2015). Effect of small interference RNA on the acetylcholine-sensitive potassium channel in H9c2 cells. *Ann Clin Lab Sci*, 45(1), 58-63.
- Heath, R. J., Goel, G., Baxt, L. A., Rush, J. S., Mohanan, V., Paulus, G. L. C., . . . Xavier, R. J. (2016). RNF166 Determines Recruitment of Adaptor Proteins during Antibacterial Autophagy. *Cell Rep*, 17(9), 2183-2194. doi:10.1016/j.celrep.2016.11.005
- Hirakata, S., & Siomi, M. C. (2016). piRNA biogenesis in the germline: From transcription of piRNA genomic sources to piRNA maturation. *Biochim Biophys Acta*, 1859(1), 82-92. doi:10.1016/j.bbagr.2015.09.002
- Hofmann, C., Vanderbruggen, H., Hofte, H., Van Rie, J., Jansens, S., & Van Mellaert, H. (1988). Specificity of *Bacillus thuringiensis* delta-endotoxins is correlated with the presence of high-affinity binding sites in the brush border membrane of target insect midguts. *Proc Natl Acad Sci U S A*, 85(21), 7844-7848. doi:10.1073/pnas.85.21.7844
- Hooper, N. M. (1994). Families of zinc metalloproteases. *FEBS Lett*, 354(1), 1-6. doi:10.1016/0014-5793(94)01079-x
- Huang, H., Li, Y., Szulwach, K. E., Zhang, G., Jin, P., & Chen, D. (2014). AGO3 Slicer activity regulates mitochondria-nuage localization of Armitage and piRNA amplification. *J Cell Biol*, 206(2), 217-230. doi:10.1083/jcb.201401002
- Huang, S., Ichikawa, Y., Igarashi, Y., Yoshitake, K., Kinoshita, S., Omori, F., . . . Asakawa, S. (2019). Piwi-interacting RNA (piRNA) expression patterns in pearl

- oyster (*Pinctada fucata*) somatic tissues. *Sci Rep*, 9(1), 247. doi:10.1038/s41598-018-36726-0
- Huang, T., & Zhang, X. (2013). Host defense against DNA virus infection in shrimp is mediated by the siRNA pathway. *Eur J Immunol*, 43(1), 137-146. doi:10.1002/eji.201242806
- Huang, X., Fejes Toth, K., & Aravin, A. A. (2017). piRNA Biogenesis in *Drosophila melanogaster*. *Trends Genet*, 33(11), 882-894. doi:10.1016/j.tig.2017.09.002
- Hutvagner, G., & Simard, M. J. (2008). Argonaute proteins: key players in RNA silencing. *Nat Rev Mol Cell Biol*, 9(1), 22-32. doi:10.1038/nrm2321
- Iwasaki, Y. W., Siomi, M. C., & Siomi, H. (2015). PIWI-Interacting RNA: Its Biogenesis and Functions. *Annu Rev Biochem*, 84, 405-433. doi:10.1146/annurev-biochem-060614-034258
- Janeway, C. A., Jr. (2013). Pillars article: approaching the asymptote? Evolution and revolution in immunology. Cold spring harb symp quant biol. 1989. 54: 1-13. *J Immunol*, 191(9), 4475-4487.
- Julenius, K., Molgaard, A., Gupta, R., & Brunak, S. (2005). Prediction, conservation analysis, and structural characterization of mammalian mucin-type O-glycosylation sites. *Glycobiology*, 15(2), 153-164. doi:10.1093/glycob/cwh151
- Junprung, W., Supungul, P., & Tassanakajon, A. (2017). HSP70 and HSP90 are involved in shrimp *Penaeus vannamei* tolerance to AHPND-causing strain of *Vibrio parahaemolyticus* after non-lethal heat shock. *Fish Shellfish Immunol*, 60, 237-246. doi:10.1016/j.fsi.2016.11.049
- Kaewkascholkul, N., Somboonviwat, K., Asakawa, S., Hirono, I., Tassanakajon, A., & Somboonviwat, K. (2016). Shrimp miRNAs regulate innate immune response against white spot syndrome virus infection. *Dev Comp Immunol*, 60, 191-201. doi:10.1016/j.dci.2016.03.002
- Khurana, J. S., Wang, J., Xu, J., Koppetsch, B. S., Thomson, T. C., Nowosielska, A., . . . Theurkauf, W. E. (2011). Adaptation to P element transposon invasion in *Drosophila melanogaster*. *Cell*, 147(7), 1551-1563. doi:10.1016/j.cell.2011.11.042
- Kitchen, G. B., Cunningham, P. S., Poolman, T. M., Iqbal, M., Maidstone, R., Baxter, M., . . . Ray, D. W. (2020). The clock gene *Bmal1* inhibits macrophage motility, phagocytosis, and impairs defense against pneumonia. *Proc Natl Acad Sci U S A*, 117(3), 1543-1551. doi:10.1073/pnas.1915932117
- Kondo, H., Tinwongger, S., Proespraiwong, P., Mavichak, R., Unajak, S., Nozaki, R., & Hirono, I. (2014). Draft Genome Sequences of Six Strains of *Vibrio parahaemolyticus* Isolated from Early Mortality Syndrome/Acute Hepatopancreatic Necrosis Disease Shrimp in Thailand. 2(2), e00221-00214. doi:10.1128/genomeA.00221-14 %J Genome Announcements
- Kumar, V., De Bels, L., Couck, L., Baruah, K., Bossier, P., & Van den Broeck, W. (2019). PirAB(VP) Toxin Binds to Epithelial Cells of the Digestive Tract and Produce Pathognomonic AHPND Lesions in Germ-Free Brine Shrimp. *Toxins (Basel)*, 11(12). doi:10.3390/toxins11120717
- Lai, H. C., Ng, T. H., Ando, M., Lee, C. T., Chen, I. T., Chuang, J. C., . . . Wang, H. C. (2015). Pathogenesis of acute hepatopancreatic necrosis disease (AHPND) in shrimp. *Fish Shellfish Immunol*, 47(2), 1006-1014. doi:10.1016/j.fsi.2015.11.008

- Lee, C. T., Chen, I. T., Yang, Y. T., Ko, T. P., Huang, Y. T., Huang, J. Y., . . . Lo, C. F. (2015). The opportunistic marine pathogen *Vibrio parahaemolyticus* becomes virulent by acquiring a plasmid that expresses a deadly toxin. *Proc Natl Acad Sci U S A*, *112*(34), 10798-10803. doi:10.1073/pnas.1503129112
- Lewis, S. H., Quarles, K. A., Yang, Y., Tanguy, M., Frezal, L., Smith, S. A., . . . Jiggins, F. M. (2018). Pan-arthropod analysis reveals somatic piRNAs as an ancestral defence against transposable elements. *Nat Ecol Evol*, *2*(1), 174-181. doi:10.1038/s41559-017-0403-4
- Li, F., & Xiang, J. (2013). Signaling pathways regulating innate immune responses in shrimp. *Fish Shellfish Immunol*, *34*(4), 973-980. doi:10.1016/j.fsi.2012.08.023
- Li, X. Z., Roy, C. K., Moore, M. J., & Zamore, P. D. (2013). Defining piRNA primary transcripts. *Cell Cycle*, *12*(11), 1657-1658. doi:10.4161/cc.24989
- Lightner, D. V. (1996). Epizootiology, distribution and the impact on international trade of two penaeid shrimp viruses in the Americas. *Rev Sci Tech*, *15*(2), 579-601. doi:10.20506/rst.15.2.944
- Lightner, D. V., Redman, R. M., Pantoja, C. R., Tang, K. F., Noble, B. L., Schofield, P., . . . Navarro, S. A. (2012). Historic emergence, impact and current status of shrimp pathogens in the Americas. *J Invertebr Pathol*, *110*(2), 174-183. doi:10.1016/j.jip.2012.03.006
- Lim, R. S., Anand, A., Nishimiya-Fujisawa, C., Kobayashi, S., & Kai, T. (2014). Analysis of Hydra PIWI proteins and piRNAs uncover early evolutionary origins of the piRNA pathway. *Dev Biol*, *386*(1), 237-251. doi:10.1016/j.ydbio.2013.12.007
- Lin, P., Cheng, T., Jin, S., Jiang, L., Wang, C., & Xia, Q. (2014). Structural, evolutionary and functional analysis of APN genes in the Lepidoptera *Bombyx mori*. *Gene*, *535*(2), 303-311. doi:10.1016/j.gene.2013.11.002
- Liu, C., Li, F., Sun, Y., Zhang, X., Yuan, J., Yang, H., & Xiang, J. (2016). Virus-derived small RNAs in the penaeid shrimp *Fenneropenaeus chinensis* during acute infection of the DNA virus WSSV. *Sci Rep*, *6*, 28678. doi:10.1038/srep28678
- Liu, F., Li, S., Liu, G., & Li, F. (2017). Triosephosphate isomerase (TPI) facilitates the replication of WSSV in *Exopalaemon carinicauda*. *Dev Comp Immunol*, *71*, 28-36. doi:10.1016/j.dci.2017.01.018
- Luangtrakul, W., Boonchuen, P., Jaree, P., Kumar, R., Wang, H. C., & Somboonwiwat, K. (2021). Cytotoxicity of *Vibrio parahaemolyticus* AHPND toxin on shrimp hemocytes, a newly identified target tissue, involves binding of toxin to aminopeptidase N1 receptor. *PLoS Pathog*, *17*(3), e1009463. doi:10.1371/journal.ppat.1009463
- Maralit, B. A., Jaree, P., Boonchuen, P., Tassanakajon, A., & Somboonwiwat, K. (2018). Differentially expressed genes in hemocytes of *Litopenaeus vannamei* challenged with *Vibrio parahaemolyticus* AHPND (VPAHPND) and VPAHPND toxin. *Fish Shellfish Immunol*, *81*, 284-296. doi:10.1016/j.fsi.2018.06.054
- Miesen, P., Joosten, J., & van Rij, R. P. (2016). PIWIs Go Viral: Arbovirus-Derived piRNAs in Vector Mosquitoes. *PLoS Pathog*, *12*(12), e1006017. doi:10.1371/journal.ppat.1006017

- Mohn, F., Handler, D., & Brennecke, J. (2015). Noncoding RNA. piRNA-guided slicing specifies transcripts for Zucchini-dependent, phased piRNA biogenesis. *Science*, 348(6236), 812-817. doi:10.1126/science.aaa1039
- Ningshen, T. J., Aparoy, P., Ventaku, V. R., & Dutta-Gupta, A. (2013). Functional interpretation of a non-gut hemocoelic tissue aminopeptidase N (APN) in a lepidopteran insect pest *Achaea janata*. *PLoS One*, 8(11), e79468. doi:10.1371/journal.pone.0079468
- Nunan, L., Lightner, D., Pantoja, C., & Gomez-Jimenez, S. (2014). Detection of acute hepatopancreatic necrosis disease (AHPND) in Mexico. *Dis Aquat Organ*, 111(1), 81-86. doi:10.3354/dao02776
- Olovnikov, I., Ryazansky, S., Shpiz, S., Lavrov, S., Abramov, Y., Vaury, C., . . . Kalmykova, A. (2013). De novo piRNA cluster formation in the *Drosophila* germ line triggered by transgenes containing a transcribed transposon fragment. *Nucleic Acids Res*, 41(11), 5757-5768. doi:10.1093/nar/gkt310
- Ortoger, N., Schuster, A. S., Oliver, D. K., Riordan, C. R., Hong, A. S., Hennig, G. W., . . . Yan, W. (2014). A novel class of somatic small RNAs similar to germ cell pachytene PIWI-interacting small RNAs. *J Biol Chem*, 289(47), 32824-32834. doi:10.1074/jbc.M114.613232
- Pacheco, S., Gomez, I., Gill, S. S., Bravo, A., & Soberon, M. (2009). Enhancement of insecticidal activity of *Bacillus thuringiensis* Cry1A toxins by fragments of a toxin-binding cadherin correlates with oligomer formation. *Peptides*, 30(3), 583-588. doi:10.1016/j.peptides.2008.08.006
- Perera, B. P. U., Tsai, Z. T., Colwell, M. L., Jones, T. R., Goodrich, J. M., Wang, K., . . . Dolinoy, D. C. (2019). Somatic expression of piRNA and associated machinery in the mouse identifies short, tissue-specific piRNA. *Epigenetics*, 14(5), 504-521. doi:10.1080/15592294.2019.1600389
- Pfaffl, M. W. (2001). A new mathematical model for relative quantification in real-time RT-PCR. *Nucleic Acids Res*, 29(9), e45. doi:10.1093/nar/29.9.e45
- Pigott, C. R., & Ellar, D. J. (2007). Role of receptors in *Bacillus thuringiensis* crystal toxin activity. *Microbiol Mol Biol Rev*, 71(2), 255-281. doi:10.1128/MMBR.00034-06
- Posiri, P., Ongvarrasopone, C., & Panyim, S. (2013). A simple one-step method for producing dsRNA from *E. coli* to inhibit shrimp virus replication. *J Virol Methods*, 188(1-2), 64-69. doi:10.1016/j.jviromet.2012.11.033
- Qin, Y., Zhou, M. T., Hu, M. M., Hu, Y. H., Zhang, J., Guo, L., . . . Shu, H. B. (2014). RNF26 temporally regulates virus-triggered type I interferon induction by two distinct mechanisms. *PLoS Pathog*, 10(9), e1004358. doi:10.1371/journal.ppat.1004358
- Queiroz, F. R., Portilho, L. G., Jeremias, W. J., Baba, E. H., do Amaral, L. R., Silva, L. M., . . . Gomes, M. S. (2020). Deep sequencing of small RNAs reveals the repertoire of miRNAs and piRNAs in *Biomphalaria glabrata*. *Mem Inst Oswaldo Cruz*, 115, e190498. doi:10.1590/0074-02760190498
- Rojas-Rios, P., & Simonelig, M. (2018). piRNAs and PIWI proteins: regulators of gene expression in development and stem cells. *Development*, 145(17). doi:10.1242/dev.161786

- Sarkar, A., Maji, R. K., Saha, S., & Ghosh, Z. (2014). piRNAQuest: searching the piRNAome for silencers. *BMC Genomics*, *15*, 555. doi:10.1186/1471-2164-15-555
- Shao, E., Lin, L., Liu, S., Zhang, J., Chen, X., Sha, L., . . . Guan, X. (2018). Analysis of Homologs of Cry-toxin Receptor-Related Proteins in the Midgut of a Non-Bt Target, *Nilaparvata lugens* (Stal) (Hemiptera: Delphacidae). *J Insect Sci.* doi:10.1093/jisesa/iex102
- Sharbati, S., Sharbati, J., Hoeke, L., Bohmer, M., & Einspanier, R. (2012). Quantification and accurate normalisation of small RNAs through new custom RT-qPCR arrays demonstrates Salmonella-induced microRNAs in human monocytes. *BMC Genomics*, *13*, 23. doi:10.1186/1471-2164-13-23
- Shu, L., & Zhang, X. (2017). Shrimp miR-12 Suppresses White Spot Syndrome Virus Infection by Synchronously Triggering Antiviral Phagocytosis and Apoptosis Pathways. *Front Immunol*, *8*, 855. doi:10.3389/fimmu.2017.00855
- Sirikharin, R., Taengchaiyaphum, S., Sanguanrut, P., Chi, T. D., Mavichak, R., Proespraiwong, P., . . . Sritunyalucksana, K. (2015). Characterization and PCR Detection Of Binary, Pir-Like Toxins from *Vibrio parahaemolyticus* Isolates that Cause Acute Hepatopancreatic Necrosis Disease (AHPND) in Shrimp. *PLoS One*, *10*(5), e0126987. doi:10.1371/journal.pone.0126987
- Soberon, M., Pardo, L., Munoz-Garay, C., Sanchez, J., Gomez, I., Porta, H., & Bravo, A. (2010). Pore formation by Cry toxins. *Adv Exp Med Biol*, *677*, 127-142. doi:10.1007/978-1-4419-6327-7\_11
- Soderhall, I., Bangyeekhun, E., Mayo, S., & Soderhall, K. (2003). Hemocyte production and maturation in an invertebrate animal; proliferation and gene expression in hematopoietic stem cells of *Pacifastacus leniusculus*. *Dev Comp Immunol*, *27*(8), 661-672. doi:10.1016/s0145-305x(03)00039-9
- Song, H., Xing, C., Lu, W., Liu, Z., Wang, X., Cheng, J., & Zhang, Q. (2019). Rapid evolution of piRNA pathway and its transposon targets in Japanese flounder (*Paralichthys olivaceus*). *Comp Biochem Physiol Part D Genomics Proteomics*, *31*, 100609. doi:10.1016/j.cbd.2019.100609
- Soonthornchai, W., Chaiyapechara, S., Klinbunga, S., Thongda, W., Tangphatsornruang, S., Yoocha, T., . . . Jiravanichpaisal, P. (2016). Differentially expressed transcripts in stomach of *Penaeus monodon* in response to AHPND infection. *Dev Comp Immunol*, *65*, 53-63. doi:10.1016/j.dci.2016.06.013
- Soto-Rodriguez, S. A., Gomez-Gil, B., Lozano-Olvera, R., Betancourt-Lozano, M., & Morales-Covarrubias, M. S. (2015). Field and experimental evidence of *Vibrio parahaemolyticus* as the causative agent of acute hepatopancreatic necrosis disease of cultured shrimp (*Litopenaeus vannamei*) in Northwestern Mexico. *Appl Environ Microbiol*, *81*(5), 1689-1699. doi:10.1128/AEM.03610-14
- Spinelli, S. V., Diaz, A., D'Attilio, L., Marchesini, M. M., Bogue, C., Bay, M. L., & Bottasso, O. A. (2013). Altered microRNA expression levels in mononuclear cells of patients with pulmonary and pleural tuberculosis and their relation with components of the immune response. *Mol Immunol*, *53*(3), 265-269. doi:10.1016/j.molimm.2012.08.008
- Stone, E. F., Fulton, B. O., Ayres, J. S., Pham, L. N., Ziauddin, J., & Shirasu-Hiza, M. M. (2012). The circadian clock protein timeless regulates phagocytosis of



- bacteria in *Drosophila*. *PLoS Pathog*, 8(1), e1002445.  
doi:10.1371/journal.ppat.1002445
- Sukthaworn, S., Panyim, S., & Udomkit, A. (2019). Functional characterization of a cDNA encoding Piwi protein in *Penaeus monodon* and its potential roles in controlling transposon expression and spermatogenesis. *Comp Biochem Physiol A Mol Integr Physiol*, 229, 60-68. doi:10.1016/j.cbpa.2018.11.022
- Tamura, K., Stecher, G., Peterson, D., Filipinski, A., & Kumar, S. (2013). MEGA6: Molecular Evolutionary Genetics Analysis version 6.0. *Mol Biol Evol*, 30(12), 2725-2729. doi:10.1093/molbev/mst197
- Tassanakajon, A., Somboonwiwat, K., Supungul, P., & Tang, S. (2013). Discovery of immune molecules and their crucial functions in shrimp immunity. *Fish Shellfish Immunol*, 34(4), 954-967. doi:10.1016/j.fsi.2012.09.021
- Tinwongger, S., Nochiri, Y., Thawonsuwan, J., Nozaki, R., Kondo, H., Awasthi, S. P., . . . Hirono, I. (2016). Virulence of acute hepatopancreatic necrosis disease PirAB-like relies on secreted proteins not on gene copy number. *J Appl Microbiol*, 121(6), 1755-1765. doi:10.1111/jam.13256
- Toth, K. F., Pezic, D., Stuwe, E., & Webster, A. (2016). The piRNA Pathway Guards the Germline Genome Against Transposable Elements. *Adv Exp Med Biol*, 886, 51-77. doi:10.1007/978-94-017-7417-8\_4
- Tran, L., Nunan, L., Redman, R. M., Mohney, L. L., Pantoja, C. R., Fitzsimmons, K., & Lightner, D. V. (2013). Determination of the infectious nature of the agent of acute hepatopancreatic necrosis syndrome affecting penaeid shrimp. *Dis Aquat Organ*, 105(1), 45-55. doi:10.3354/dao02621
- Van Rie, J., Jansens, S., Hofte, H., Degheele, D., & Van Mellaert, H. (1990). Receptors on the brush border membrane of the insect midgut as determinants of the specificity of *Bacillus thuringiensis* delta-endotoxins. *Appl Environ Microbiol*, 56(5), 1378-1385. doi:10.1128/aem.56.5.1378-1385.1990
- Velazquez-Lizarraga, A. E., Juarez-Morales, J. L., Racotta, I. S., Villarreal-Colmenares, H., Valdes-Lopez, O., Luna-Gonzalez, A., . . . Ascencio, F. (2019). Transcriptomic analysis of Pacific white shrimp (*Litopenaeus vannamei*, Boone 1931) in response to acute hepatopancreatic necrosis disease caused by *Vibrio parahaemolyticus*. *PLoS One*, 14(8), e0220993. doi:10.1371/journal.pone.0220993
- Victorio-De Los Santos, M., Vibanco-Perez, N., Soto-Rodriguez, S., Pereyra, A., Zenteno, E., & Cano-Sanchez, P. (2020). The B Subunit of PirAB(vp) Toxin Secreted from *Vibrio parahaemolyticus* Causing AHPND Is an Amino Sugar Specific Lectin. *Pathogens*, 9(3). doi:10.3390/pathogens9030182
- Visetnan, S., Supungul, P., Tassanakajon, A., Donpudsa, S., & Rimphanitchayakit, V. (2017). A single WAP domain-containing protein from *Litopenaeus vannamei* possesses antiproteinase activity against subtilisin and antimicrobial activity against AHPND-inducing *Vibrio parahaemolyticus*. *Fish Shellfish Immunol*, 68, 341-348. doi:10.1016/j.fsi.2017.07.046
- Wang, W., Han, B. W., Tipping, C., Ge, D. T., Zhang, Z., Weng, Z., & Zamore, P. D. (2015). Slicing and Binding by Ago3 or Aub Trigger Piwi-Bound piRNA Production by Distinct Mechanisms. *Mol Cell*, 59(5), 819-830. doi:10.1016/j.molcel.2015.08.007

- Watanabe, T., Cheng, E. C., Zhong, M., & Lin, H. (2015). Retrotransposons and pseudogenes regulate mRNAs and lncRNAs via the piRNA pathway in the germline. *Genome Res*, 25(3), 368-380. doi:10.1101/gr.180802.114
- Xiol, J., & Pillai, R. S. (2012). Molecular biology. Outsourcing genome protection. *Science*, 337(6094), 529-530. doi:10.1126/science.1227095
- Xu, C., Wang, B. C., Yu, Z., & Sun, M. (2014). Structural insights into *Bacillus thuringiensis* Cry, Cyt and parasporin toxins. *Toxins (Basel)*, 6(9), 2732-2770. doi:10.3390/toxins6092732
- Ye, W., Liu, X., Guo, J., Sun, X., Sun, Y., Shen, B., . . . Zhu, C. (2017). piRNA-3878 targets P450 (CpCYP307B1) to regulate pyrethroid resistance in *Culex pipiens pallens*. *Parasitol Res*, 116(9), 2489-2497. doi:10.1007/s00436-017-5554-3
- Yeh, M. S., Kao, L. R., Huang, C. J., & Tsai, I. H. (2006). Biochemical characterization and cloning of transglutaminases responsible for hemolymph clotting in *Penaeus monodon* and *Marsupenaeus japonicus*. *Biochim Biophys Acta*, 1764(7), 1167-1178. doi:10.1016/j.bbapap.2006.04.005
- Zhang, S., Cheng, H., Gao, Y., Wang, G., Liang, G., & Wu, K. (2009). Mutation of an aminopeptidase N gene is associated with *Helicoverpa armigera* resistance to *Bacillus thuringiensis* Cry1Ac toxin. *Insect Biochem Mol Biol*, 39(7), 421-429. doi:10.1016/j.ibmb.2009.04.003
- Zhang, X., Liang, Z., Zhang, Y., Zhu, M., Zhu, Y., Li, S., . . . Wang, J. (2019). Specific PIWI-interacting small noncoding RNA expression patterns in pulmonary tuberculosis patients. *Epigenomics*, 11(16), 1779-1794. doi:10.2217/epi-2018-0142
- Zhang, Y., Zhao, D., Yan, X., Guo, W., Bao, Y., Wang, W., & Wang, X. (2017). Identification and Characterization of *Hyphantria cunea* Aminopeptidase N as a Binding Protein of *Bacillus thuringiensis* Cry1Ab35 Toxin. *Int J Mol Sci*, 18(12). doi:10.3390/ijms18122575
- Zheng, H., Guo, Z., Zheng, X., Cheng, W., & Huang, X. (2018). MicroRNA-144-3p inhibits cell proliferation and induces cell apoptosis in prostate cancer by targeting CEP55. *Am J Transl Res*, 10(8), 2457-2468.
- Zheng, Z., Li, R., Aweya, J. J., Yao, D., Wang, F., Li, S., . . . Zhang, Y. (2021). The PirB toxin protein from *Vibrio parahaemolyticus* induces apoptosis in hemocytes of *Penaeus vannamei*. *Virulence*, 12(1), 481-492. doi:10.1080/21505594.2021.1872171

**VITA**

**NAME** Waruntorn Luangtrakul

**DATE OF BIRTH** 25 November 1992

**INSTITUTIONS ATTENDED** Chulalongkorn University

**HOME ADDRESS** 367/69 Jarunsanitwong Road. Bangkok Noi, Bangkok 10700

**PUBLICATION** Luangtrakul, W., Boonchuen, P., Jaree, P., Kumar, R., Wang, H. C., & Somboonwiwat, K. (2021). Cytotoxicity of *Vibrio parahaemolyticus* AHPND toxin on shrimp hemocytes, a newly identified target tissue, involves binding of toxin to aminopeptidase N1 receptor. *PLoS Pathog*, 17(3), e1009463.

